DEVELOPMENT OF A PRODUCTION ESTIMATION MODEL FOR TUNNEL BORING MACHINES (TBMs)

by

SAEED JANBAZ

Presented to the Faculty of the Graduate School of

The University of Texas at Arlington in Partial Fulfillment

of the Requirements

for the Degree of

DOCTOR OF PHILOSOPHY

THE UNIVERSITY OF TEXAS AT ARLINGTON

December 2017

Dedication

To Loving Memory of My Mother,

And To My Family.

Acknowledgements

I would like to express my thanks to all individuals who encouraged me and helped me during my studies to accomplish my goals in my graduate studies at University of Texas at Arlington. Special thanks are due to Dr. Mohammad Najafi, my Ph.D. dissertation advisor, for guiding and supporting me during my studies and for providing me with invaluable information, recommendations, and suggestions to accomplish my research goals. Thanks are also due to Dr. Mohsen Shahandashti, Dr. Xinbao Yu, and Dr. Asish Basu, my committee members, for their support and advice. Thanks are due to Robbins Company for their support of my research.

Most importantly, many thanks are due to my family who patiently supported me throughout my studies at the University of Texas at Arlington. Words alone cannot express my gratitude and my thanks that I always owe them. In this regard I would like to thank my father who always supports and encourages me and I would like to thank my mother, may she rest in peace, for all the support she has given me; I know and feel that her spirit watches over me.

Lastly, I offer my regards to all Civil Engineering Department faculty and staff at the University of Texas at Arlington, and the entire Center for Underground Infrastructure Research and Education (CUIRE) members and students who supported me in any respect during the completion of my studies.

November 9th, 2017

Abstract

DEVELOPMENT OF A PRODUCTION ESTIMATION MODEL

FOR TUNNEL BORING MACHINES (TBMs)

Saeed Janbaz, PhD

The University of Texas at Arlington, 2017

Supervising Professor: Mohammad Najafi

Advance rate (AR) estimation is a crucial factor at the conceptual phase of a tunneling project for preliminary estimation of tunnel boring machines' (TBMs') usage. The primary objective of this research is to develop order of magnitude performance charts for advance rate of TBMs that can be used using the limited information about the tunneling progress at the conceptual phase. The secondary objective of this dissertation is to evaluate factors that impact TBM progress in large diameter applications. Tunnel diameter and uniaxial compressive strength of ground are found to be some of the primary parameters for prediction of advance rate. Statistical analysis was used to produce an advance rate formula. Then performance charts were developed for specific rock conditions. The results were tested with use of case studies. The results of this dissertation showed that the highest amount of overestimation for case studies considered by these performance charts was 16%. The outcome of this dissertation can assist in prediction of tunnel boring machine's advance rate at the conceptual stage of a tunneling project based on uniaxial compressive strength of rock and diameter of the tunnel.

Table of Contents

List of Illustrations

List of Tables

Chapter 1 INTRODUCTION

INTRODUCTION

Tunneling developed during the industrialization at the start of the 19th century with building of the railway network (Maidl et al. 2008). The first stage of the developing mechanization of tunneling was the development of efficient drills for drilling holes for the explosives for drill and blast (Maidl et al. 2008). The first tunneling machines were not actually tunnel boring machines (TBMs). They did not work the entire face with their excavation tools. Rather the intention was to break out a groove around the tunnel perimeter. After this process, the TBM was withdrawn and the remaining core loosened with explosives. This was the basic principle of the TBM as was designed and built in 1846 by the Belgian engineer Henri Joseph Maus for the Mount Cenis Tunnel (Maidl et al. 2008). The breakthrough in the development of today's TBMs did not occur until the 1950s, when the first open gripper TBM with disc cutters as its only tools was developed by the mining engineer James S. Robbins (Maidl et al. 2008). Tunnel Boring Machines (TBMs) are popular in underground construction and tunneling projects in different ground conditions.

TUNNELING METHODS

There are various types of construction techniques developed for construction of tunnels as discussed in the following sections.

Hand Mining Method

Hand mining is a viable and cost effective method of constructing a tunnel. The main limitation is size. Hand mining will not be a viable method where the tunnel is too

small for worker entry and in large tunnels where there is a large volume of material to be excavated (VTC, 2017). Figure 1-1 illustrates hand mining operations.

Figure 1-1 Hand Mining (Jjboring, 2017)

Drill and Blast Method

Drill and blast tunneling involves controlled use of explosives to break rock. Drill and blast tunneling is a form of subsurface construction. Using jack hammers, blast holes are drilled on the tunnel face. Explosives are loaded in the blast holes and then blasting is taken place (VTC, 2017). Figure 1-2 shows the tunnel face after blasting.

Figure 1-2 Tunnel Surface after Blast (Tunneltalk, 2017a)

Cut and Cover Method

Cut and cover method is generally used to build shallow tunnels. In this method, a trench is cut in the soil and it is covered by some support which can be capable of bearing load on it. In this method, the excavation sides are vertical and temporary supported are provided. The main problems associated with cut and cover method are the stability of the ground, impact on the existing underground services & utilities and traffic disruption in urban areas (VTC, 2017). Figure 1-3 shows this method in construction.

Figure 1-3 Cut and Cover Construction (Tunneltalk, 2017b)

Tunnel Boring Machine

To avoid the need of miners working in compressed air and to eliminate the risk of collapse of tunnel face, tunnel boring machines (TBM) are developed for such purpose (VTC, 2017). By definition, all machines used for boring tunnels are tunnel boring machines. However, a TBM often refers to a large diameter cylindrical shield, equipped with a rotating cutterhead at the front, a mucking device, and frequently an automatic segment erector (VTC, 2017). Some limitations of TBMs are, high initial cost renders it expensive for short tunnels, high cost for wear and tear when driving tunnels in hard rock, and it is limited to driving circular tunnels and cannot be used for other cross section (VTC, 2017). Figure 1-4 shows a TBM entering the exit shaft.

Figure 1-4 TBM at Exit Shaft (Mole, 2017)

Pipe Jacking Method

This method can be used for the installation of pipes from 3 inches to 12 ft diameter, but it is mainly employed on the larger diameter pipes of over 3 ft (VTC, 2017). This method is very suitable for installing services under roads and railway embankments without creating disturbance to traffic. The method consists of forming pits at both ends of the proposed tunnel. A thrust wall is constructed to provide jacking reaction and pipe segments are jacked into the soil. This method uses small TBMs known as micro TBMs at the face (VTC, 2017).

The excavated spoil is liquefied by mixing with bentonite slurry and removed by pump and pipeline. For large diameter pipes or for long pipes, the friction will be very great and it creates problems in providing suitable jacking reaction (VTC, 2017). A

method to counteract the frictional forces is use of intermediate jacking stations (Najafi, 2013). The intermediate jacks are fixed on steel sleeves which are installed at suitable intervals along the pipe length. The line is then jacked forward in a caterpillar fashion. In addition, bentonite slurry can be introduced from the rear of the driving shield as lubricant to reduce the friction (Najafi, 2013). Figure 1-5 shows a pipe jacking in operation.

Figure 1-5 Pipe Jacking (Herrenknecht, 2017a)

Box Jacking Method

Box jacking is a trenchless technology method for installing a prefabricated box through the ground from a drive shaft to a receiving shaft (Najafi, 2013).Box jacking method is similar to pipe jacking, but in this case, instead of pipe sections, specially made boxes are driven into the soil. Excavation at the face can be done with different methods, such as manually or by mechanically using specifically made cutterheads. Excavated materials (spoils) are collected and transported within the box (Najafi, 2013). Box jacking operation is shown in Figure 1-6.

Figure 1-6 Box Jacking Operation (Source: Dr. Najafi, 2017)

RESEARCH NEEDS

To accurately predict the advance rate of TBMs, a variety of information regarding project site and specific conditions, such as, ground conditions, machine specifications, surface congestions, tools used, etc., are needed. The penetration rate (PR) and advance rate (AR) of the TBM can be used to estimate machine productivity. PR is usually reported in terms of ft/hr and it is mostly related to ground conditions and TBM specifications such as diameter (Robbins, 1992). AR is the average progress of the completed tunnel (with supports erected) and it can be predicted using the PR and utilization rate (UR) of TBM. UR is the time that the machine is excavating divided by the total cycle time. The relationship between AR, PR and UR can be shown as Eq. 1-1:

$AR = PR \times UR$ (Eq. 1-1)

Eq. 1-1 states that any increase in utilization rate will directly increase the advance rate. It also states that even if the PR may be high in a project, it could still have

low advance rate because of low utilization rate and vice versa. Many researchers such as Rostami (1997), Yagiz (2002), and Gong (2005), have made an effort to model TBM performance for prediction of the penetration rate. Literature review shows that there have been a lot of studies on accurate prediction of PR, with some considering different geological parameters in recent years but the amount of work on prediction of TBM advance rate is very limited and the number of research studies is quite low compared to the volume of research on prediction of the PR (Farrokh, 2013). The existing systematic work on prediction of TBM AR includes the work by the Earth Mechanics Institute (EMI) of Colorado School of Mines (CSM) that can be found in Ozdemir and Sharp (1991), the Norwegian Institute of Technology (NTH) (Johannssen, 1988, Bruland, 1998a, 1998b), the Q_{TBM} method (Barton, 2000), the neural network method (Alvarez, 2000), and the Fuzzy Logic-Based Utilization Predictor Model (Kim, 2004).

Farrokh (2013) compared different previously defined models for AR. He found that the difference between predicted and observed values can sometimes be in excess of 100%. This finding is in agreement with Goel (2008), which two AR models, namely Q_{TBM} (Barton, 2000) and RME (Bieniawski et al., 2008) models, where tested for a Himalayan tunnel. Many of the information (such as, bore logs) needed for the complex models developed by researchers are not available to tunneling contractors at the conceptual phase To estimate the production rate of the TBM, the current models that exist in the literature cannot be used as they require specific data which will be available later in the project. Therefore, simple advance rate models are needed using limited available information about the project alongside the historical information of other TBM projects.

TBM PRODUCTIVITY PARAMETERS

Advance rate of TBMs is affected by many different parameters. Some parameters affect the advance rate directly while others have more of an indirect effect on productivity. The following sections introduce main parameters and how they affect the advance rate.

Underground Conditions

Underground conditions such as type and behavior of soil (formation, soft, hard, compressive and shear strength, etc.) and rock (hardness, texture, tenacity, formation, etc.), watertable, etc., have a direct impact on the TBM advance rate. In rock mechanics and engineering geology, according to ISRM (1978), the boundary between rock and soil is defined in terms of the uniaxial compressive strength (UCS) and not in terms of structure, texture or weathering. A material with the strength less than 36 psi is considered as soil (ISRM, 1978). The higher the UCS of the ground, the stronger the material the TBM bores. The ground UCS has a direct impact in calculation of penetration rate (PR) and utilization rate (UR) (Farrokh, 2013).

Tunnel Diameter

Tunnel diameter affects the TBM production rate directly. As the tunnel diameter increases, the cross section of the tunnel increases which, means that more soil needs to be excavated and it will take longer to be bored and transport the spoils. Larger tunnel diameter decreases the revolution per minute (RPM) of TBM as described in Chapter 4 of this dissertation.

TBM Characteristics

TBM related factors such as operator and TBM backup system impact advance rate of TBM. Behind all types of tunnel boring machines, inside the finished part of the tunnel, are trailing support decks known as the backup system. Support mechanisms located on the backup can include: conveyors or other systems for muck removal, slurry pipelines if applicable, control rooms, electrical systems, dust removal, ventilation and mechanisms for transport of precast segments. This dissertation considers the average advance rate of TBMs. Generally the backup system would cause productivity issues in tunnels of extremely long alignment, but this issue is usually solved by excavating interval access shafts (Jencopale, 2013).

Project Site Conditions and Unforeseen Events

In any tunneling project, specific site conditions such as, weather, traffic, working hours, and etc., affect the production rate of the project. For example, these conditions could delay the spoil removal from the project site or delay the delivery of tunnel segmental lining. Also unforeseen events or so-called acts of God, could impact the productivity dramatically. These conditions are out of the scope of this dissertation.

OBJECTIVES

The primary objective of this dissertation is to develop a prediction model for TBM advance rate using available data in the conceptual phases of a tunneling project. Historical data from various tunneling projects can provide similar information at the conceptual phase as contractors have experience with different ground conditions and

TBM specifications. These historical data can be used to produce a model for TBM productivity at the conceptual phase.

CONTRIBUTIONS TO THE BODY OF KNOWLEDGE

The followings are the main contributions of this research:

1. Producing rough order of magnitude estimates of TBM productivity based on UCS and diameter.
2. Developing performance charts that use above information as input data.

SCOPE

To predict the advance rate, the penetration rate and utilization rate will be predicted. The study will focus on shielded TBMs since they are more common amongst the recent tunneling projects. The TBM advance rate prediction model will provide a basis for the productivity that the project needs at the conceptual phase.

The scope of this research includes various literature reviews of existing TBM advance rate prediction methods, statistical analysis of TBM advance rate records within various ground conditions, and the development of prediction models for estimation of machine hourly advance rates. The scope of this study was limited to the following due to time and resource restrictions to prepare this dissertation:

1. The dissertation is positioned in conceptual phase where limited information is available for feasibility analysis.
2. Shielded TBMs. Gripper TBMs are not included.
3. Diameters between 5 ft to 40 ft.
4. Ground conditions of up to 36,000 psi uniaxial compressive strength.

Conceptual Phase

A schematic flow diagram of the sequential actions to realize a project is shown in Figure 1-7 (Halpin, 2006). The first step in any project is the establishment of a need and a conceptual definition of the facility at “zero design” that will meet owner’s requirements (Halpin, 2006). In conceptual phase, the client's needs for the constructed facility are expressed. The needs are stated in broad terms rather than in terms of specifics and the operational details of the later phases (Abdul-Kadir and Price, 1995). In a project environment, the conceptual phase is at a macro level, and hence it is strategically important (Abdul-Kadir and Price, 1995). It is common practice to present conceptual documentation to potential funding sources (Halpin, 2006). The conceptual phase has the most influence on the course of the phases to come: the detailed engineering, procurement, construction and startup phases. The success of these phases very much depends upon the decisions made during the conceptual phase (Abdul-Kadir and Price, 1995).

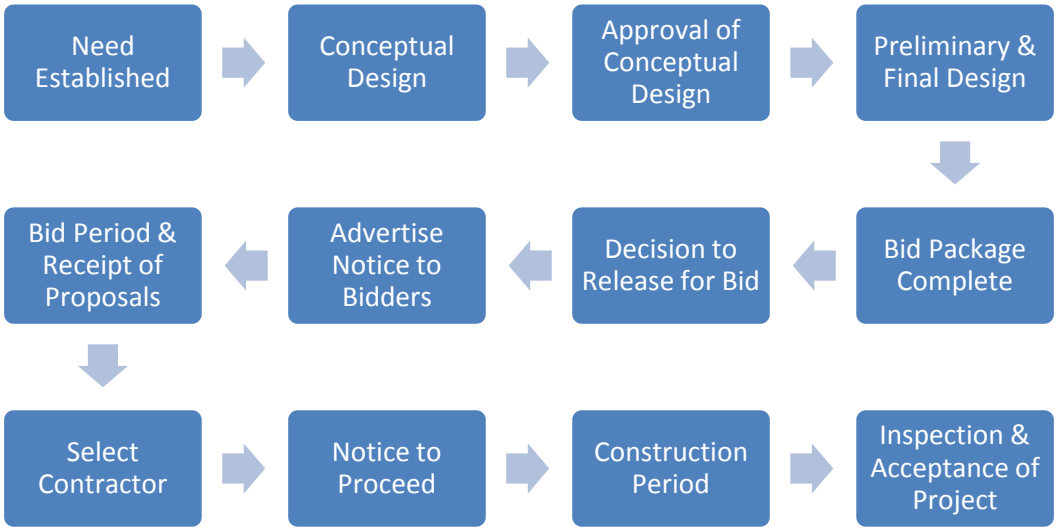

Figure 1-7 Project Development Cycle (Halpin, 2006)

METHODOLOGY

The below steps were followed to accomplish goals of this research:

1. A literature review was conducted on penetration and utilization rate of prediction models.
2. Collection of TBM data from the literature.
3. Data analysis and interpretation using statistical methods and regression analysis to develop proper formulas for estimation of TBM penetration and utilization rate.
4. Validation of the prediction models by comparison with various case studies.
5. Fine-tuning the results.

Figure 1-8 shows a flowchart for the methodology of this research.

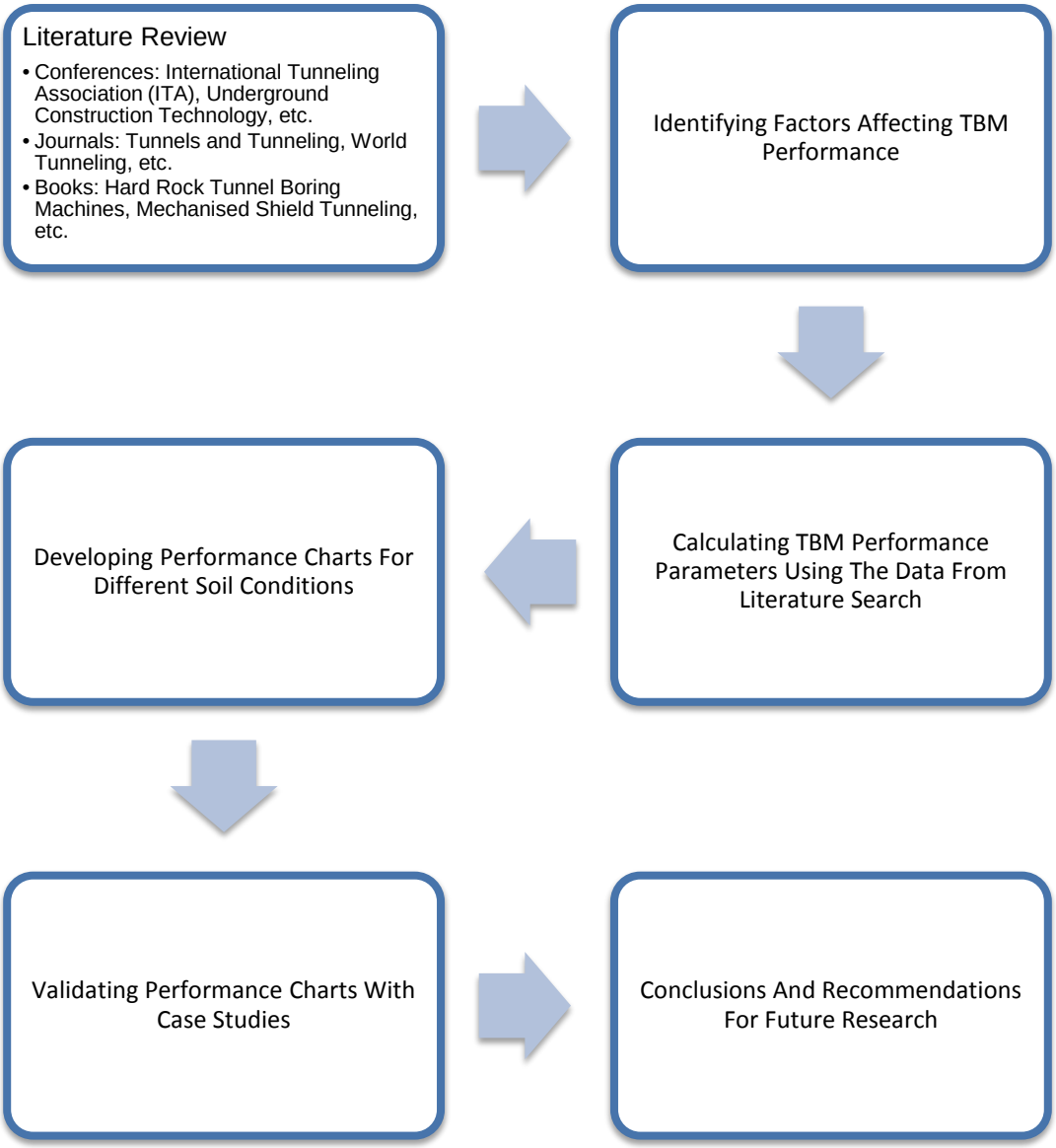

Figure 1-8 Methodology

HYPOTHESIS

The performance charts developed with this dissertation will provide a rough order of magnitude estimation of hourly advance rate of TBMs. These performance charts will provide advance rate prediction in the conceptual phase of the project. It is expected that the performance charts developed with this dissertation allow contractors and design engineers select a TBM based on uniaxial compressive strength of rock and diameter of the tunnel.

STRUCTURE OF THIS DISSERTATION

Chapter 1 presents the research needs, objectives, scope, methodology, and contributions of this study to the technical knowledge in this field.

Chapter 2 provides a description of various TBMs and how they work.

Chapter 3 covers the background and literature review on application of TBMs and productivity prediction, and their main performance parameters.

Chapter 4 presents the statistical analysis to find different parameter of advance rate formula.

Chapter 5 presents the performance charts for hourly advance rate of various size TBMs for various ground conditions and compares the results of the performance charts with case studies.

Finally, in Chapter 6, summary and conclusions are presented followed by explanation for the limitations of the current study and recommendations for future research.

CHAPTER SUMMARY

This chapter presented the research needs, objectives, scope, methodology, and contributions of this study to the technical knowledge in this field. Prediction of TBM advance rate in the conceptual phase of a tunneling project, when the information about the project is limited is important for initial scheduling and budgeting. The advance rate prediction will use the data that might be available at the conceptual stage of a tunneling project, such as, strength of rock and diameter of the tunnel.

Chapter 2 TBM DESCRIPTION

INTRODUCTION

Chapter 1 provided an introduction to this dissertation. In this chapter, different types of TBMs with their working mechanism will be explained. In recent years, the range of application of mechanized tunneling has been remarkably extended. In the past a stable rock mass and the necessity of no or at least only minor support measures served as a prerequisite for machine tunneling in rock (Maidl et al., 2008).

TUNNEL BORING MACHINE (TBM)

TBMs are used in a variety of ground conditions and range in size from just under 7 ft to over 35 ft in diameter (Maidl et al., 2008). They can negotiate large curves within limits and can cut soft grounds as low as 200 psi UCS, such as fault breccia to hard with more than 36,250 psi UCS, such as igneous rocks (Maidl et al., 2008). Table 2-1 summarizes some of the advantages and limitations of the TBM excavation method.

Table 2-1 TBM Advantages and Limitations (Modified from Maidl et al., 2008)

Advantages	**Limitations**
Higher tunneling advance rate	More geological information needed
Exact excavation profile	High investment
Automated and continual work process of tunneling	Longer lead time for machine designing and manufacturing
Lower personnel expenditure	Specific profile (circular)
Better working conditions and safety	Limits on curve driving
Mechanization and automation of the drive	Detailed planning required
N/A	Limits of adaptation to highly variable ground conditions
N/A	Limits on adaptation to high water inflow
N/A	Limits on transportation system

Different types of TBM have been developed for variety ground conditions. The range of application of TBMs has expanded considerably in the past two decades (Maidl et al., 2008). A comprehensive tunneling machine classification and selection chart has been developed by the International Tunneling Association (ITA). For simplicity, it is possible to classify the TBMs into three classes according to Barla and Pelizza (2000). Figure 2-1 shows this classification with more information for each type provided at the following sections.

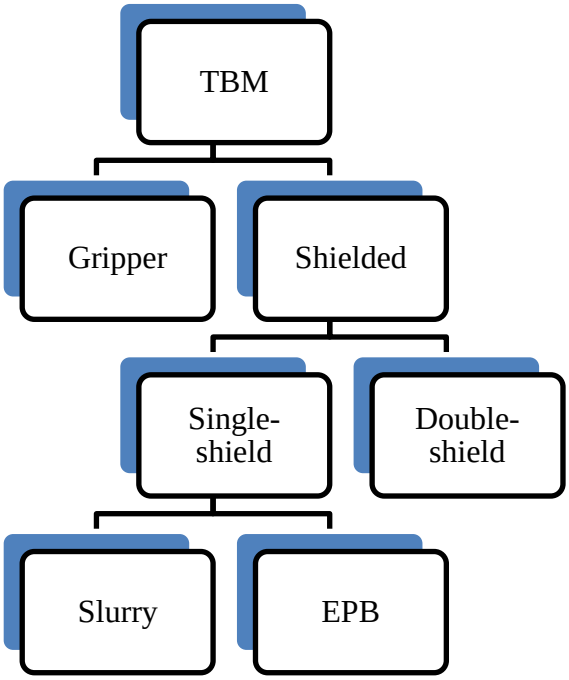

Figure 2-1 TBM Classification (Modified from Barla and Pelizza, 2000)

The cyclic process of a typical TBM tunnel boring and material handling can be shown in Figure 2-2.

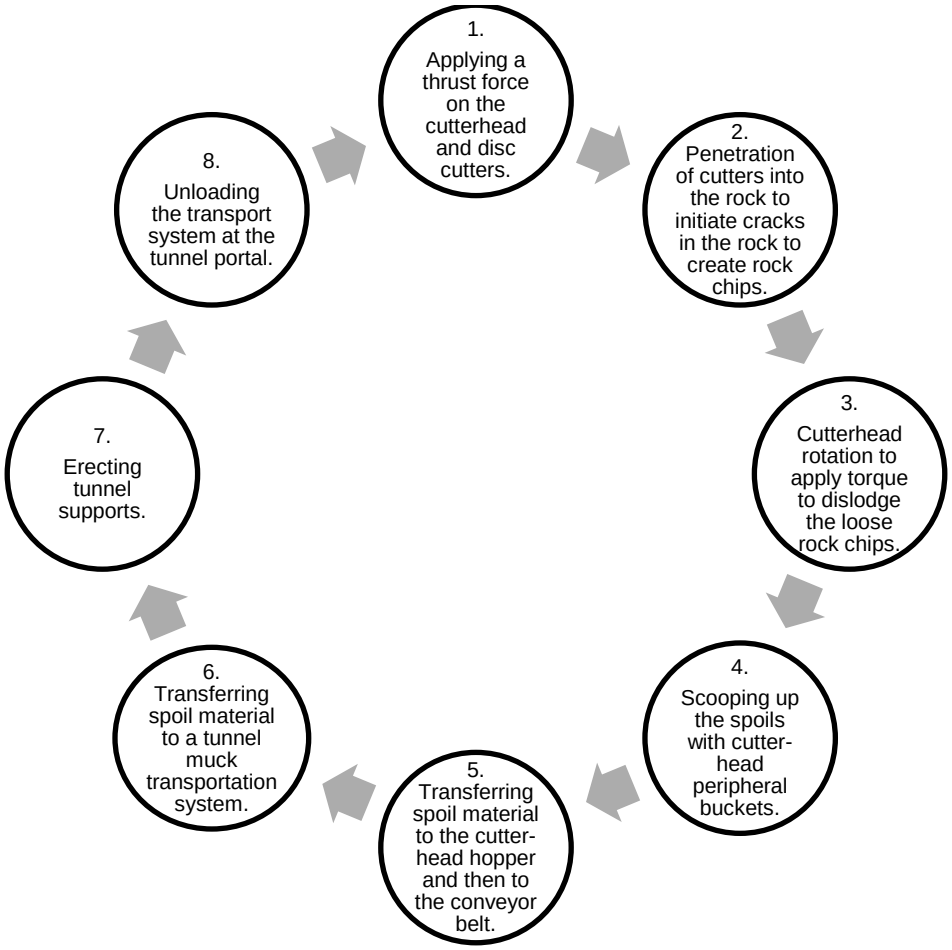

Figure 2-2 Cyclic Process of a Typical TBM Operation

Gripper TBM

Applicability

A gripper TBM is suitable for application in a rock mass in which a support of the excavated cross-section in the area of the temporary face and of the machine is not required or may be achieved with minor efforts, e. g., rock bolts, steel sets and shotcrete, applied locally at the roof of the tunnel. The boring system consists of the cutterhead, the cutting tools (discs), the cutterhead bearing and drive. The cutterhead is driven by hydraulic or electric motors and is mounted on the main beam.

The thrust, gripper and bracing system consist of the thrust cylinders, the gripper jacks, the gripper plates as well as the front leg and the rear leg. Figure 2-3 shows a TBM with the gripper shoe.

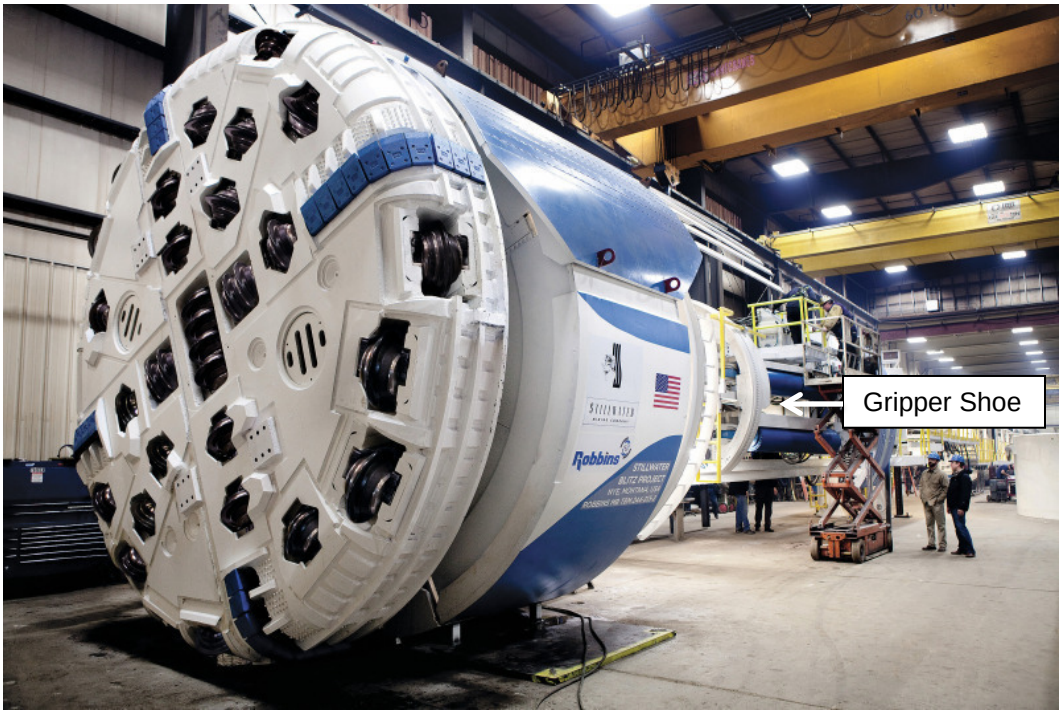

Figure 2-3 Gripper TBM (Tunnelingonline, 2017)

Operation

In Figure 2-4, the boring cycle of a gripper TBM is illustrated. The thrust cylinders, which are located between the gripper unit and the cutterhead, push the cutterhead against the temporary face while the machine is sliding on an invert shield or sliding shoe (Figure 2-4a). Pairs of gripper plates, which are pushed against the sidewalls via hydraulic jacks during the phase of advance, serve as an abutment for the thrust force and the cutterhead torque. During the phase of advance, the rear leg is lifted (Figure 2-

4a). At the end of the phase of advance, which is designated as stroke, the rear leg is extended and the grippers are retracted (Figure 2-4b).

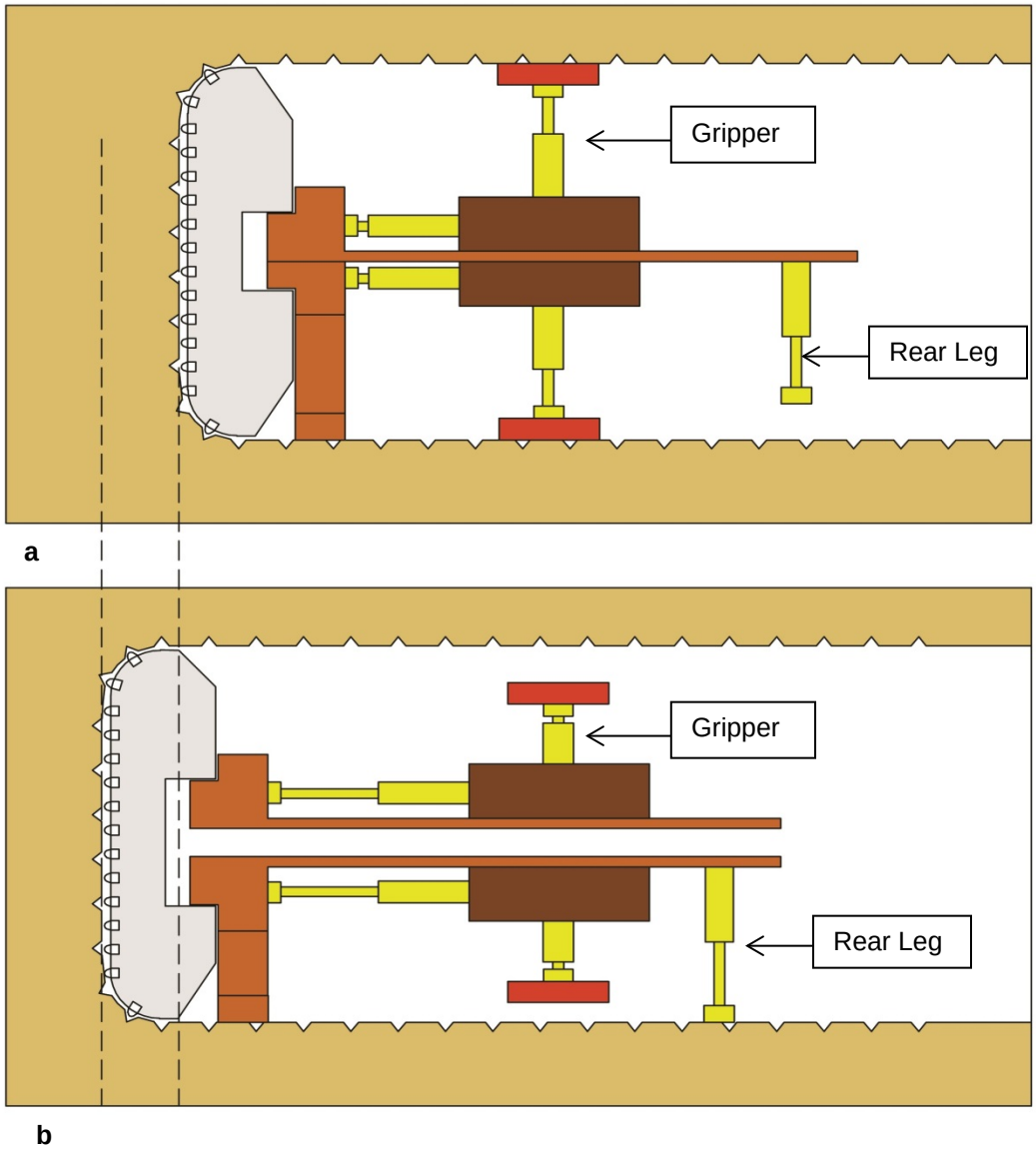

Figure 2-4 Boring cycle of a Gripper TBM

a) TBM advancing, gripper extended, rear leg retracted;

b) Repositioning of the gripper assembly, gripper retracted, rear leg extended

For repositioning of the gripper assembly for the next boring cycle, the thrust cylinders are also retracted and the gripper unit is sliding forward. Then, the rear leg is lifted and the new stroke begins.

The double gripper system consists of two bracing planes, the front and the rear gripper unit. The main beam, which is bearing the cutterhead and the drive, is supported by the exterior shell and movable in longitudinal direction. Machines with double gripper system are guided mainly by the gripper units, while in machines with single gripper system also the thrust cylinders are used for steering.

Gripper TBMs are mostly equipped with partial shields or hoods because also in stable rock conditions rockfall is to be expected locally. The partial shields or hoods serve as protection against falling rock and are often extended backwards by lamellae. Such a lamella roof, also denoted as finger shield, bridges the unsupported area between the shield and the area in which the support will be installed.

With the so-called partial or cutterhead shields with radially movable segments, a supporting pressure on the rock mass around the cutterhead can be applied (Maidl et al., 2001). Partial shields protect the cutterhead against falling rock and thus can avoid a blockade of the cutterhead. With lateral, radially movable bracing shields as well as with a vertically adjustable sliding shoe and invert shield, respectively, the position of the cutterhead can be fixed. A steel dust shield integrated in the cutterhead shield protects the working room from dust and small rock particles.

For the support of the excavation contour in the machine area of a gripper TBM, steel sets, steel meshes, rock bolts and shotcrete can be used. The steel sets and meshes are installed as a headgear normally immediately behind the cutterhead, using a ring erector and a wire mesh erector. With the drilling equipment, boreholes for rock bolts, exploration drillings and advancing support in form of injections can be carried out.

The support of the entire cross section will usually be completed in the backup area. The application of shotcrete in the machine area is extremely difficult due to problems regarding space, dust and rebound, and leads to a considerable reduction of the performance rates. Furthermore, the shotcrete would be damaged by the bracing forces induced by the gripper plates. Shotcrete in the machine area, therefore, is applied only over short tunnel sections, e.g., in the area of fault zones.

During the advance of a gripper TBM, the chips created by the rolling disk cutters at the temporary face are picked up by the buckets located at the periphery of the cutterhead and transported via hoppers onto a belt conveyor. In tunnel boring machines with large diameters and a center free bearing of the cutterhead, the belt conveyor can be arranged centrally. The conveyor belt is led through the main beam to a hand-over point. From there, the excavated material is transported via rail conveyance, dumpers or belt conveyors further through the tunnel.

Shielded TBM

Applicability

Shielded tunnel boring machines (Figure 2-5) are utilized, if the rock mass, because of its too low strength, is not able to carry the bracing forces of a gripper TBM, which are necessary to transmit the required thrust forces. A shielded TBM without facilities for a face support can also be applied, if the excavation contour is not stable and if rock collapse may occur. The shield skin, which covers the entire machine, serves as a temporary support. As final support, usually pre-cast lining segments of reinforced concrete are used. The lining segments are installed under the protection of the rear part of the shield, the so-called tail-skin. Unlike to a gripper TBM the completed segmental lining serves as an abutment for the thrust force (Figures 2-5 and 2-6).

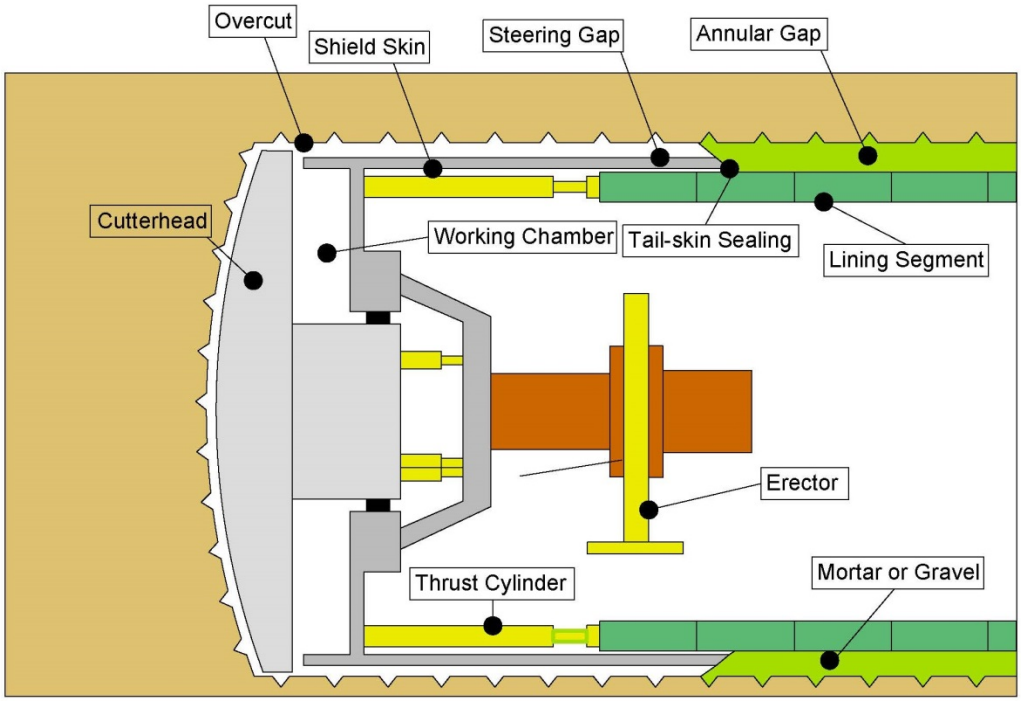

Figure 2-5 Shielded TBM

Operation

The cutterhead usually has a slightly larger diameter than the shield skin. This causes a so-called overcut to avoid that the shield gets stuck. The space between the shield skin and the excavation contour is referred to as steering gap (Figure 2-5). In unstable rock mass or soil the steering gap may be close.

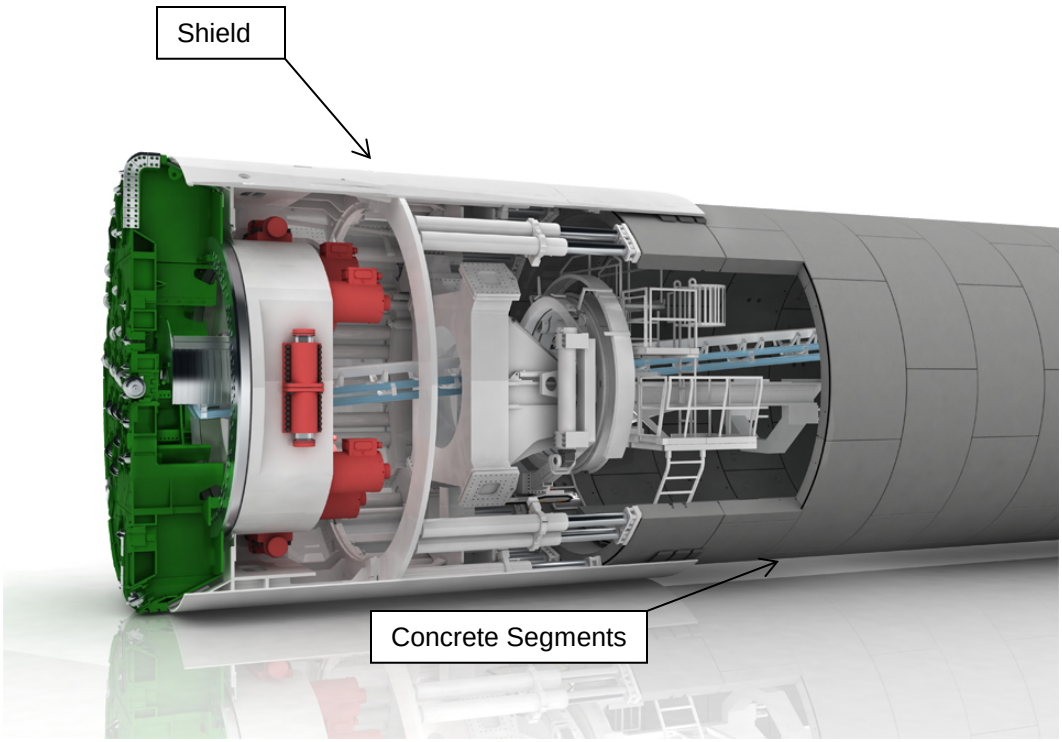

Figure 2-6 Single Shield TBM (Herrenknecht, 2017b)

The interface between the segmental lining and the excavation contour, the so-called annular gap, is normally grouted with mortar using injection lines which are integrated in the tail-skin (Figure 2-5). The mortar in the annular gap leads to a bedding of the segmental lining which is maintained to a large extent also after setting of the grout. A complete bedding of the segmental lining is necessary to keep the bending moments and deformations of the lining small. Sufficient bedding and a completely filled annular gap, respectively, is also required to carry the loads exerted by the thrust cylinders, particularly during driving of curves. For taking over the cutterhead torque, the shearing bond between the segmental lining and the rock mass is needed.

Between the shield skin and the segmental lining, a so-called tail-skin sealing is mounted to avoid leakage of the annular grout into the machine area (Figure 2-5).In

Figure 2-7, the boring cycle of a shielded TBM consisting of the phase of advance and of the installation of the segmental lining is illustrated. During boring, the thrust cylinders push the shield forward (Figure 2-7a).

After the end of the stroke, the boring is interrupted and the segments are installed (Figure 2-7b). During installation, the jack of the corresponding segment is retracted and, when the mounting is completed, extended against the segment installed. After the assembly of the last segment of the ring the new stroke begins.

Double-shield TBM

The double-shield TBM (Figure 2-8), also referred to as telescopic shield TBM, represents a combination of a gripper TBM and a shielded TBM. It is composed of a front shield with cutterhead, main bearing and drive as well as of a tail shield including grippers, gripper jacks, cutterhead jacks and shield jacks.

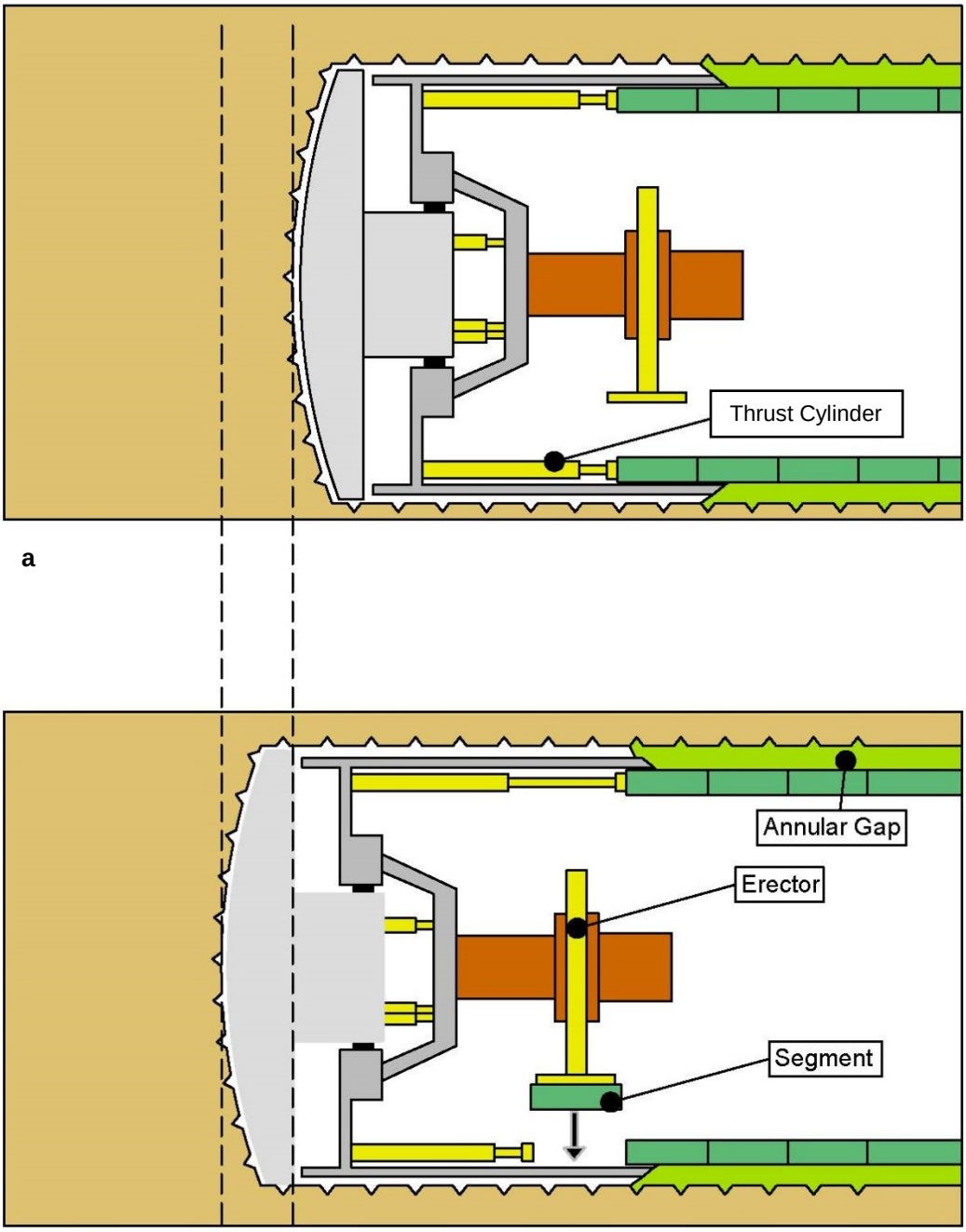

Figure 2-7 Boring Cycle of a Shielded TBM

a) TBM advancing;

b) Installation of segmental lining

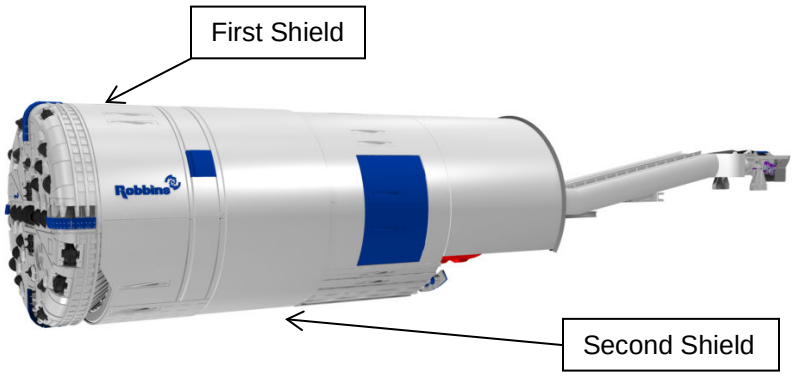

Figure 2-8 Double Shield TBM (Wpengine, 2017)

Operation

In Figure 2-9, the boring cycle of a double-shield TBM is illustrated. Compared with a shielded TBM, the double-shield TBM has the advantage that the segmental lining can be erected simultaneously with boring. During boring the tail shield serves as an abutment of the front shield with the cutterhead. The tail skin remains stationary, because it is supported by the gripper bracing. The cutterhead jacks, which are arranged between the front shield and the tail shield, are extended to push the cutterhead forward. The installation of the segmental lining is carried out in the same way as for a shielded TBM. After the stroke and the ring assembly are completed, the grippers are retracted and the tail shield is pushed forward by the shield jacks which are supported by the last installed segmental ring. Then, the new stroke begins.

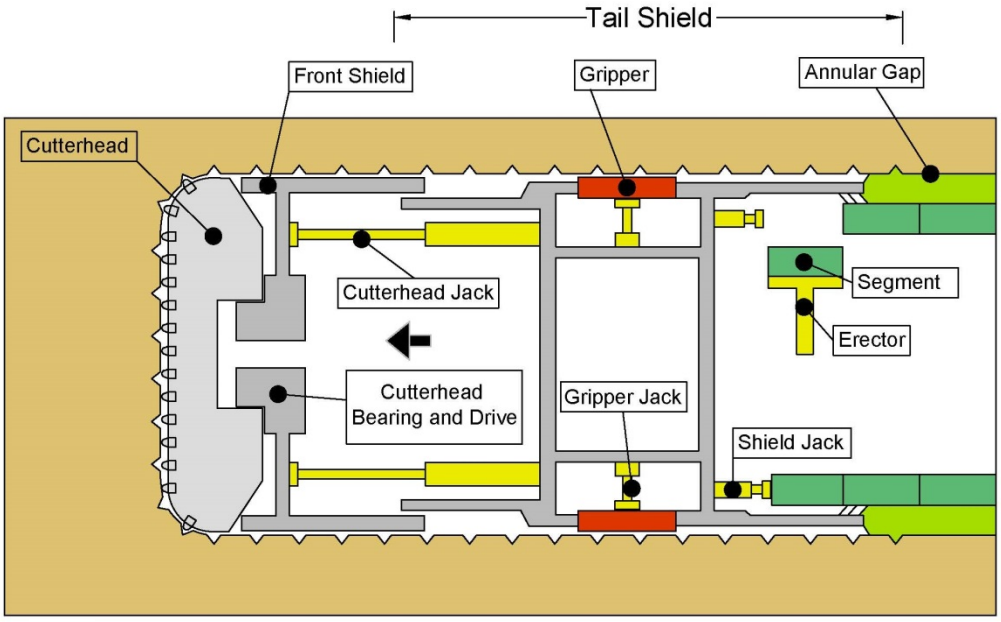

a

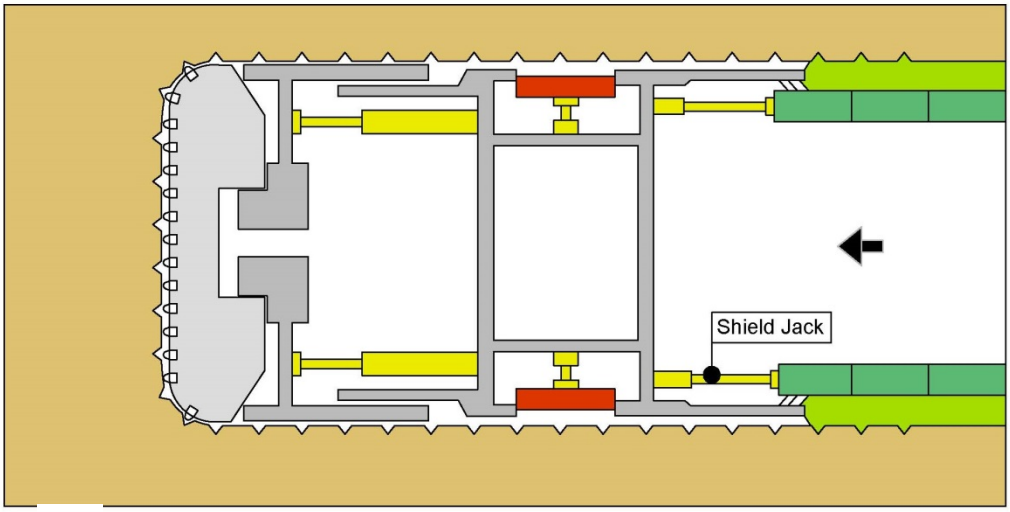

b

Figure 2-9 Boring Cycle of a Double-shield TBM

a) Stroke and installation of segmental lining, grippers extended;

b) Pushing forward of the tail shield, grippers retracted

Shielded TBM with Slurry Face Support

Applicability

As support medium of a shielded TBM with slurry face support (Figures 2-10, and 2-11), a mix of water with clay powder or bentonite and/or polymers, which is referred to as slurry, is used. The density or unit weight of the slurry can be adapted to the ground conditions within a certain range. Tunnel boring machines of this type are applied, if the ground surrounding the excavated cross-section and the temporary face must be supported or if in highly permeable ground the inflow of water is to be avoided. The extraction chamber also referred to as pressure chamber, which is located behind the cutterhead, is shut-off against the tunnel by a pressure wall (Figure 2-10). The supporting pressure has to balance at least the horizontal rock mass pressure and a potential water pressure (Figure 2-10).

With regard to the shield machines it is to be distinguished between slurry shields and hydro shields or mix shields, respectively. In a slurry shield, the supporting pressure is controlled directly by pumping the slurry in or out of the extraction chamber. In the case of a hydro or mix shield, the support pressure is regulated by a compressed air buffer which is located in the pressure chamber behind a submerged wall (Figure 2-10).

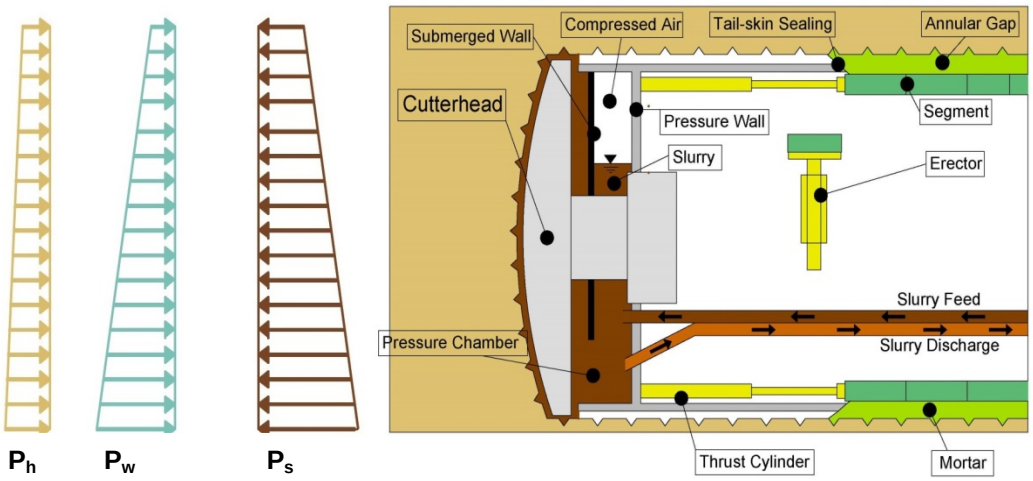

P_h: Horizontal ground pressure
P_w: Water pressure
P_s: Support pressure at the face

Figure 2-10 Shielded TBM with Slurry Face Support

Operation

The bentonite-soil mix is hydraulically transported via a slurry discharge pipe. The liquid and solid parts of the bentonite-soil mix are separated by a separator outside the tunnel. In case that access into the extraction chamber becomes necessary, e.g., for tool change, repair or removal of an obstacle, the slurry has to be partly or completely replaced by compressed air. With compressed air, drainage as well as a temporary face support can be achieved during the access into the extraction chamber. A lock in the roof area enables the access into the extraction chamber.

According to Krause (1987), the range of application of slurry shield machines in soil can be characterized by a band of grain size distributions including predominantly sands and fine gravels. In case of soils with higher cohesive fractions, there is the risk of

adhesion at the cutting wheel or in the extraction chamber. Furthermore, cohesive soils lead to an increased effort for separation of the bentonite-soil mix.

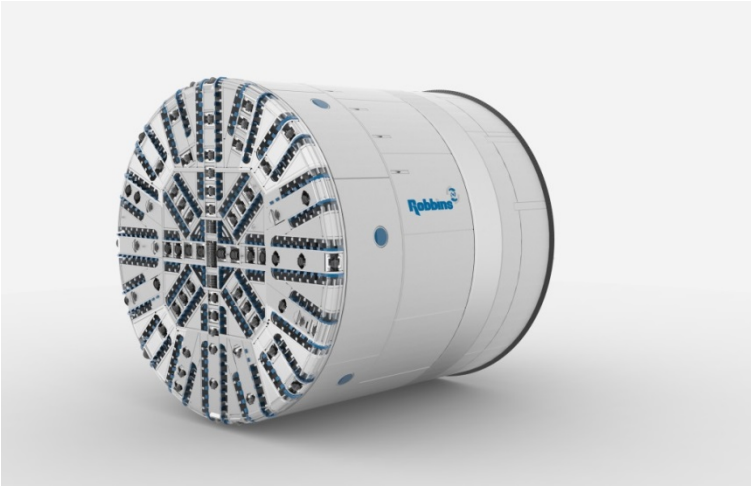

Figure 2-11 Slurry TBM (Robbins, 2017a)

Shielded TBM with Earth Pressure Balanced (EPB) Face

Applicability

The supporting pressure of a shielded TBM with earth pressure balanced face is obtained by the resistance of the excavated soil and rock respectively, which is transformed into an earth mud. The latter is formed with the excavation tools and the mixing tools at the temporary face and in the extraction chamber, potentially with the aid of liquid or foam conditioning agents. The heading with earth pressure balanced face is also referred to as EPB mode.

EPB machines are frequently utilized if tunnel sections have to be driven in both, soil and rock. They are also applied in formations with different and frequently changing ground conditions ("mixed-face-conditions") or in heavily weathered rock. Therefore, in addition to the cutter discs, drag picks are mounted as excavation tools at the cutterhead (Figure 2-12). With the latter, soil and rock with low strength can be excavated.

Figure 2-12 EPB TBM with Cutterdiscs and Drag Picks (Robbins, 2017b)

Operation

The extraction chamber is shutoff against the tunnel by a pressure wall similar to slurry machines (Figure 2-13). The supporting pressure has to balance at least the horizontal rock mass pressure and a potential water pressure P_w (Figure 2-13). The force at the pressure wall induced by the thrust cylinders is transferred to the earth mud and monitored by pressure gages which are mounted at the pressure wall.

The earth mud is conveyed by a screw conveyor (Figure 2-13). The supporting pressure is controlled by the TBM advance speed and the rate of revolutions of the screw conveyor.

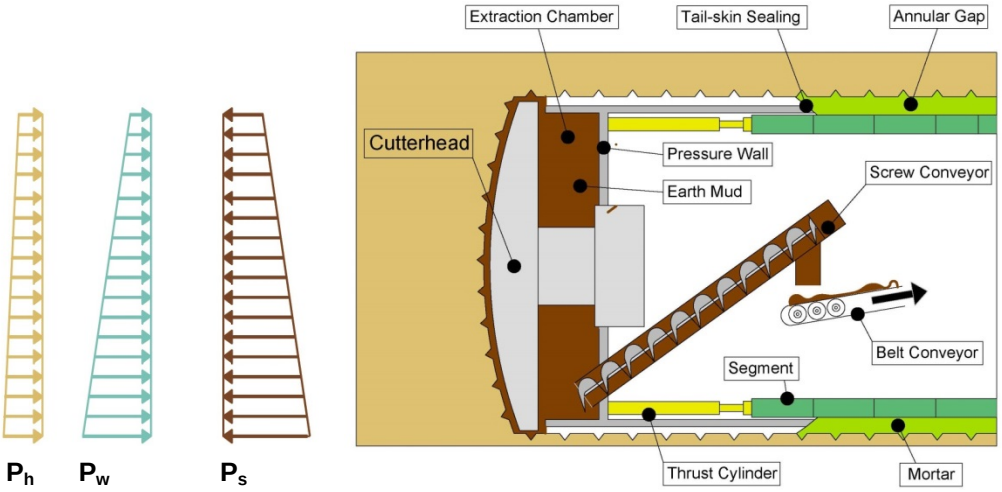

P_h: Horizontal ground pressure
P_w: Water pressure
P_s: Support pressure at the face

Figure 2-13 EPB TBM

For the transformation of the excavated chips into an earth mud, clay suspensions, polymer suspensions or solutions and foam agents, which are referred to as conditioning agents, can be added to the muck in the extraction chamber or already at the temporary face.

The requirements for the application of an EPB TBM in rock are as follows:

- The intact rock can be transformed into an earth mud, if necessary with the aid of conditioning agents,
- The high cutterhead torque, which is required for EPB headings, can be carried by skin friction and inclination of the thrust cylinders and,
- The (conditioned) excavated material can be ecologically deposited.

TBM with Convertible Mode

Applicability

TBMs with convertible mode, which allow for a change of driving mode during excavation, can be usefully utilized in varying ground and groundwater conditions. By machine modifications these types of TBM enable a better adjustment to the ground conditions encountered in the corresponding tunnel sections. In the past, a number of convertible shielded machines for tunneling in soil were developed, which allow for different combinations of modes, such as open mode, EPB mode, slurry mode or compressed air mode.

A convertible TBM normally is designed for the mode which is expected to occur predominantly. For the combination of two tunnel concepts, however, compromises are necessary, because the machine must be designed for both, the predominantly and the less frequently occurring mode. For each individual case it must be checked if based on the predicted ground conditions a frequent change of modes is to be expected. The inevitable technical compromises and the conversion times from one mode to another can lead to drastically reduced rates of performance and therefore are of great importance for an economical assessment.

CHAPTER SUMMARY

This chapter presented descriptions of various tunnel boring machines, which included the following types:

- Gripper TBM
- Shielded TBM
    - Single Shield TBM
    - Double Shield TBM
    - Slurry Face TBM
    - Earth Pressure Balanced Face TBM

The operation process of each TBM type is explained along with a schematic design of the operation. The process of a typical TBM tunnel boring and material handling can be summarized as follows:

1. Applying a thrust force on the cutter head and disc cutters.
2. Penetration of cutters into the rock to initiate cracks in the rock to create rock chips.
3. Cutterhead rotation to apply torque to dislodge the loose rock chips.
4. Scooping up the spoils with cutterhead peripheral buckets.
5. Transferring rock material to the cutter-head hopper and then to the conveyor belt.
6. Transferring rock material to a tunnel muck transportation system.
7. Erecting tunnel supports.
8. Unloading the transport system at the tunnel portal.

Chapter 3 LITERATURE REVIEW

INTRODUCTION

Chapter 2 provided a description of how different tunnel boring machines work. In this chapter a literature review on advance rate prediction of TBMs is presented. TBM advance rate (AR) is one of the key parameters required to calculate the time to complete a tunnel. As a definition, AR is the average rate of TBM progress in a specific period of time which is usually expressed in the unit of ft/day. This parameter is obtained directly as a product of Penetration Rate (PR which is sometimes referred to as rate of penetration or ROP) and utilization rate (UR) as shown in Eq. 1-1.

Robbins (1992) noted the geologically related conditions and tunnel diameter as the most important factors influencing AR. During the past few decades, many studies have been carried out to develop TBM performance prediction models, but the main focus of most of these studies has been on penetration rate (PR) prediction. The following sections illustrate the various works done by researchers on prediction of PR and AR.

PENETRATION RATE PREDICTION MODELS

Early Models

The development of PR prediction models started in 1973 by Tarkoy. Tarkoy (1973) presented a model for PR prediction of TBMs in specific ground conditions such as limestone, shale, sandstone, quartzite, orthoquartzite, schist, and dolomite using empirical information. As the first model in this field, it was a great start but the amount of data used was limited. Roxborough and Phillips (1975) presented a model for ground conditions with UCS of 10,000-29,000 psi, Tensile strength of 800-2,000 psi, and TBM diameter of 12-14 ft. The limitation of their model was the small range and size of TBM diameters and also the model did not account for soft ground conditions with UCS of less than 10,000 psi.

A model was presented for penetration per revolution (PRev) by Graham (1976). This model calculated the PRev using the UCS of ground conditions and the average normal force on cutter discs. The major drawback of this model was that the penetration per revolution was given with no model for calculation of TBM revolutions; therefore using this model for PR prediction was difficult as the users had to predict the TBM's RPM.

Ozdemir (1978) introduced a model based on the Robbins Company data in ground conditions such as granite, quartzite, schist, and shale. This model was based on limited studies and mostly focused on ground conditions with UCS above 17,000 psi. Farmer and Glossop (1980) developed a model for prediction of PRev based on the data collected from six TBM tunneling projects. This model used the tensile strength of the ground and the average normal force on cutter discs to predict the PRev. but like the Graham (1976) model, the means for predicting the RPM of TBM were not given.

In 1982, Cassinelli predicted the PR using new factor in calculations called Rock Structure Rating (RSR). RSR is a quantitative method for describing quality of a rock

mass for appropriate ground support. The model solely relied on RSR in a linear regression model to predict PR. Snowdon et al. (1982), introduced a formula through engineering calculations that demonstrated the relationship between the cutter disc average normal and rolling force, and the penetration per revolution of TBM.

Lislerud et al. (1983) provided their PR model based on excavation records in Norway in shale, limestone, gneiss, and basalt. The model relied on limited number of excavation records in soft ground conditions. Nelson et al. (1983) developed a PR model for tunnels in sedimentary rocks. Their model was based on the information of four tunnels and the specifics of their ground conditions were not given.

A model was introduced by Bamford (1984). The model used the data of tunneling in claystone from Thompson project and this fact limited its application for future project use, unless they were in the same ground condition and TBM size. Sanio (1985) investigated the effect of foliation on penetration rate. Foliation in geology refers to repetitive layering in metamorphic rocks. This layering weakens the rock and thus, causes ease of boring operation.

Hughes (1986) investigated TBMs in sandstone. His research was limited to penetration per revolution of up to 0.4 in./rev in sandstone, but did not consider other ground conditions. Another PR model was introduced by Howarth et al. (1986). This model was based on the excavation information in sandstone and marble which was done by a fixed and certain RPM. Also in 1986, Boyd presented a model for penetration rate that was based on cutterhead power, specific energy, and tunnel cross section area. This model used the cross section of tunnel directly in the model and no research was done for RPM or utilization rate of the TBM.

Sato et al. (1991) followed Sanio's (1985) work and used the same approach. The major difference about Sato et al. (1991) research with Sanio (1985) was that it

focused completely on TBMs with full face cutterhead. Further in 1991, Innaurato et al. (1991) presented an updated version of the method provided by Cassinelli (1982). This model used UCS and RSR to predict PR. The updated version was based on 112 homogeneous sections of tunneling, but unfortunately no information was provided on the number of bored tunnels.

Models With Multiple Parameters

In 1993, Rostami and Ozdemir developed the Colorado School of Mines (CSM) model. A specialized test was introduced with this model called Linear Cutting Machine (LCM) test. The model was based on the LCM test results and that was a limitation, since the test could only be done in the Colorado School of Mines laboratory.

Sundin and Wanstedt (1994) developed a very specific model for penetration rate with very specific boundaries. The model was not applicable outside these boundaries which limited its application. The model was developed for granite, micaschist, gneiss with UCS ranging from 9,500-29,000 psi, point load strength of 145-1,300 psi, Cerchar Abrasivity Index (CAI) of 1.9-5.9, and toughness of 2.2-3.3.

In 1997, Rostami updated the Colorado School of Mines (CSM) model using more LCM tests and proposed a function for PRev based on normal and rolling cutter disc forces. Bruland (1998) introduced the Norwegian University of Science and Technology (NTNU) model. This model predicted the penetration per revolution of TBM using three factors; equivalent cutter thrust (Mekv), critical cutter thrust (M1), and penetration coefficient (b). Laughton (1998), using probabilistic tools, introduced a model for PR. This research lacked significantly in having information from similar tunneling projects. Barton in 1999 developed a model for PR called Qtbm. This model had a new parameter called Barton rock mass quality rating for TBM driven tunnels (Q_{TBM}).

According to Barton (1999), the PR is 5 times Q_{TBM}. Also in 1999, Cheema modified the CSM model based on the information of one project.

In 2005, Ribacchi and Lembo Fazio introduced a new formula to calculate the specific penetration rate (SP) which is the inverse of field penetration index (FPI). This formula needed a specific variable called rock mass uniaxial compressive strength (UCS_{cm}) which was calculated using regular UCS and rock mass rating (RMR). Hassanpour et al. (2009) introduced a formula for field penetration index (FPI). The formula used a factor called rock mass cuttability index (RMCI) which a different formula was given for. These formulas were developed based on the information of only two projects. Khademi et al. (2010) also introduced a complex FPI formula using UCS, rock quality designation (RQD), and RMR joint condition partial rating (J_c). This formula was only based on the information from one project.

Computer-Aided Models

Alvarez (2000) developed a neuro-fuzzy model for PR. This is a neural network modeling system that combines the human-like style of fuzzy systems with the learning and connectionist structure of neural networks. The main strength of neuro-fuzzy system is that they are “universal approximations” with the ability to solicit interpretable IF-THEN rules. Yagiz (2002) used the information of one project to modify the CSM model. This model introduced new methods of calculation but the whole process was based on CSM model.

ADVANCE RATE PREDICTION MODELS

Advance rate prediction models can be categorized by their approach in predicting AR. These approaches are explained in the following sections.

Indirect Approach

This is a simple approach to AR prediction. In such models the geotechnical and TBM specifications are accounted for, but these models do not rely on a good database and their lack of updating limits their range of application. The best thing about such models is that they are easy to use and if they rely on a good database they can be very useful. Examples for indirect approach models are the CSM model, work done by Sharp and Ozdemir (1991), US Army (1997), ITA model (2000), Rostami et al. (1993 and 1997), and Bruland (1998).

Semi-Direct Approach

This approach is very similar to indirect approach. The major difference is that these models need to rely on a good database. However the downside is the fact that these models have many input parameters with complex relationships and often require uncommon tests. The work by Barton (1999, 2000, and 2011) is using a semi-direct approach. This model relies on a good database and introduces a new parameter that is needed by the model called the Barton rock mass quality rating (Q_{TBM}).

Probabilistic Approach

Such models truly help in making an informed decision and account for randomness and approximation for many parameters through case studies. The major problem with such models is their lack of formula and persistent need for a database. These models are not easy to use and without their database they are useless. Nelson et al. (1994a, 1994b, and 1999), Laughton et al. (1995), Abd Al Jalil (1998), and Laughton (1998), are amongst the researchers that developed probabilistic models.

Computer-Aided Approach

These models have a very complex underlying structure and they usually are not available in public domain. Like the probabilistic models, these models do not provide a formula and might be over-fitting their prediction. The best quality of such models is the fact that they need to rely on a very good comprehensive database which they do and these models account for the complex relationships between parameters. Only Alvarez (2000) developed a computer-aided model, and since such models do not provide a formula to use, they are not very popular and there has not been an interest by researcher to follow suit.

Direct Approach

Direct approach introduces the AR as a straight function of a parameter. Bieniawski et al. (2006) has developed a direct model. The developed model showed that the AR is a direct function of rock mass excavability (RME) as introduced by the authors. This model has a very limited database and in their formula does not consider one major parameter, namely the tunnel diameter.

Rock Mass Excavability (RME), is boreability predictor of a rock mass that a TBM is encountering. Bieniawski et al. (2006) proposed a classification for RME. Thuro and Plinninger (2003) were among other researchers who investigated RME in drilling and blasting and cutting by TBMs and road headers. There are five factors directly related to rock mass characteristics in RME model. The suggested ratings of the RME model are in agreement with Thuro and Plinninger (2003) study results. Initially RME was applied to the data from 14 miles of four tunnels bored with four TBMs in Spain. A number of statistical correlations have been established between RME and the Average Rate of Advance (ARA). In recently published works by Bieniawski et al. (2007a, 2008), three

main correction factors for the prediction of advance rate were introduced by considering the influences of the TBM crew, tunnel excavation length, and tunnel diameter. Some extensions were recently offered by Bieniawski et al. (2008) for other types of TBMs as well. The RME system was also utilized for cutter consumption prediction (Bieniawski et al., 2009). Khademi et al. (2009) offered a fuzzy logic model for application of the RME system. It should be noted that RME calculations are easier using classic ratings since RME authors have offered continuous rating charts.

CHAPTER SUMMARY

A review of the available literature indicated that many models are limited to TBMs operating in a relatively limited range of geologic settings. Simpler models were often preferred because of their ease of use, but they included only a few basic input parameters and could only offer a limited range of application. As such many of the parameters that influenced TBM performance in more variable ground conditions were unaccounted for in the modeling process. Probabilistic models offered a more complex methodology for estimating performance. These models should only be used when it could be demonstrated that the detailed information (e.g., probability distribution functions for various parameters) of a similar tunnel is available to support the prediction of TBM performance on a new project. These models used performance data collected from similar case histories. If there were significant differences in ground conditions or technology choices between the new drive and case histories within the database, substantial errors were likely to be introduced in the estimates when using these models. Another potential problem, which was also common for computer-aided models is that in practice these models were rarely used for TBM performance prediction purposes, even though they offered several advantages over the other methods (e.g., having a higher

correlation coefficient and taking complex formula structures wherever needed). This was due to the lack of transparency of the process.

Chapter 4 SOIL/ROCK CLASSIFICATION AND DATA ANALYSIS

INTRODUCTION

Chapter 3 provided a literature review on different methods of estimating penetration rate (PR) and advance rate (AR). The PR itself in Eq. 1-1 can be divided into two major components as shown in Eq. 4-1:

$$PR = PRev.RPM \quad \text{(Eq. 4-1)}$$

Where PRev is penetration per revolution and RPM is revolutions per minute of the machine. In this chapter, using the historical information, different regression models will be obtained to explain the three main factors (PRev, RPM, and UR) influencing the AR. Also a soil and rock classification will be provided to be used in development of performance charts.

THE UNIAXIAL COMPRESSIVE STRENGTH (UCS)

As said previously, in rock mechanics and engineering geology, the boundary between rock and soil is defined in terms of the uniaxial compressive strength and not in terms of structure, texture or weathering (ISRM, 1978). Several classifications of the compressive strength of rocks are presented. A material with the strength ≤ 36.25 psi is considered as soil; refer to ISRM (1978). The uniaxial compressive strength can be determined directly by uniaxial compressive strength tests in the laboratory, or indirectly from point-load strength test. The uniaxial compressive strength of the rock constitutes the highest strength limit of the actual rock mass.

ISRM (1980) recommended that the uniaxial compressive strength of the rock material in an area is given as the mean strength of rock samples taken away from faults, joints and other discontinuities where the rock may be more weathered. When the rock material is markedly anisotropic in its strength, the value used should correspond to the

direction along which the smallest mean strength was found. However, in such cases it is usually of importance to record the uniaxial compressive strength also in other directions. Many compressive strength tests are made on dry specimens. ISRM (1980) suggested that the samples should be tested at water content pertinent to the application.

The uniaxial compressive test is time-consuming and is also restricted to those relatively hard, unbroken rocks that can be machined into regular specimens. Although the strength classification is based on laboratory tests, it can be approximated by simple methods. An experienced person can make a rough five-fold classification of rock strength with a hammer or pick. Deere and Miller (1966) have shown that rock strength can be estimated with a Scmidt hammer and a specific gravity test with enough reliability to make an adequate strength characterization. According to Patching and Coates (1968) the rock strength can be quickly and cheaply estimated in the field, and more precision can be attained, if required, by laboratory tests. Also from a fully description of a rock including composition and possible anisotropy and weathering it may in many instances be possible to estimate its strength.

COMPRESSIVE STRENGTH ASSESSED FROM FIELD TESTS

Sometimes, particularly at an early stage in the description of the rock mass, strength may be assessed without testing (ISRM, 1980). Such a first estimate of the uniaxial compressive strength (UCS) may be made by visual and sensory description of hardness of rock or consistency of a soil (Piteau, 1970; Herget, 1982). The strength can be judged from simple hardness tests in the field with geological pick by observing the resistance, as shown in Table 4-1.

The clays in grade S1 - S6 can be silty clays and combinations of silts and clays with sands, generally slow draining. The hammer test should be made with a geologist's

hammer on pieces about 4 inches thick placed on a hard surface, and tests with the hand should be made on pieces about 1.5 inches thick. The pieces must not have incipient fractures, and therefore several should be tested. For anisotropic rocks tests should be carried out in different directions to the structure. The lowest representative values should be applied.

Table 4-1 Simple Field Identification

Compressive Strength of Rock and Clay (ISRM, 1978)

Grade	Term	Field Identification	Approx. UCS (psi)
S1	Very soft clay	Easily penetrated several inches by fist.	< 3.62
S2	Soft clay	Easily penetrated several inches by thumb.	3.62 – 7.25
S3	Firm clay	Can be penetrated several inches by thumb with moderate effort.	7.25 – 14.5
S4	Stiff clay	Readily intended by thumb, but penetrated only with great effort.	14.5 – 36.25
S5	Very stiff clay	Readily intended by thumbnail.	36.25 – 72.5
S6	Hard clay	Intended with difficulty by thumbnail.	> 72.5
R0	Extremely weak rock	Intended by thumbnail.	36.25 - 145
R1	Very weak rock	Crumbles under firm blows with point of geological hammer; can be peeled by a pocket knife.	145 - 725
R2	Weak rock	Can be peeled by a pocket knife with difficulty, shallow identifications made by firm blow with point of geological hammer.	725 - 3625
R3	Medium strong rock	Cannot be scraped or peeled with a pocket knife; specimen can be fractured with single firm blow of geological hammer.	3625 - 7250
R4	Strong rock	Specimen requires more than one blow of geological hammer to fracture it.	7250 - 14500
R5	Very strong rock	Specimen requires many blows of geological hammer to fracture it.	14500 - 36250
R6	Extremely strong rock	Specimen can only be chipped with geological hammer	> 36250

A common and functional tunneling classification of soft ground was provided by Terzaghi. This classification called “Tunnelman’s Ground Classification,” is essentially based upon standup time of the ground. A modified version of the Terzaghi soft ground classification is presented in Table 4-2 (Iseley et al., 1999).

STRENGTH ASSESSMENT FROM ROCK NAME

The rock types often give relative indications of their inherent properties (Piteau, 1970; Patching and Coates, 1968). For many rocks, however, the correlation between the petrographic names of rocks and their mechanical properties may be poor, caused by difference in composition, grain size, porosity, cementation, anisotropy within each type. Nevertheless, a great deal of associated information about a rock can be inferred from its geological name, such as whether it may be homogeneous, layered, schistose or irregular (Hansen, 1988).

Table 4-2 Tunnelman's Ground Classification (Iseley et al., 1999)

Classification		Behavior	Typical Soil Type
Firm		Heading can be advanced without initial support, and final lining can be constructed before ground starts to move.	Loess above watertable; hard clay, marl, cemented sand and gravel when not highly overstressed.
Raveling	**Slow Raveling**	Chunks or flakes of material begin to drop out of the arch or walls sometimes after the ground has been exposed, due to loosening.	Residual soils or sand with small amounts of binder may be fast raveling below the watertable, slow raveling above. Stiff fissured clay may be slow or fast raveling depending upon degree of overstress.
	Fast Raveling	In fast raveling ground, the process starts within a few minutes, otherwise the ground is raveling.	
Squeezing		Ground squeezes or extrude plastically into tunnel, without visible fracturing or loss of continuity, and without perceptible increase in water content. Ductile, plastic yield and flow due to overstress.	Ground with low frictional strength. Rate of squeeze depends on degree of overstress. Occurs at shallow to medium depth in clay at very soft to medium consistency.
Running	**Cohesive Running**	Granular materials without cohesion are unstable at a slope greater than their angle of repose. When exposed at steeper slopes they run like granulated sugar or dune sand until the slope flattens to the angle of repose.	Clean, dry granular materials, apparent cohesion in moist sand, or weak cementation in any granular soil, may allow the material to stand for a brief period of raveling before it breaks down and runs. Such behavior is cohesive running.
	Running		
Flowing		A mixture of soil and water flows into the tunnel like a viscous fluid. The material can enter the tunnel from the invert as well as from the face, crown, and walls, and can flow for great distance, completely filling the tunnel in some cases.	Below the watertable in silt, sand, or gravel without enough clay content to give significant cohesion and plasticity. May also occur in highly sensitive clay when such material is disturbed.
Swelling		Ground absorbs water, increases in volume, and expands slowly into the tunnel.	Highly pre-consolidated clay with plasticity index in excess of about 30, generally containing significant percentages of montmorillonite.

Table 4-3 Normal Range of Compressive Strength of Some Common Rock Types

(Modified from Hansen, 1988 and Hoek and Brown, 1980)

Rock Name	Uniaxial Compressive Strength UCS psi			**Rock Name**	Uniaxial Compressive Strength UCS psi		
	Low	Ave.	High		Low	Ave.	High
Sedimentary Rocks				**Metamorphic Rocks**			
Anhydrite		17,405		Amphibolite	10,878	18,130	36,260
Coal	2,321	3,046	3,771	Amphibolitic gneiss	13,779	23,206	33,359
Claystone	290	725	1,450	Augen gneiss	13,779	23,206	33,359
Conglomerate	10,153	12,328	14,500	Black shale	5,076	10,153	15,229
Coral chalk	435	1,450	2,611	Garnet mica schist	10,878	15,229	18,855
Dolomite	8,702	14,500	43,500	Granite gneiss	11,603	17,405	22,481
Limestone	7,250	14,500	26,107	Granulite	11,603	21,756	40,611
Mudstone	6,527	13,779	21,031	Gneiss	11,603	18,855	26,832
Shale	5,222	13,779	24,947	Gneiss granite	9,428	15,229	20,306
Sandstone	10,878	17,405	23,206	Greenschist	9,428	10,878	12,328
Siltstone	1,450	11,603	26,107	Greenstone	17,405	24,656	40,611
Tuff	435	3,626	21,756	Greywacke	14,500	17,405	21,031
Igneous Rocks							
Andesite	10,878	20,306	43,500	Marble	8,702	18,855	33,359
Anorthosite	5,802	18,130	30,458	Mica gneiss	7,977	11,603	14,500
Basalt	14,500	23,931	51,488	Mica quartzite	6,527	12,328	18,130
Diabase (dolerite)	32,924	40,611	46,267	Mica schist	2,901	11,603	24,656
Diorite	14,500	20,306	27,557	Mylonite	9,428	13,054	17,405
Gabbro	27,557	34,809	41,336	Phyllite	3,046	7,250	11,603
Granite	13,779	23,206	33,359	Quartz sandstone	10,153	17,405	25,382
Granodiorite	10,879	15,229	19,580	Quartzite	10,878	21,031	35,534
Monzonite	12,328	21,031	33,359	Quartzitic phyllite	6,527	14,500	22,481
Nepheline syenite	18,130	23,931	29,000	Serpentinite	9,428	19,580	29,000
Norite	42,061	43,221	47,282	Slate	17,405	27,557	43,500
Pegmatite	5,657	7,250	8,992	Talc schist	6,527	9,428	13,054
Rhyolite		12,328					
Syenite	10,878	21,756	33,359				
Ultra basic rock	11,603	23,206	52,214				

Soil materials:
Very soft clay = 3.62 psi Soft clay = 3.62-7.25 psi Firm clay = 7.25-14.5 psi
Stiff clay = 14.5-36.25 psi Very stiff clay = 36.25-72.5 psi Hard clay > 72.5 psi
Silt, sand: assume = 0.014-0.145 psi

DATA ANALYSIS

The database used in this dissertation was extracted from Farrokh (2013) and is provided in Appendix B. This database consisted of two separate databases that were compiled from the review of various technical sources. This database has been assembled with the objective of developing a new performance model with data from more than 300 projects from around the world as described in the following sections. The information in this database reflects average values for each parameter over the total length of the tunnels.

Tunnel Location and Application

Figure 4-1 shows the tunnel application counts in Farrokh (2013) database and their locations.

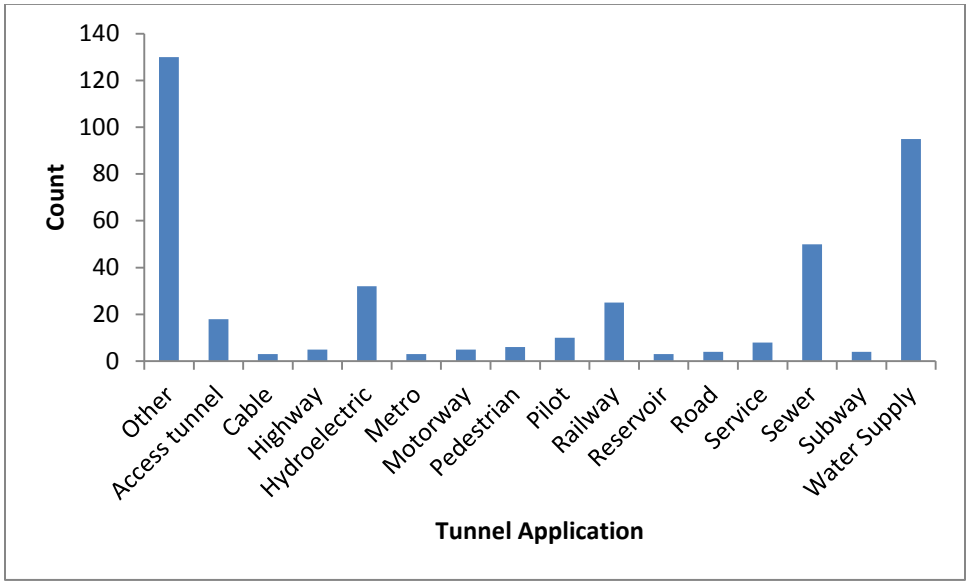

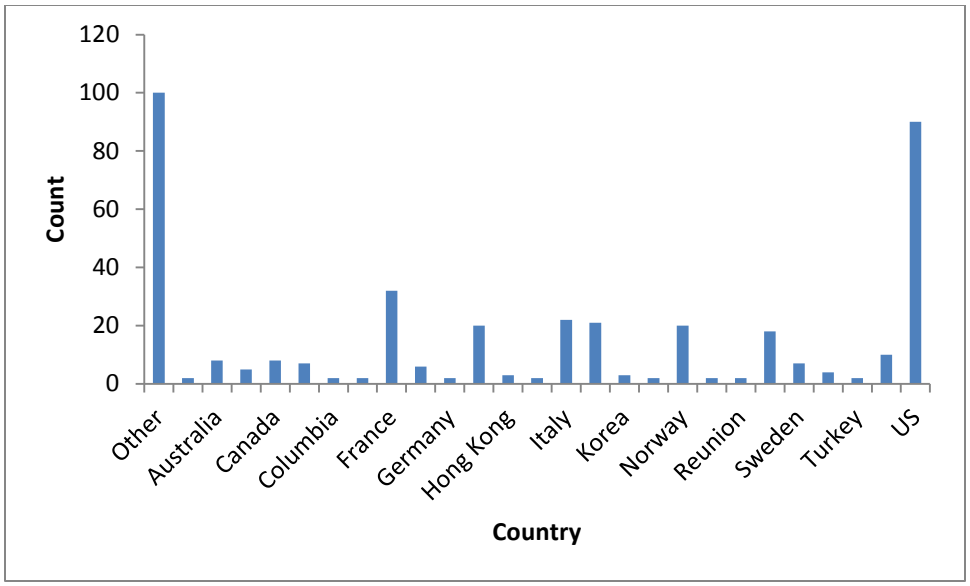

Figure 4-1 Histograms for Tunnel Applications and Locations (Farrokh, 2013)

Tunnel Diameter

Figure 4-2 shows a histogram plot of the diameter of TBMs in the data base. As can be seen, a range of 10-22 ft dominates the available cases in the database which reflects the common application range of TBMs.

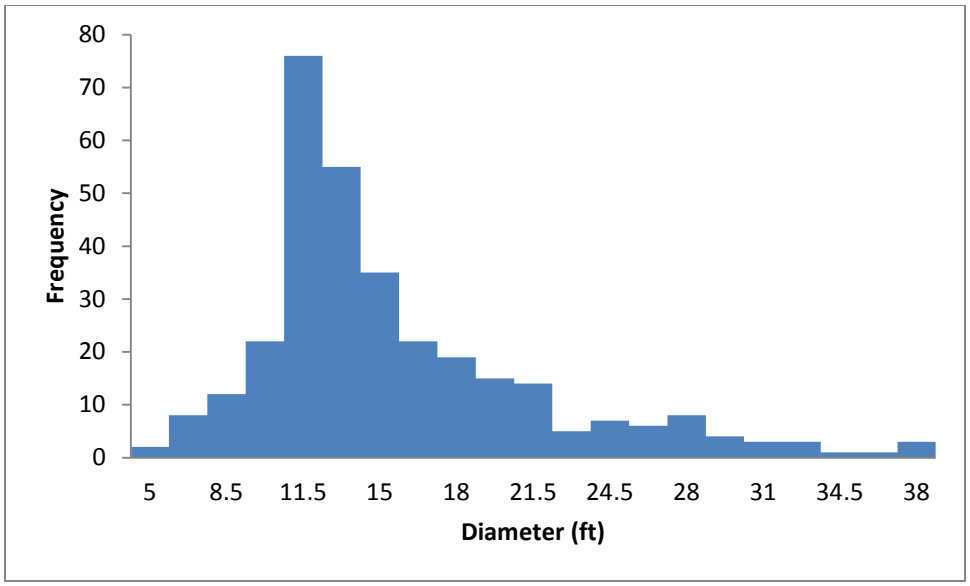

Figure 4-2 Histogram for Tunnel Diameter (Farrokh, 2013)

Uniaxial Compressive Strength

Uniaxial compressive strength (UCS) is a commonly-used representative of ground strength in almost all of TBM tunnel projects (Farrokh, 2013). Figure 4-3 shows the histogram for different ground UCS encountered in the database.

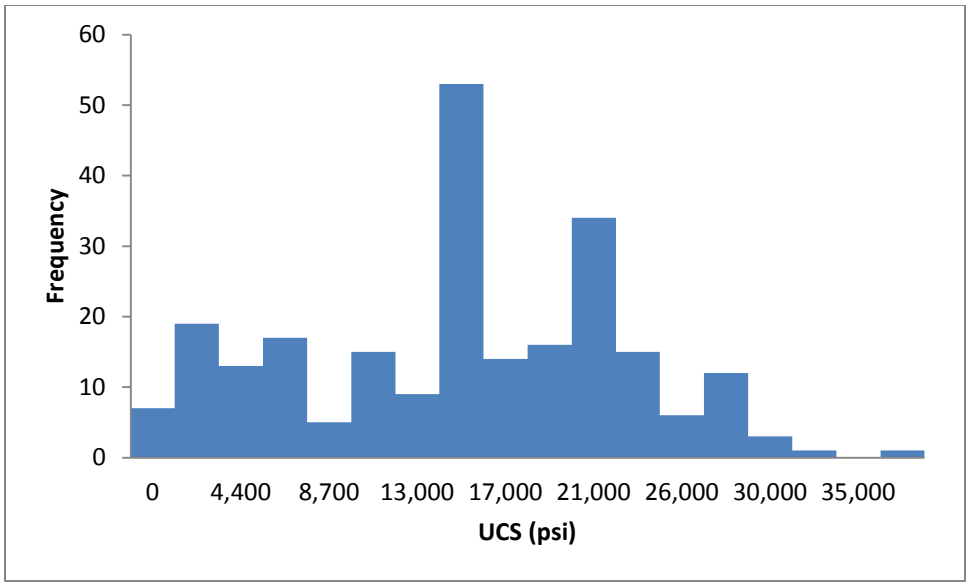

Figure 4-3 Histogram for Different Ground UCS (Farrokh, 2013)

In this dissertation, a series of different regression models are obtained to achieve the highest adjusted R^2. The reason for using adjusted R^2 over regular R^2, as the primary deciding factor, is that adjusted R^2 value takes the complexity of the fitted line in consideration as well. The goal in obtaining a suitable regression model is to explain as many data sets as possible while trying to keep the model simple and prevent over-fitting. Different regression lines have been fitted to each data set trying to achieve the best results. These regression lines include Exponential, Linear, Logarithmic, Polynomial Order-2, Polynomial Order-3, and Power Law.

EVALUATION OF PENETRATION PER REVOLUTION, PRev

PRev is the amount of penetration the TBM can achieve per one revolution of its cutter head. PRev has an inverse relationship with field penetration index (FPI) as shown in Eq. 4-2:

PRev = Fn/FPI (Eq. 4-2)

Where Fn stands for the average normal force on cutter discs of TBM. Consider the model introduced by Khademi et al. (2010), the bivariate analysis shows that UCS by itself accounted for 70% of the variation of the FPI (Farrokh, 2013) and, therefore PRev. Adding three more parameters led to only a marginal increase in R^2 from 0.7 to 0.77. This means that the effects of the additional parameters were largely overshadowed by UCS. PRev is at a maximum at higher UCS levels. This is a logical trend and is in agreement with several research studies such as those reported by Laughton (1998), Robbins (1992), Hassanpour et al. (2009), and Khademi et al. (2010). In simpler terms, it can be concluded that a major factor affecting the PRev is the ground condition of the project. The higher the UCS, the lower the PRev. Figure 4-4 shows the chosen regression model for database.

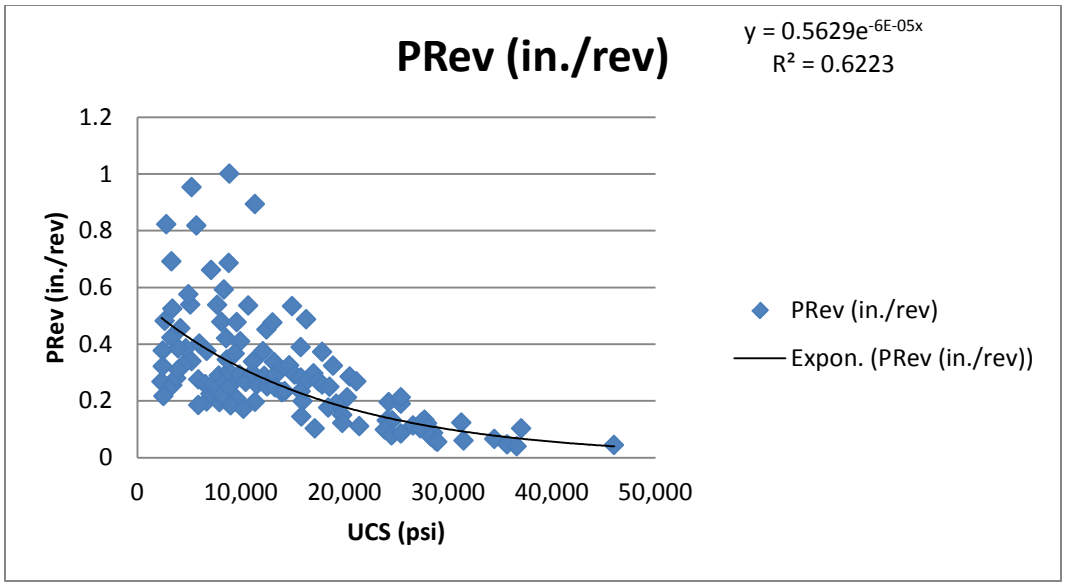

SUMMARY OUTPUT

Regression Statistics	
Multiple R	0.78886862
R Square	0.622313699
Adjusted R Square	0.619112968
Standard Error	0.417570915
Observations	120

ANOVA

	df	*SS*	*MS*	*F*	*Significance F*
Regression	1	33.90163304	33.90163304	194.4285944	1.03908E-26
Residual	118	20.57512534	0.174365469		
Total	119	54.47675838			

	Coefficients	*Standard Error*	*t Stat*	*P-value*
Intercept	-0.57462719	0.070567619	-8.142930112	4.51726E-13
UCS	-5.75363E-05	4.12631E-06	-13.94376543	1.03908E-26

Figure 4-4 Exponential Regression Analysis of UCS vs. PRev

Figure 4-4 showed the exponential regression model on the data set with the highest adjusted R^2 value of 62% amongst all attempted regression models (see Appendix A), therefore this regression model is chosen to be used in the making of TBM performance charts in chapter 5.

EVALUATION OF MACHINE REVOLUTION PER MINUTE, RPM

Larger diameter machines have lower RPMs. This fact was obvious in our RPM vs. diameter data base as shown in Figure 4-5. It needs to be mentioned that in the RPM data set, we have different RPMs for the same size of TBM. The reason for that is the fact that the manufacturer of the TBM will give the highest possible RPM of the machine to their customer, but in reality the applicable cutterhead speed or RPM, would differ based on the project. The RPM data set includes the actual TBM RPMs that were used for various projects. Therefore for the same size, although they are both capable of doing the same RPM freely, we have different field RPMs which were recorded from the projects.

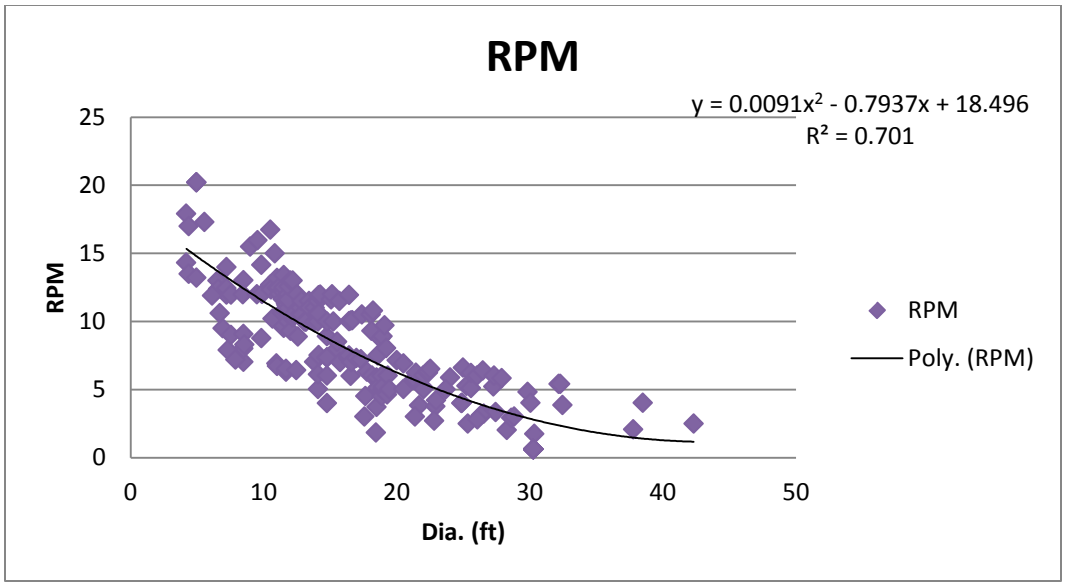

SUMMARY OUTPUT

Regression Statistics	
Multiple R	0.837260543
R Square	0.701005217
Adjusted R Square	0.697938603
Standard Error	2.270075795
Observations	198

ANOVA

	df	*SS*	*MS*	*F*	*Significance F*
Regression	2	2355.987412	1177.993706	228.5926457	7.53706E-52
Residual	195	1004.882602	5.153244114		
Total	197	3360.870014			

	Coefficients	*Standard Error*	*t Stat*	*P-value*
Intercept	18.49613874	0.813529855	22.73566069	9.81647E-57
Dia.	-0.793678354	0.090758992	-8.744900446	1.03754E-15
Dia. Square	0.009080448	0.00226061	4.016813546	8.41577E-05

Figure 4-5 Polynomial Order-2 Regression Analysis of RPM vs. Dia.

Figure 4-5 showed the Polynomial Order-2 regression analysis with the adjusted R^2 value of 70%. Increasing the degree of the fitted line to Polynomial Order-3 (Figure A-9) will not make a difference in the adjusted R^2 value. Also the linear regression (Figure A-7) has an adjusted R^2 value of 67% and the fitted line formula is much simpler, but this regression yields negative values for the upper boundary of the data set, therefore it is rejected. The chosen regression fitted line for use in performance charts in Chapter 5, is Polynomial Order-2 regression (Figure 4-5).

EVALUATION OF MACHINE UTILIZATION RATE, UR

The utilization rate, by definition, is the time that the cutterhead works, divided by the total time of one cycle. There are many different factors affecting the UR of a TBM tunneling operation. The affecting factors differ based on the approach that the researcher is taking to obtain the UR. There are two major approached to UR: Direct and Indirect approach.

Direct Approach

In the direct approach to estimate the utilization rate of TBM, the main focus is on the boring operation. As per the definition of UR, the boring time in a cycle divided by the total time of the cycle yields the UR. The boring cycle of a TBM mainly consists of two activities: boring and erecting support. It should be noted that the boring cycle of TBM should not be confused as the whole tunneling project cycle which includes the back-up system of TBM. When the whole tunneling cycle is considered, the back-up system and the activities outside the boring cycle come into play. But in the direct approach to find the influencing factors to UR, only the boring cycle of the TBM is considered and it is assumed that the back-up system will do its job completely.

Indirect Approach

Indirect approach looks at the whole tunneling cycle and instead of looking at the factors that directly influence the UR, pays more attention to the down-times of the whole system. Therefore in order to find the boring time, the down times are deducted from the total time of the operation. A very thorough study of the down times was conducted by Farrokh (2013). Also a very complex model was created by Farrokh (2013) to estimate the UR of an operation. This model was extremely accurate based on the case studies it was tested on (almost 99% accuracy). But the down fall of such model was the fact that it was not given for easy use by the author as it used proprietary software to do the estimation. In the indirect approach many factors such as the operation experience of the crew affect the down-times of TBM and therefore it's UR.

Influencing Factors

In this dissertation, the direct approach has been opted and by looking at the cycle of TBM, it is evident that the major factors influencing the boring time of the machine would be the ground conditions and the size of TBM. Obviously as the ground gets stronger (higher UCS), the penetration per revolution decreases, which in turn, means that it will take a longer time to bore the ground. Also the size of the machine could impact the boring process as the larger diameter TBMs have lower cutterhead speeds as shown previously in Figure 4-5. The following sections will evaluate the effect of TBM diameter and ground conditions on UR.

Correlation Between UR and Diameter

TBMs with larger diameter have lower cutterhead speeds. A series of regression analyzes was made on UR vs. TBM diameter to determine what the correlation between

these two parameters is. Figures A-11 through A-16 in Appendix A, show these regressions. Various attempts are made to fit a regression line on the UR vs. Diameter data set, and the highest adjusted R^2 value came to be 1%. It can be concluded that a correlation between these two parameters is non-existent since no regression can be fitted to the data set to explain the relationship.

Correlation Between UCS and UR

Increase in boring time results in having higher utilization percentage. Figures 4-6 and A-17 through A-21 in Appendix A show the regression analyzes to determine the best fitted line to the UR vs. UCS data set. Figure A-20 in Appendix A shows the Polynomial Order-3 regression which has the highest adjusted R^2 of 72%. Although this fitted regression line is achieving the highest adjusted R^2 of all the regression analyzes, its formula is quite complex and the scatter diagram of the data set does not indicate a need for such degree of formula (lack of existence of two opposite curves to indicate a need for Polynomial Order-3). The use of such regression might cause over-fitting of data.

The second highest adjusted R^2 belongs to Polynomial Order-2 regression (Figure A-19) with the value of 66%. This adjusted R^2 is only slightly higher (2% higher) than the linear regression (Figure 4-6, adjusted R^2 of 64%); therefore it is not logical to increase the complexity of the fitted line formula to achieve 2 more percent in adjusted R^2 value. The Linear regression (Figure 4-6) is chosen to be used in the production of performance charts in Chapter 5.

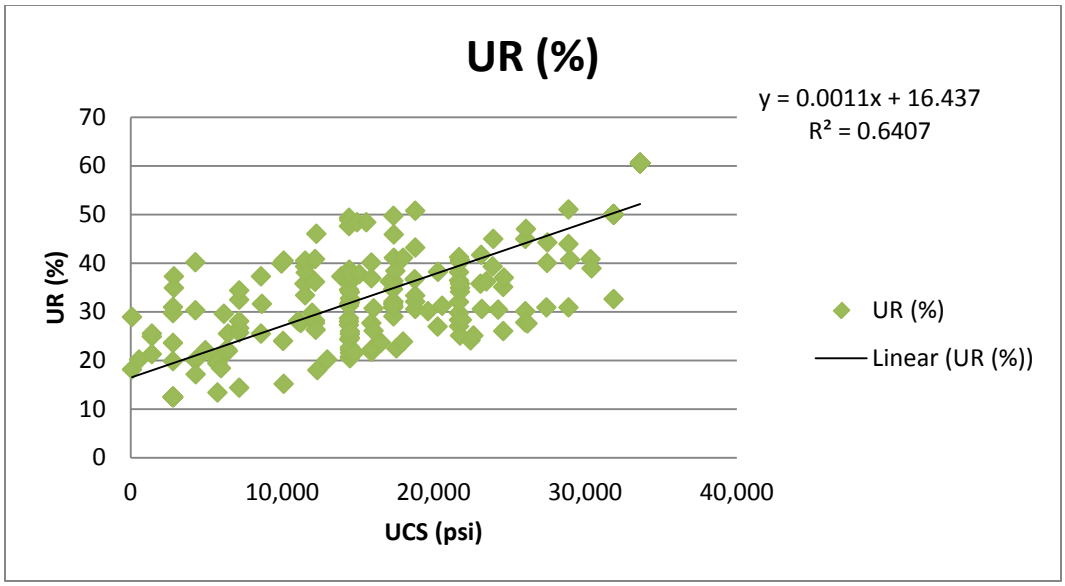

SUMMARY OUTPUT

Regression Statistics	
Multiple R	0.800431514
R Square	0.640690609
Adjusted R Square	0.63902714
Standard Error	8.137861649
Observations	218

ANOVA

	df	*SS*	*MS*	*F*	*Significance F*
Regression	1	25506.69247	25506.69247	385.1532275	6.61274E-50
Residual	216	14304.55512	66.22479223		
Total	217	39811.24759			

	Coefficients	*Standard Error*	*t Stat*	*P-value*
Intercept	16.43683178	1.13346357	14.50142043	9.96204E-34
UCS	0.001061432	5.40848E-05	19.62532108	6.61274E-50

Figure 4-6 Linear Regression Analysis of UR vs. UCS

CHAPTER SUMMARY

In this chapter different ways of identifying ground conditions for tunneling projects were introduced. The two main approaches were estimating the uniaxial compressive strength of soil and rock by field identification and rock names. Also this chapter presented the statistical analysis of various data sets for different parameters involved in advance rate formula.

For each data set, different regression analyzes were conducted. The major factors to choose the correct fitted line to our data sets were the significance of the regression model through F-Test, and the adjusted R^2. The major reason in favoring adjusted R^2 over the regular R^2 is that the adjusted R^2 considers the complexity of the formula. Also the effort has been made to choose the regression model that will not cause overfitting of the fitted line to the data set.

Chapter 5 RESULTS AND DISCUSSION

INTRODUCTION

Chapter 4 introduced different soil classifications and showed the various conducted statistical analysis on different data sets. The regressions chosen from the analysis will be used in this chapter to develop performance charts for various soil and rock classification.

This chapter will introduce the performance charts and their analysis. The most important part of the performance chart analysis would be its validation which will be conducted through the use of multiple real-life case studies.

PERFORMANCE CHARTS

The advance rate formula developed, based on Chapter 4, is shown in Eq. 5-1:

AR (ft/hr) = 5 × PRev (in./rev.) × RPM (rev./min) × UR (%) (Eq. 5-1)

Where AR is the advance rate in ft/hr, PRev is penetration per revolution in in./rev., RPM is the TBM's revolution per minute, UR is the utilization rate in percentage, and 5 is the conversion factor. The corresponding best fitted line equations for each of the parameters in the formula were found in Chapter 4.

Based on the soil and rock classifications introduced (Chapter 4), different performance charts will be produced. Each performance chart will be based on a lower and upper boundary of UCS and its axis will be diameter of tunnel (TBM) and AR.

Clay and Extremely Weak Rock Performance Chart

This performance chart will correspond to the ground conditions of less than 3.62 psi UCS to 145 psi UCS. According to Table 4-1, grades S1 to S6 with R0 will be included in this category. The difference in lower and upper boundary of this chart is not wide, therefore causing the graphs to overlap on each other. Figure 5-1 shows this performance chart.

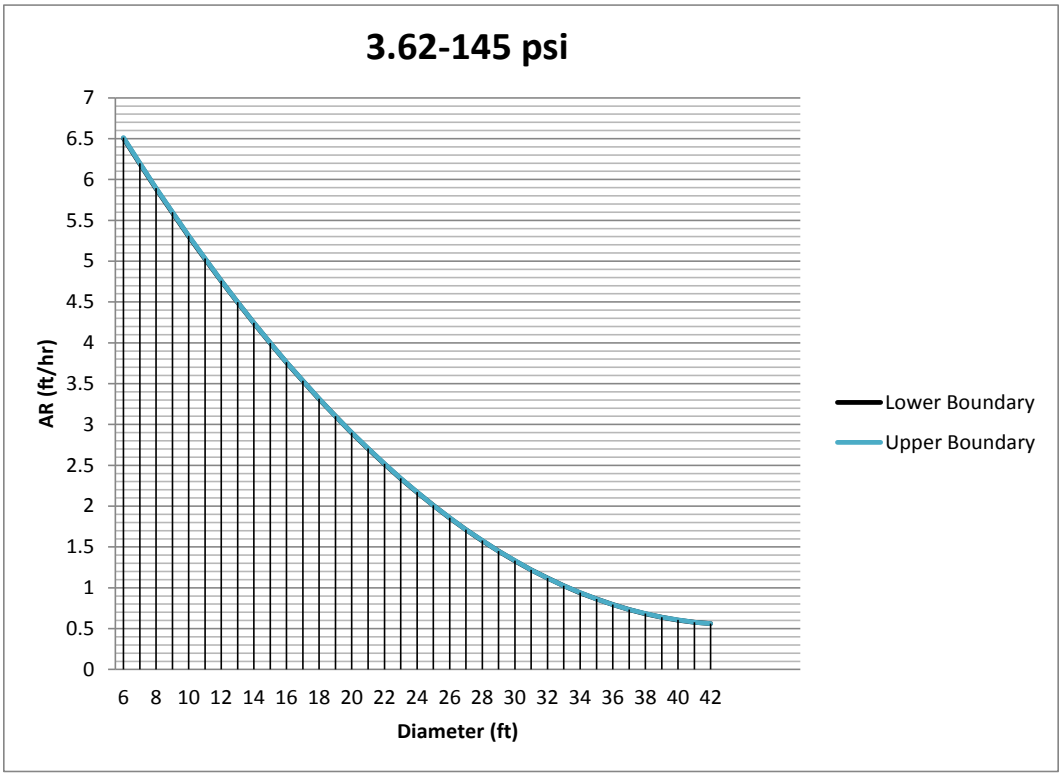

Figure 5-1 Clay and Extremely Weak Rock Performance Chart

Very Weak Rock Performance Chart

The lower and upper boundaries of this performance chart are 145 psi UCS and 725 psi UCS respectively. These boundaries correspond to grade R1 of Table 4-1. Similar to very soft ground performance chart (Figure 5-1), the upper boundary of this chart also overlaps the lower boundary. Figure 5-2 shows this performance chart.

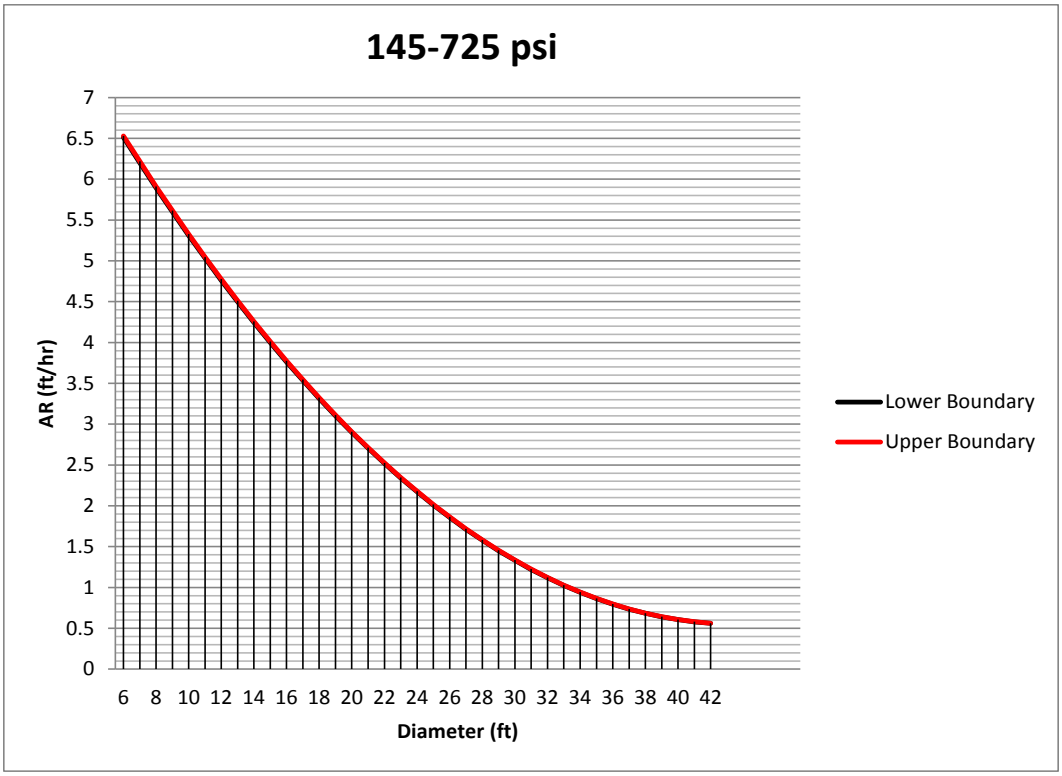

Figure 5-2 Very Weak Rock Performance Chart

Weak Rock Performance Chart

The boundaries for this performance chart come from the grade R2 of Table 4-1. The lower boundary is 725 psi UCS and the upper boundary is 3,625 psi UCS. In this performance chart it can be observed that the upper boundary is slightly offsetting the lower boundary. Figure 5-3 shows this performance chart.

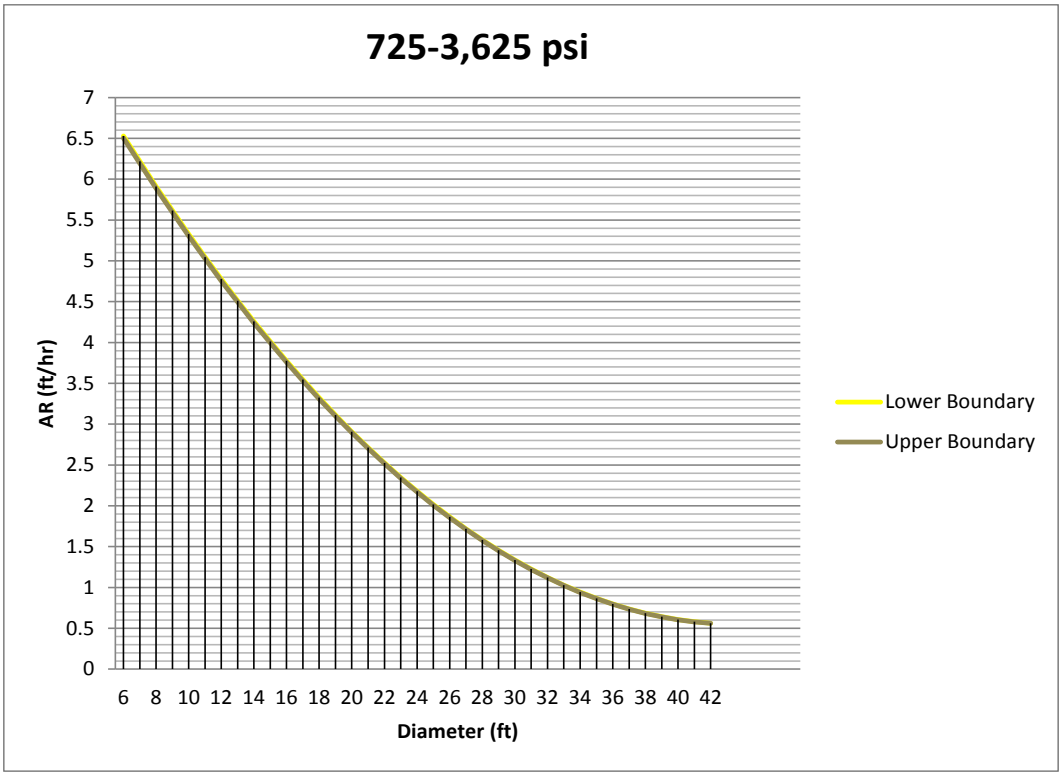

Figure 5-3 Weak Rock Performance Chart

Medium Strong Rock Performance Chart

Medium strong ground conditions are referred to any ground with UCS in the range of 3,625 psi and 7,250 psi. This UCS range corresponds to grade R3 of Table 4-1. In this performance chart (as shown in Figure 5-4), the gap between the lower boundary and upper boundary of the performance chart increases as the ground condition UCS range gets wider.

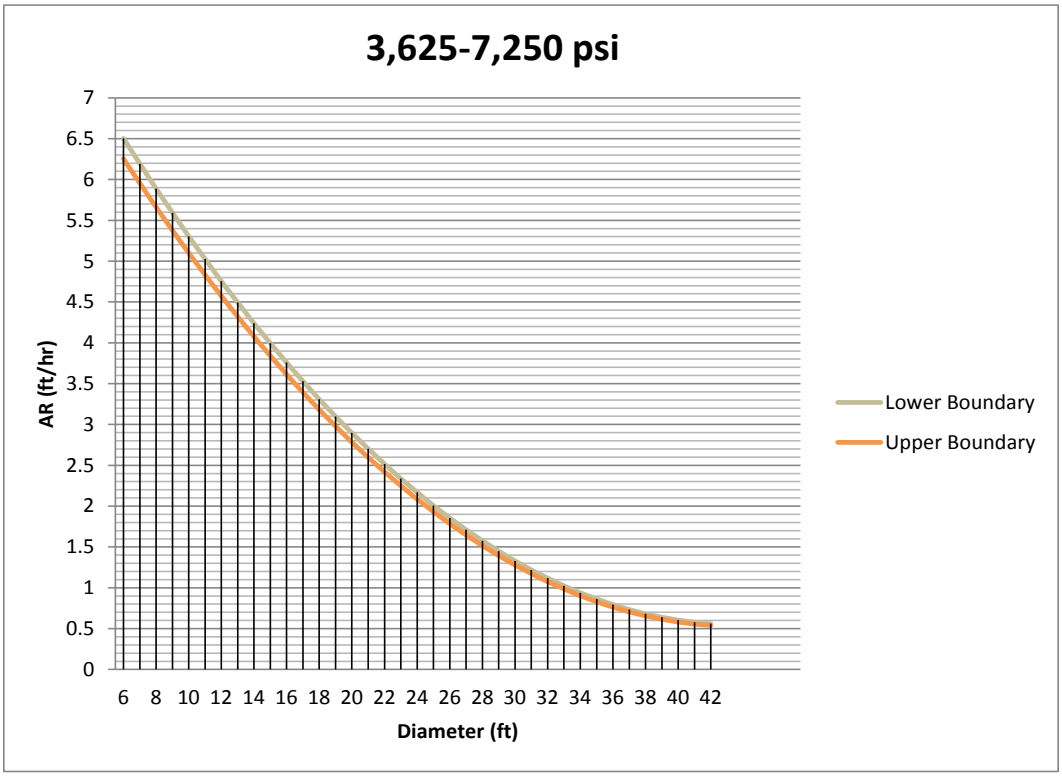

Figure 5-4 Medium Strong Rock Performance Chart

Strong Rock Performance Chart

Strong grounds are basically strong rocks. The UCS of this ground type is 7,250 psi and 14,500 psi for lower and upper boundaries respectively. Such UCS levels are in accordance with grade R4 of Table 4-1. This performance chart is illustrated in Figure 5-5.

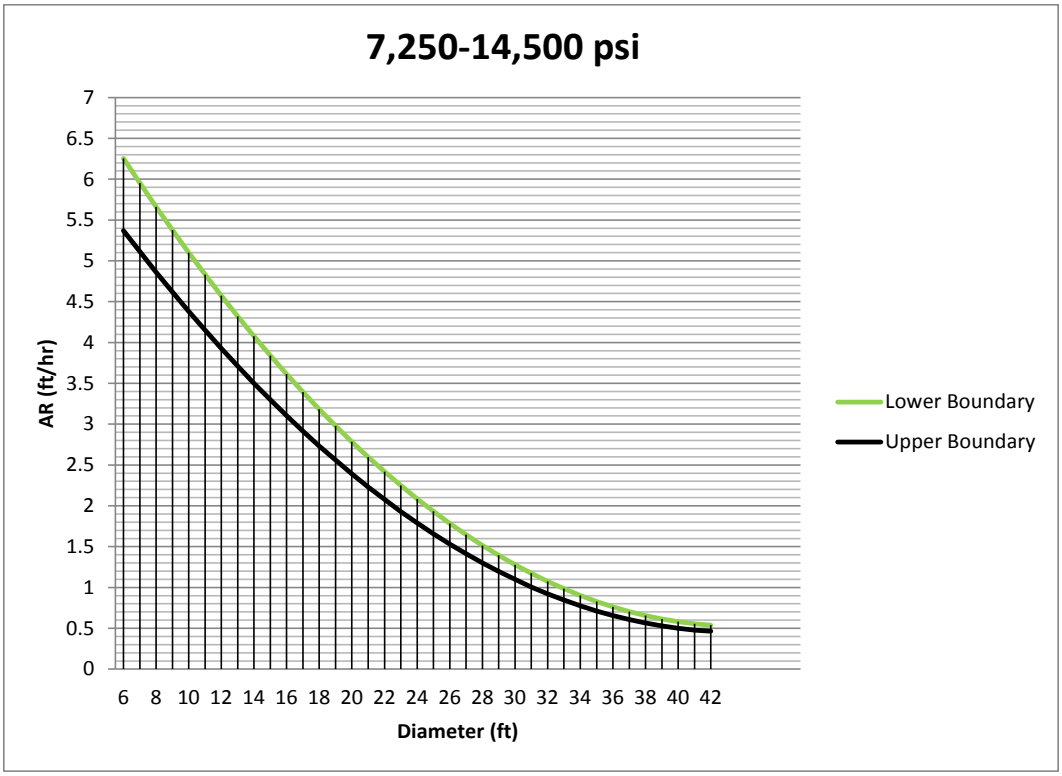

Figure 5-5 Strong Rock Performance Chart

Very Strong Rock Performance Chart

This performance chart (Figure 5-6) is useful for UCS levels of 14,500 psi to 36,250 psi and above. The upper boundary of this chart is for extremely strong rocky conditions. The corresponding grades from Table 4-1 for this chart are R5 and R6.

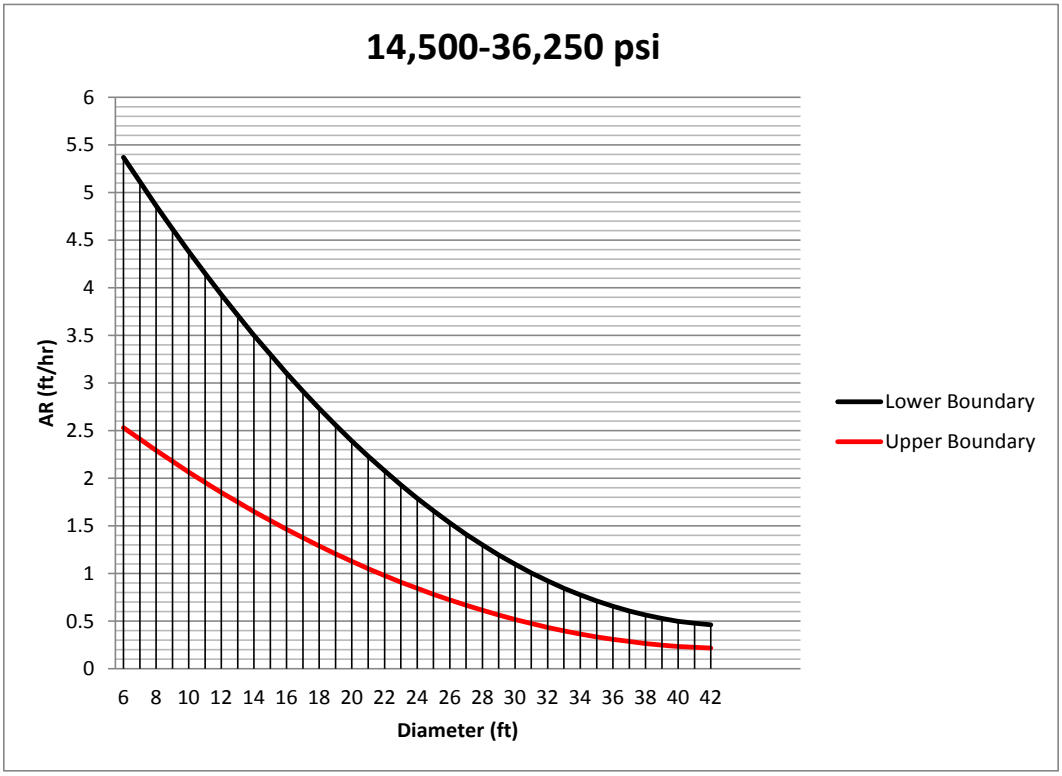

Figure 5-6 Very Strong Rock Performance Chart

PERFORMANCE CHART COMPARISON

Figure 5-7 shows all performance chart curves together. As it can be seen, up to 3,625 psi UCS levels, the graphs almost completely overlap. This fact is indicating that for ground conditions of grades S1 to S6 and R0 to R2 from Table 4-1, there is not a noticeable change in the AR values for different diameters of TBM (see Appendix B for the data).

Figure 5-7 also illustrates that as the ground conditions get stronger (higher UCS), the advance rate decreases for the same diameter which is logical trend since in stronger grounds, we have less penetration. Table B-1 in Appendix B shows the data for performance charts.

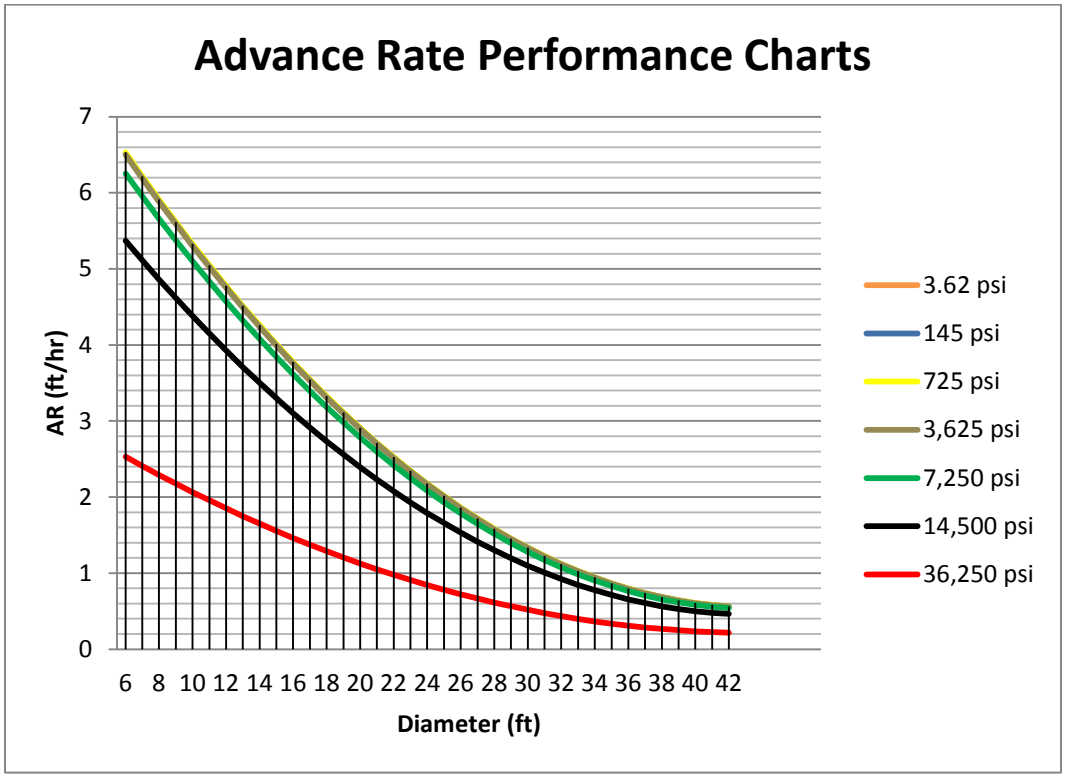

Figure 5-7 Comparison of Advance Rate Performance Charts

A very interesting point that should be noted about the performance charts is that as the diameter of TBM increases, all graphs seem to be converging. This could be due to the fact that for extremely large diameter TBMs, the effect of the size of the TBM over shadows ground condition parameters.

CASE STUDY ANALYSIS

In this section of this chapter, various real-life case studies will be presented and the average advance rate from each case study will be compared the predicted value from the corresponding performance chart.

Chengdu Metro Line 2—Chengdu, China

General Information

- 31.45 miles of tunnel, split into 18 sections specified for EPB TBMs
- Ground consists of clayey and sandy soils with layered strata of pebbles, cobbles, and boulders. The pebbles, cobbles, and boulders have a high compressive strength (7,250 psi to 14,500 psi) and can result in abrasive ground conditions. The area's high groundwater levels interact with this matrix to form permeable ground conditions.
- This type of ground is unusual in China, and the Chengdu Metro represents the first instance of TBM tunneling in conditions with high cobble/pebble content and high groundwater in China.

Figure 5-8 Robbins 20.53 ft Diameter EPB Used on Line 2

Robbins Technical Documents, Appendix C

The average advance rate for the entire project, both sections of tunnel, has been 223 ft per week. This amount is equal to 2.23 ft/hr of average advance rate. Also this project's TBM has a diameter of 20.53 ft.

The ground conditions of this project were of grade R4 from Table 4-1 and therefore, the performance chart appropriate for prediction is strong rock performance chart (Figure 5-5). Using the project TBM's diameter, the AR for the lower and upper boundaries of UCS comes to be 2.68 ft/hr and 2.3 ft/hr.

The average prediction of the performance chart is 2.49 ft/hr, which is 11% higher than the actual AR of the project.

Guangzhou Metro, Guang-Fo Line—Guangzhou, China

General Information

- The 20 mile long Guang-Fo line is China's first ever inter-city rail line, and will cut travel times between the cities of Guangzhou and Foshan to about 50 minutes by 2012.
- Ground consisted of a complex layered profile, ranging from highly weathered to slightly weathered granite, coarse sand, and silt at pressures up to 4 bar. About 70% of the tunneling was through a mixed face, with the alignment above the spring line in soft soils and the bottom half of the tunnel in rock of at least 7,250 psi UCS. The remaining 30% consisted of flowing sand with high water content.
- Robbins supplied two 20.53 ft diameter EPBs with mixed ground cutterheads.

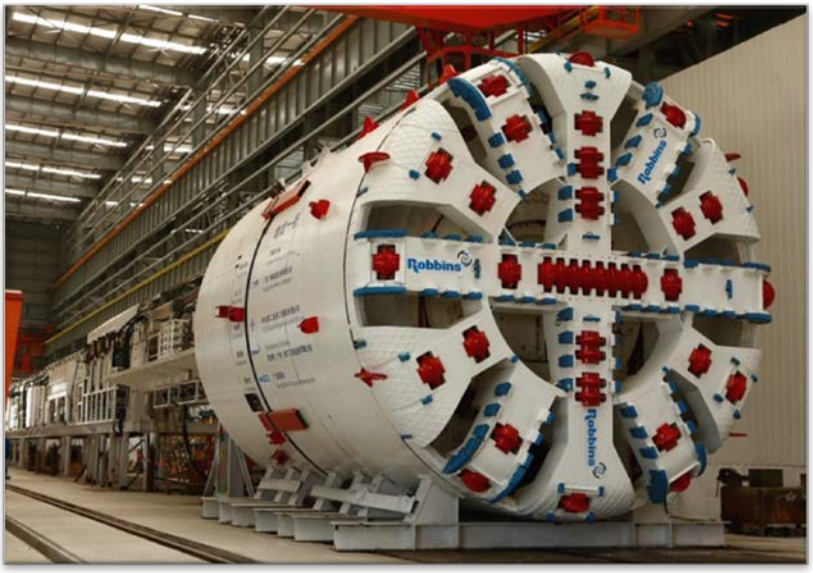

Figure 5-9 Robbins 20.53 ft Diameter EPB Used on Guang-Fo Line

Robbins Technical Documents, Appendix C

The average advance rate for the entire project was 2.3 ft/hr (see Appendix C). This project's TBM has a diameter of 20.53 ft.

Based on the ground condition information of the project, the performance chart appropriate for prediction is strong rock performance chart (Figure 5-5). Using the project TBM's diameter, the AR for the lower and upper boundaries of UCS comes to be 2.68 ft/hr and 2.3 ft/hr.

The average prediction of the performance chart is 2.49 ft/hr, which is 8% higher than the actual AR of the project.

Mexico City Metro Line 12—Mexico City, MX

General Information

- The Robbins EPB excavated 4.8 miles of the Mexican Federal District's first new rail route in ten years, traveling between the southern neighborhoods of Tláhuac and Mixcoac. During tunneling, the machine will pass through seven cut and cover station sites.
- The 33.5 ft diameter EPB is the largest TBM ever to bore in Mexico.
- Geotechnical investigations of the metro tunnel area showed an abundance of lake clays, interspersed with sections of sand, gravel, and boulders up to 800 mm in diameter. Long dormant and eroded volcanoes are buried throughout the area, where they have deposited volcanic rock and fields of boulders in the drained lake bed where modern Mexico City was founded. This type of soil composition is highly unusual, and has only one other analog in the world—in Sapporo, Japan.

- The Robbins EPB was assembled using Onsite First Time Assembly (OFTA) in just ten weeks. Components were lowered into the 17 m deep launch shaft, located on Ermita Iztapalapa Avenue in downtown Mexico City.

Figure 5-10 TBM Exit into the Ermita Station

Robbins Technical Documents, Appendix C

This project had a very large TBM with diameter of 33.5 ft. Considering the ground conditions, the project was mostly in soft grounds except when it encountered volcanic boulders. Based on this information, grade R3 from Table 4-1 is a logical choice. This ground condition's performance chart is shown in Figure 5-4 as medium strong rock performance chart.

Based on Figure 5-4, the average predicted advance rate is 0.96 ft/hr. The average advance rate of the whole project was 1.2 ft/hr. The predicted AR value is 20% lower than the actual advance rate.

New Delhi Metro Extension Project Phase II—New Delhi, India

General Information

- Two 21.4 ft diameter Robbins EPBs were commissioned to bore the BC-16 contract of the New Delhi Metro Extension Project, Phase II, running between Udyog Bhawan and Jor Bagh areas in Delhi. Each TBM bored parallel tunnels of 1.2 miles in length, with an intermediate station in between.
- Approximately 10 mi of TBM drives were involved in Phase II of the project, with about 19 mi of underground works in total including cut and cover stations. The 14 other TBMs were manufactured by competitors. The project was on a tight schedule, which called for all tunneling to be complete by December 2009, in advance of the 2010 Commonwealth Games.
- Ground conditions consisted of watery to sticky clay, silty sand, and gravels with pressures up to 3 bar.

Figure 5-11 Robbins 21.4 ft Diameter EPB in the Shop

Robbins Technical Documents, Appendix C

This project had two 21.4 ft shielded earth pressure balance TBMs. The average advance rate for the complete project considering both TBMs was 2.25 ft /hr. The ground conditions of this project fall into the clay and extremely weak rock category. The performance chart for such ground condition is Figure 5-1.

Based on the information from this project and performance chart from Figure 5-1, the predicted average AR comes to be 2.63 ft/hr. This prediction is 16% higher than the actual average project AR.

Upper Northwest Interceptor Sewer 1 & 2—Sacramento, California, USA

General Information

- The Robbins 13.9 ft diameter EPB excavated a 3.7 mile long tunnel for Sacramento's Upper Northwest Interceptor (UNWI) sewer project. The sewer line will convey up to 560 million liters (148 million gallons) of wastewater per day. The tunnels, for project owner Sacramento Regional County Sanitation District (SRCSD), will add capacity to existing interceptor systems in the area that are close to overflowing during heavy rains.
- The EPB was designed for use with a novel tunnel liner, never before used in the U.S. Precast concrete segments 9 inches thick were molded with embedded PVC sheets 0.07 inches thick. Designed as a single pass system, the PVC inner liner protects the sewer from corrosive gases that can degrade concrete.
- Bore holes along the tunnel alignment indicated layers of clay and sand, with no boulders expected. Below the spring line, the tunnel profile consisted mostly of sand, while the upper portion of the tunnel face was in clay.

Figure 5-12 Robbins 13.9 ft Diameter EPB in the Shop

Robbins Technical Documents, Appendix C

This project has been excavated in very soft grounds such as clay and sand with no boulders. The ground conditions of this project suggest Figure 5-1, clay and extremely weak rock performance chart, to be used for prediction purposes. The average advance rate recorded for this project has been 351 ft per week which equals to 4.38 ft/hr. According to Figure 5-1, the average advance rate predicted is 4.27 ft/hr, which is 2% lower than that of the project.

Zhengzhou Metro, Line 1—Zhengzhou, China

General Information

- Once complete in 2013, Line 1 of Zhengzhou Metro will include 16 mi of tunnel and 22 stations. The Zhengzhou Metro company has invested Yuan 10.2 billion (USD 1.5 billion / EUR 1.1 billion) in the new metro lines, which will total 117 mi by their completion between 2015 and 2030.
- The parallel 2.2 mi long tunnels pass through four intermediate stations between Kaixuan and Tongbo areas of the city
- Ground consists of soft soils including clay, fine sand, loess, and pebbles.
- Robbins supplied two 20.6 ft diameter EPBs with soft ground cutterheads.

Figure 5-13 Robbins 20.6 ft Diameter EPB Used for Zhengzhou Metro Line 1

Robbins Technical Documents, Appendix C

This project has advanced 314 ft on average per week throughout the whole project. As far as ground conditions are concerned, the project has been in clay and sand which means that the suitable performance chart for AR prediction purposes is the clay and extremely weak rock performance chart from Figure 5-1.

The performance chart AR prediction for this project is 2.78 ft/hr which is almost 12% lower than the actual average AR of the project, 3.14 ft/hr.

VALIDATION

The performance charts, entitled CUIRE Model, presented in this chapter were tested and validated through the use of six case studies. Also the results from the RME model presented by Bieniawski et al. (2008) are presented and compared with the results of the CUIRE Model for the same case studies.

RME Model

This model calculates the rock mass excavability (RME) for ground conditions and based on the calculated RME and adjustment factors, attempts to predict the AR. The RME is calculated using five input parameters having these initial ratings:

- Uniaxial compressive strength of intact rock material, UCS: 0 - 15 rating points;
- Drilling rate index, DRI: 0 - 15 points;
- Number of discontinuities present at tunnel face, their orientation with respect to tunnel axis and homogeneity at tunnel face: 0 - 40 points;
- Stand up time of the tunnel front: 0 - 25 points; and
- Water inflow at tunnel front: 0 - 5 points.

The sum of the ratings of the above parameters varies between 0 - 100 rating points and it is expected that the higher the RME value, the easier and more productive the excavation of the tunnel.

To include other important factors such as the diameter of the tunnel or the experience and efficiency of the TBM crew calls for introduction of the term, average rate of advance (ARA) real (ARA_R). At the same time the ARA derived directly from the RME is designated as ARA theoretical (ARA_T). The applicable relationship is as follows:

$$ARA_R = ARA_T \times F_E \times F_A \times F_D \quad \text{(Eq. 5-2) (Bieniawski et al., 2008)}$$

Where ARA_R = real advance rate (ft/hr)

ARA_T = theoretical advance rate (ft/hr)

F_E = factor of crew efficiency;

F_A = factor of team adaptation to the terrain; and

F_D = factor of tunnel diameter.

The RME value for each case study presented in this research was calculated. The adjustment factors were found for the case studies and therefore, the ARA_R was calculated.

Validation

A summary of validation can be found below in Table 5-1. As it is illustrated in Table 5-1, the highest overestimation error by the developed performance charts (CUIRE Model) is 16% and the highest underestimation is 20%. In the case of the underestimation, the models are being conservative and their result would not affect the schedule of a project adversely. Considering overestimation, the models have quite a fair

accuracy. Table 5-1 also shows the comparison between the CUIRE model and the RME model.

Table 5-1 Summary of CUIRE Performance Chart Compared with Bieniawski et al. (2008) RME Model

Case Study	Actual AR (ft/hr)	Predicted AR by Bieniawski et al. (2008) RME Model (ft/hr)	Bieniawski et al. (2008) RME Error (%)	Predicted AR by CUIRE Model (ft/hr)	CUIRE Error (%)
Chengdu Metro Line 2—Chengdu, China	2.23	4.52	+102	2.49	+11
Guangzhou Metro, Guang-Fo Line—Guangzhou, China	2.3	4.52	+96	2.49	+8
Mexico City Metro Line 12—Mexico City, MX	1.2	3.5	+191	0.96	-20
New Delhi Metro Extension Project Phase II—New Delhi, India	2.25	4.7	+108	2.63	+16
Upper Northwest Interceptor Sewer 1 & 2—Sacramento, California, USA	4.38	7.25	+65	4.27	-2
Zhengzhou Metro, Line 1—Zhengzhou, China	3.14	4.89	+55	2.78	-12

Contribution to Body of Knowledge

Farrokh (2013) has done a review of existing models in the literature and concludes that the existing models overestimate the advance rate sometimes in excess of 100%. These results are in agreement with Goel (2008), which evaluated the Q_{tbm} and RME models for a Himalayan tunnel.

As it can be observed from Table 5-1, the model presented by this research does not result in excessive overestimation. The highest overestimation value in Table 5-1 for CUIRE performance charts was 16% that is lower than that of existing models in the literature reported by Farrokh (2013).

Limitations of Study

This dissertation has been positioned in conceptual phase of a tunneling project where limited information is available for feasibility analysis. Only shielded TBMs are considered and gripper TBMs are not included. The diameters for TBMs are between 5 ft to 40 ft and the ground condition UCS is up to 36,000 psi. The results of this dissertation have been validated with limited information from 6 case studies received from Robbins Company.

CHAPTER SUMMARY

This chapter presented various performance charts for TBM productivity perdition based on the ground conditions and TBM diameter. These performance charts were then used in comparison with real life case studies to be tested for accuracy and validation. The results from validation of the performance charts showed that at most, these charts overestimated the advance rate of a project by 16%, which is fairly low compared to the existing advance models in the literature.

Chapter 6 CONCLUSIONS AND RECOMMENDATIONS FOR FUTURE RESEARCH

CONCLUSIONS

Prediction of advance rate is the most crucial factor in of a TBM tunneling project. For the project to be a success, the planning process must provide a realistic evaluation of TBM advance rate. The primary goal of this study was to develop a new model that can be used in the time to complete tunnel calculations in various ground conditions. The proposed model improved the previous TBM performance prediction models. Statistical analyzes were conducted to seek correlations between ground/rock parameters and TBM performance parameters to result in TBM performance charts.

Various regression attempts were made on datasets to achieve the best fitted line to explain as many data as possible. The criteria for choosing the best regression model were the adjusted R^2, results from the statistical F-Test, and prevention of overfitting. The reason for choosing adjusted R^2 over regular R^2 in the analysis was the fact that adjusted R^2 takes the regression formula complexity in consideration as well. The results from the statistical F-Test on regression models indicated if the regression model is significant at all.

Different methods were presented for quantification/classification of soil/rock. Using the ground/rock quantification/classification and the formulas for different regression lines serving as parameters in the calculation of advance rate, various performance charts were presented. The following summarizes the most important findings of this study:

- Literature search conducted with this dissertation showed that the existing TBM performance prediction models do not offer accurate estimate of TBM performance and in some cases overestimate the performance in excess of 100%.

- Previous studies suggested adding various parameters rated to soil and rock conditions are increasing the effect of soil/rock parameters. The new suggested soil/rock parameter already exist in the more general term used as UCS, therefore this might be the cause for their overestimation.
- The approach taken by previous researchers in evaluating utilization rate is an indirect approach whereas in this study a direct approach was chosen. The indirect approach considers the downtimes of the operation without considering that as the boring operation is in process, many of the so-called activities causing downtimes can happen simultaneously and will not cause a decrease in UR. This could possibly be another source causing overestimation in previously developed models.
- The analysis of the developed performance charts shows that for soil/rock conditions of up to 3,625 psi UCS, a major change in the AR values cannot be detected. This is in agreement with the field identification of these conditions as it states that there is no need for excessive power to bore in such conditions.
- The validation of performance charts presented in this study with real-life cases shows a maximum of 16% and 20% overestimation and underestimation for the projects respectively. The underestimation is in the researcher's favor as it is providing conservative results.
- A comparison of the results from the performance charts presented by this study and the evaluation of the existing models in the literature done by Farrokh (2013), shows the accuracy of this study's model is higher.
- The low levels of over and under estimation of AR values presented by the performance charts of this study are due to using direct approach in calculation of factors affecting AR. This direct approach prevents the effect multiplication of

various parameters on the AR model and therefore, prevents excessive overestimations.

RECOMMENDATIONS FOR FUTURE RESEARCH

Based on the conclusions and findings of this study, the following recommendations for future study of performance prediction of tunnel boring machines, are provided:

Recommendations for the Tunneling Industry

- Development of a public database for the TBM projects. This study shows that with more data, researchers have a better understanding of the affecting factors for TBM tunneling projects.
- Development of a database for the time of each activity in a TBM tunneling project for future optimization of these activities. This optimization would help the tunneling industry achieve higher advance rates.
- A survey study of tunneling industry to find out about models that are practically being used and also the industry's suggestions on how the academia can help in furthering their practice.

Recommendations for Future Researchers

- A study on the impacts of tunneling depth on the advance rate of TBM tunneling operation.
- Analysis of the effects of unexpected changes in the ground conditions of tunneling projects to measure the amount of disruptions and delays to project schedule.
- Development of a simulated model for the performance of tunnel boring machines considering the effects of various project site conditions.

- Development of scheduling baseline for tunneling projects as a starting point in scheduling for contractors, engineers, and owners.

Appendix A

Data Analysis

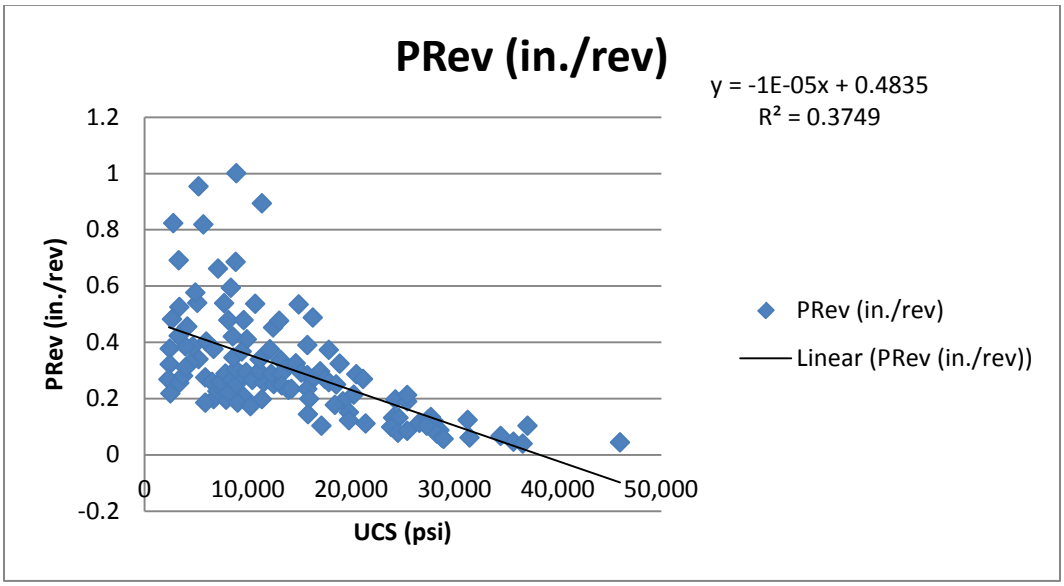

SUMMARY OUTPUT

Regression Statistics	
Multiple R	0.612289699
R Square	0.374898676
Adjusted R Square	0.369601207
Standard Error	0.152121225
Observations	120

ANOVA

	df	*SS*	*MS*	*F*	*Significance F*
Regression	1	1.63766521	1.63766521	70.769397	1.07983E-13
Residual	118	2.730622317	0.023140867		
Total	119	4.368287528			

	Coefficients	*Standard Error*	*t Stat*	*P-value*
Intercept	0.483453961	0.025707807	18.8057252	2.65205E-37
UCS	-1.26457E-05	1.50322E-06	-8.412454873	1.07983E-13

Figure A-1 Linear Regression Analysis of UCS vs. PRev

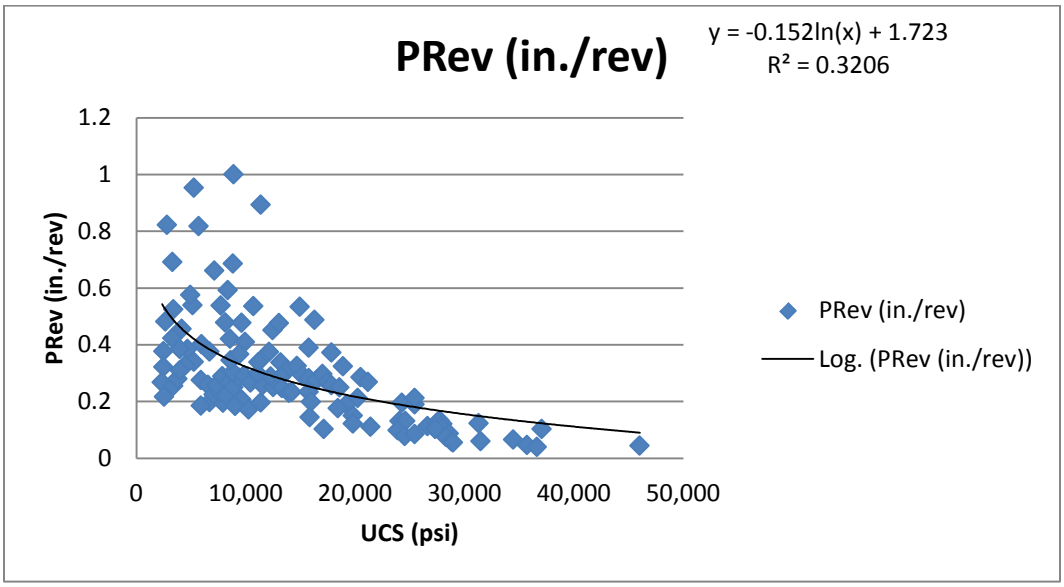

SUMMARY OUTPUT

Regression Statistics	
Multiple R	0.566200347
R Square	0.320582833
Adjusted R Square	0.314825061
Standard Error	0.158592579
Observations	120

ANOVA

	df	*SS*	*MS*	*F*	*Significance F*
Regression	1	1.400397993	1.400397993	55.67827281	1.58782E-11
Residual	118	2.967889535	0.025151606		
Total	119	4.368287528			

	Coefficients	*Standard Error*	*t Stat*	*P-value*
Intercept	1.723006854	0.191060218	9.018135075	4.18128E-15
LnUCS	-0.152074538	0.020380443	-7.461787508	1.58782E-11

Figure A-2 Logarithmic Regression Analysis of UCS vs. PRev

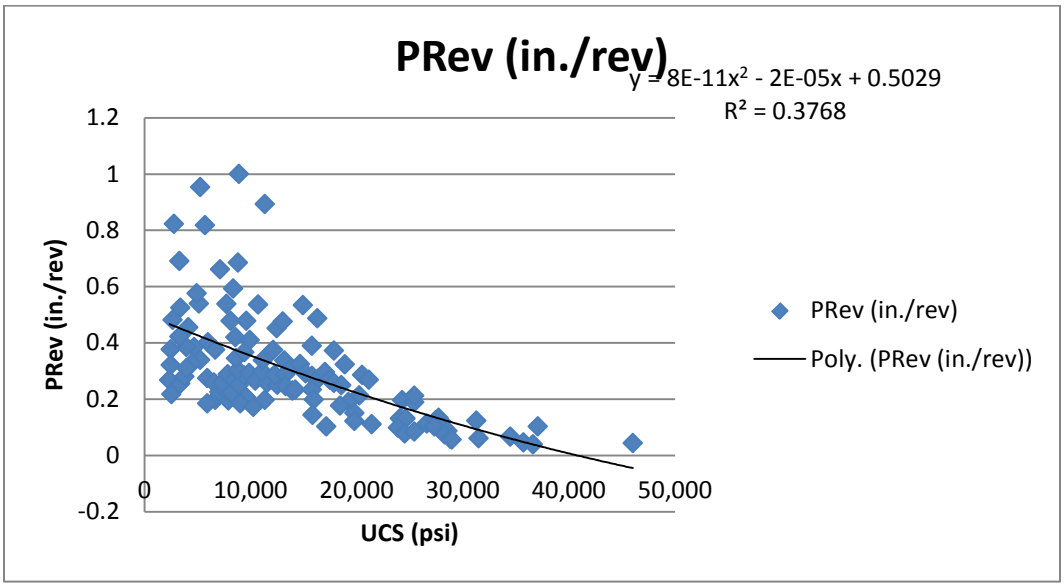

SUMMARY OUTPUT

Regression Statistics	
Multiple R	0.613864347
R Square	0.376829436
Adjusted R Square	0.366176948
Standard Error	0.152533819
Observations	120

ANOVA

	df	*SS*	*MS*	*F*	*Significance F*
Regression	2	1.646099326	0.823049663	35.37478065	9.64951E-13
Residual	117	2.722188202	0.023266566		
Total	119	4.368287528			

	Coefficients	*Standard Error*	*t Stat*	*P-value*
Intercept	0.502920951	0.04135094	12.16226168	1.68742E-22
UCS	-1.56514E-05	5.21469E-06	-3.00140013	0.003285626
UCS Square	8.13425E-11	1.35103E-10	0.602079193	0.548286434

Figure A-3 Polynomial Order-2 Regression Analysis of UCS vs. PRev

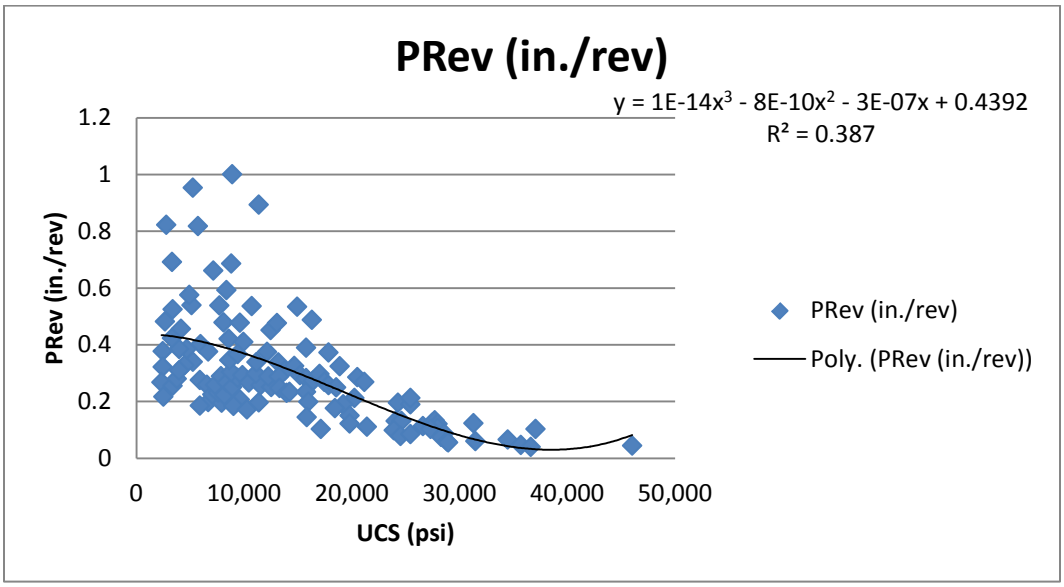

SUMMARY OUTPUT

Regression Statistics	
Multiple R	0.622098957
R Square	0.387007113
Adjusted R Square	0.371153848
Standard Error	0.151933776
Observations	120

ANOVA

	df	*SS*	*MS*	*F*	*Significance F*
Regression	3	1.690558344	0.563519448	24.41182489	2.56421E-12
Residual	116	2.677729184	0.023083872		
Total	119	4.368287528			

	Coefficients	*Standard Error*	*t Stat*	*P-value*
Intercept	0.439190369	0.061687262	7.11962818	9.7087E-11
UCS	-2.75856E-07	1.22362E-05	-0.022544171	0.982052612
UCS Square	-8.13368E-10	6.58594E-10	-1.23500662	0.2193237
UCS Cube	1.41421E-14	1.01903E-14	1.387795908	0.167859187

Figure A-4 Polynomial Order-3 Regression Analysis of UCS vs. PRev

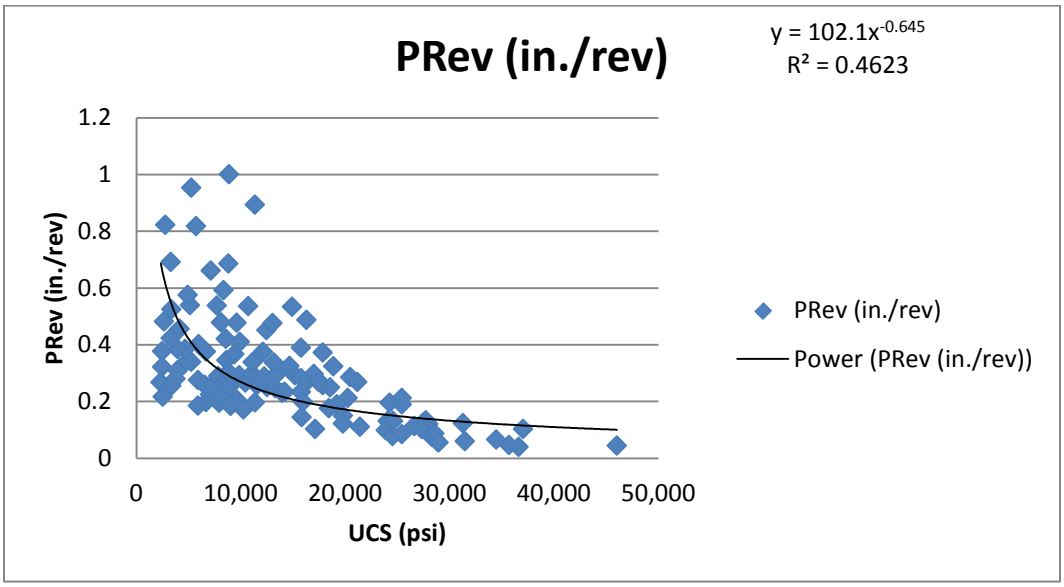

SUMMARY OUTPUT

Regression Statistics	
Multiple R	0.679949338
R Square	0.462331102
Adjusted R Square	0.457774586
Standard Error	0.498221061
Observations	120

ANOVA

	df	*SS*	*MS*	*F*	*Significance F*
Regression	1	25.18629973	25.18629973	101.4659212	1.34545E-17
Residual	118	29.29045865	0.248224226		
Total	119	54.47675838			

	Coefficients	*Standard Error*	*t Stat*	*P-value*
Intercept	4.625940731	0.600218655	7.707092567	4.45272E-12
UCS	-0.644930549	0.064025481	-10.07302939	1.34545E-17

Figure A-5 Power Law Regression Analysis of UCS vs. PRev

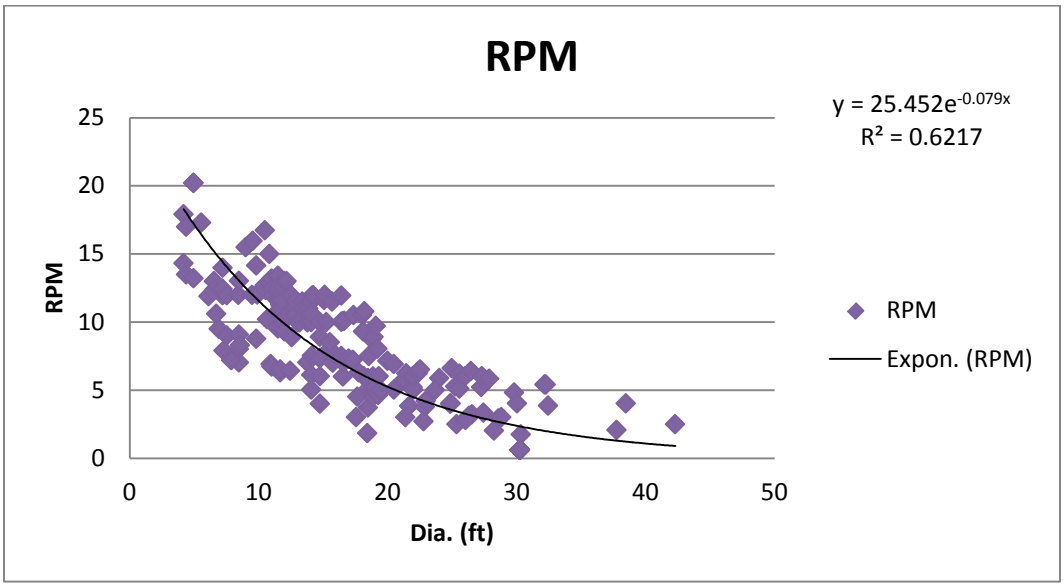

SUMMARY OUTPUT

Regression Statistics	
Multiple R	0.788469553
R Square	0.621684237
Adjusted R Square	0.619754054
Standard Error	0.477805577
Observations	198

ANOVA

	df	*SS*	*MS*	*F*	*Significance F*
Regression	1	73.53158354	73.53158354	322.0857343	3.0682E-43
Residual	196	44.74644121	0.228298169		
Total	197	118.2780247			

	Coefficients	*Standard Error*	*t Stat*	*P-value*
Intercept	3.236806113	0.082207377	39.37366987	4.95022E-95
Dia.	-0.078946267	0.004398918	-17.94674718	3.0682E-43

Figure A-6 Exponential Regression Analysis of RPM vs. Dia.

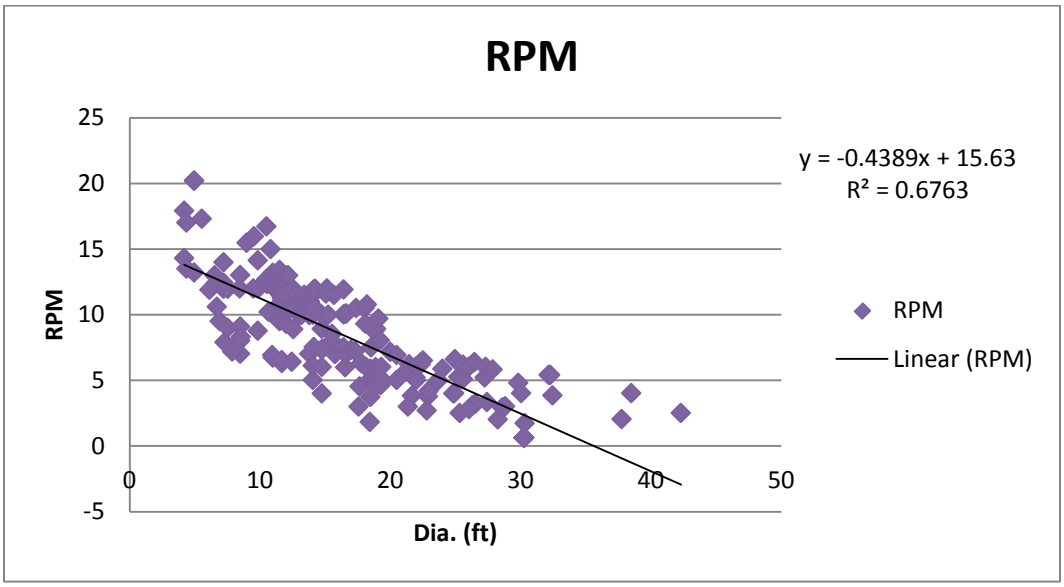

SUMMARY OUTPUT

Regression Statistics	
Multiple R	0.822353717
R Square	0.676265635
Adjusted R Square	0.674613929
Standard Error	2.356091886
Observations	198

ANOVA

	df	*SS*	*MS*	*F*	*Significance F*
Regression	1	2272.840895	2272.840895	409.4346443	6.88111E-50
Residual	196	1088.029119	5.551168976		
Total	197	3360.870014			

	Coefficients	*Standard Error*	*t Stat*	*P-value*
Intercept	15.62957116	0.405370181	38.55629222	1.89297E-93
Dia.	-0.438913722	0.021691364	-20.23449145	6.88111E-50

Figure A-7 Linear Regression Analysis of RPM vs. Dia.

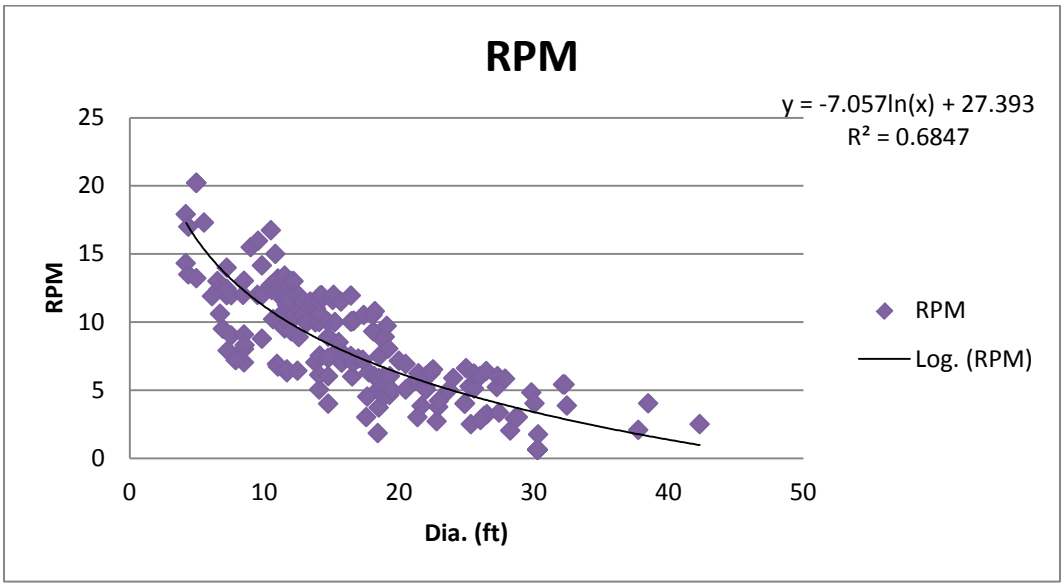

SUMMARY OUTPUT

Regression Statistics	
Multiple R	0.82744349
R Square	0.684662728
Adjusted R Square	0.683053865
Standard Error	2.325334714
Observations	198

ANOVA

	df	*SS*	*MS*	*F*	*Significance F*
Regression	1	2301.062434	2301.062434	425.5567194	5.20589E-51
Residual	196	1059.80758	5.407181533		
Total	197	3360.870014			

	Coefficients	*Standard Error*	*t Stat*	*P-value*
Intercept	27.39344717	0.946902686	28.92952738	1.15637E-72
LnDia.	-7.057304937	0.342105579	-20.62902614	5.20589E-51

Figure A-8 Logarithmic Regression Analysis of RPM vs. Dia.

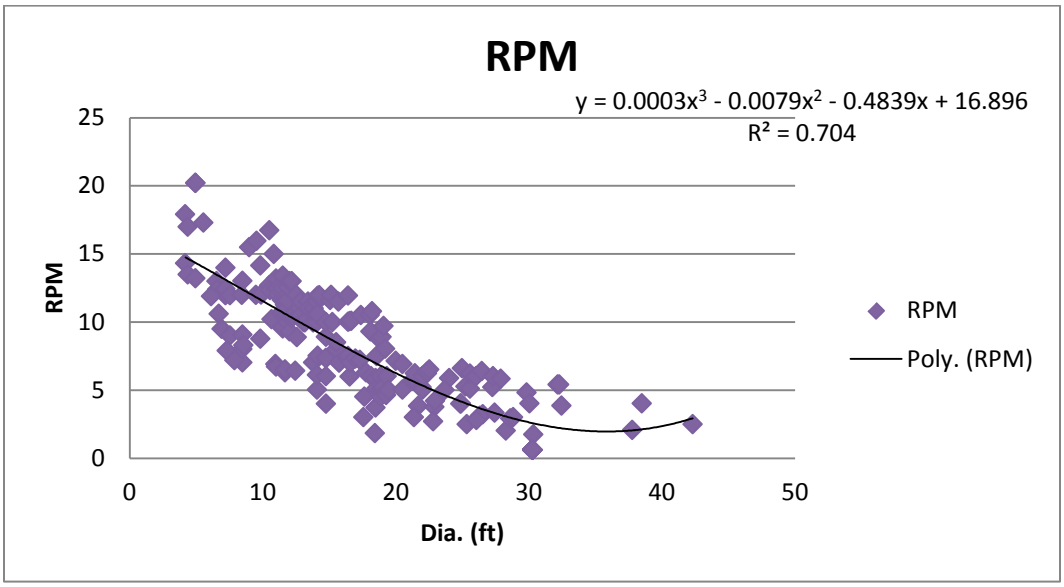

SUMMARY OUTPUT

Regression Statistics	
Multiple R	0.839024679
R Square	0.703962411
Adjusted R Square	0.69938451
Standard Error	2.264636079
Observations	198

ANOVA

	df	*SS*	*MS*	*F*	*Significance F*
Regression	3	2365.926159	788.6420531	153.7740623	4.93018E-51
Residual	194	994.943855	5.128576572		
Total	197	3360.870014			

	Coefficients	*Standard Error*	*t Stat*	*P-value*
Intercept	16.89646982	1.406813161	12.0104576	3.31263E-25
Dia.	-0.483920613	0.240228346	-2.014419284	0.045346418
Dia. Square	-0.007888029	0.012396075	-0.636332773	0.525309596
Dia. Cube	0.000272482	0.000195736	1.392090275	0.165488835

Figure A-9 Polynomial Order-3 Regression Analysis of RPM vs. Dia.

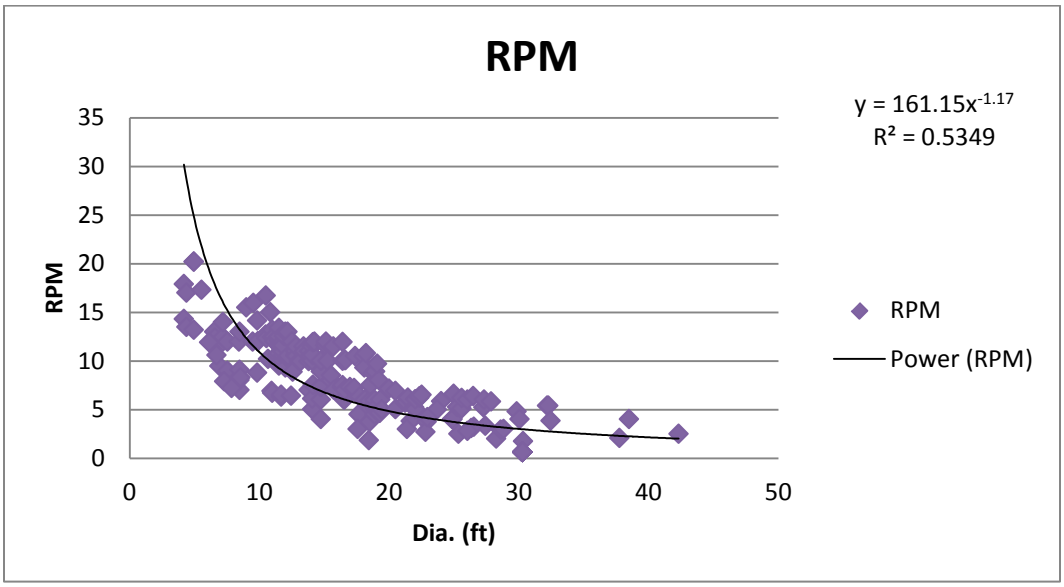

SUMMARY OUTPUT

Regression Statistics	
Multiple R	0.731345887
R Square	0.534866807
Adjusted R Square	0.532493679
Standard Error	0.529800864
Observations	198

ANOVA

	df	*SS*	*MS*	*F*	*Significance F*
Regression	1	63.26298945	63.26298945	225.3846765	2.05034E-34
Residual	196	55.01503529	0.280688956		
Total	197	118.2780247			

	Coefficients	*Standard Error*	*t Stat*	*P-value*
Intercept	5.082364762	0.215740925	23.55772217	4.47153E-59
Dia.	-1.170171556	0.077944835	-15.01281707	2.05034E-34

Figure A-10 Power Law Regression Analysis of RPM vs. Dia.

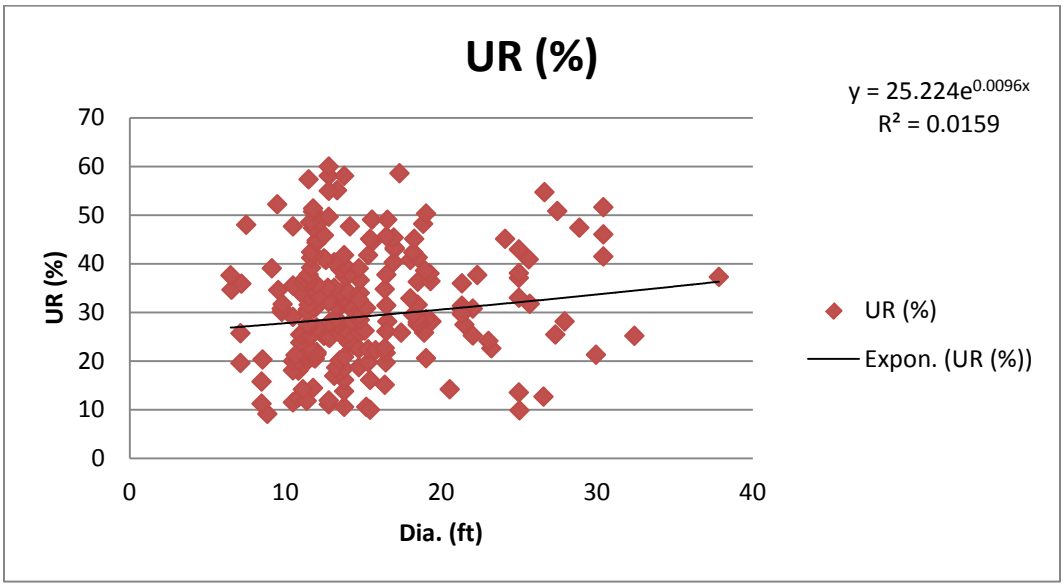

SUMMARY OUTPUT

Regression Statistics	
Multiple R	0.125922503
R Square	0.015856477
Adjusted R Square	0.011501859
Standard Error	0.396709965
Observations	228

ANOVA

	df	*SS*	*MS*	*F*	*Significance F*
Regression	1	0.573063721	0.573063721	3.641301963	0.057630091
Residual	226	35.56760805	0.157378797		
Total	227	36.14067177			

	Coefficients	*Standard Error*	*t Stat*	*P-value*
Intercept	3.22779743	0.080617488	40.03842707	1.3641E-104
Dia.	0.009626619	0.005044817	1.908219579	0.057630091

Figure A-11 Exponential Regression Analysis of UR vs. Dia.

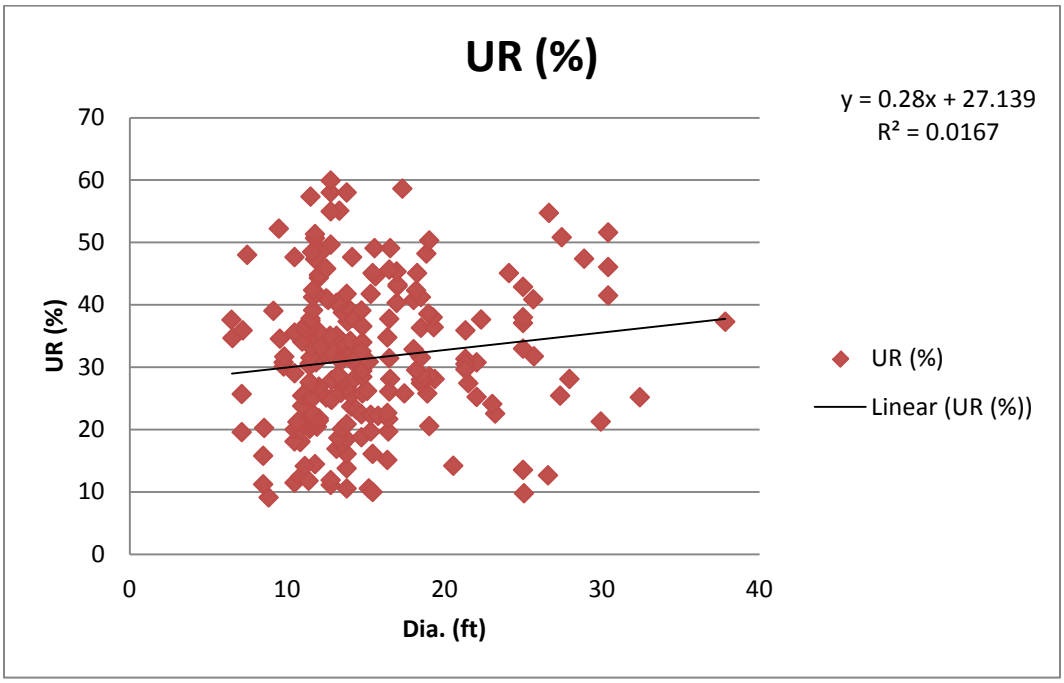

SUMMARY OUTPUT

Regression Statistics	
Multiple R	0.129262863
R Square	0.016708888
Adjusted R Square	0.012358042
Standard Error	11.23449039
Observations	228

ANOVA

	df	*SS*	*MS*	*F*	*Significance F*
Regression	1	484.7084874	484.7084874	3.840377087	0.051261497
Residual	226	28524.31302	126.2137744		
Total	227	29009.02151			

	Coefficients	*Standard Error*	*t Stat*	*P-value*
Intercept	27.13915765	2.283019027	11.88739881	1.24268E-25
Dia.	0.279970726	0.142864948	1.959688008	0.051261497

Figure A-12 Linear Regression Analysis of UR vs. Dia.

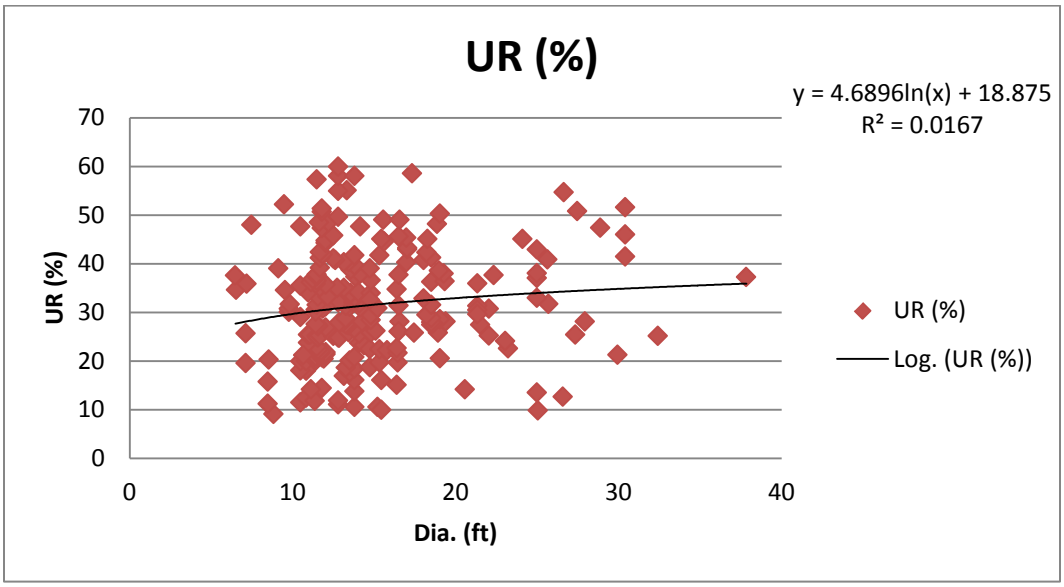

SUMMARY OUTPUT

Regression Statistics	
Multiple R	0.129156503
R Square	0.016681402
Adjusted R Square	0.012330435
Standard Error	11.23464741
Observations	228

ANOVA

	df	*SS*	*MS*	*F*	*Significance F*
Regression	1	483.9111606	483.9111606	3.833952646	0.051454858
Residual	226	28525.11035	126.2173024		
Total	227	29009.02151			

	Coefficients	*Standard Error*	*t Stat*	*P-value*
Intercept	18.87452872	6.424269719	2.93800378	0.003645537
LnDia.	4.689564297	2.395019879	1.958048173	0.051454858

Figure A-13 Logarithmic Regression Analysis of UR vs. Dia.

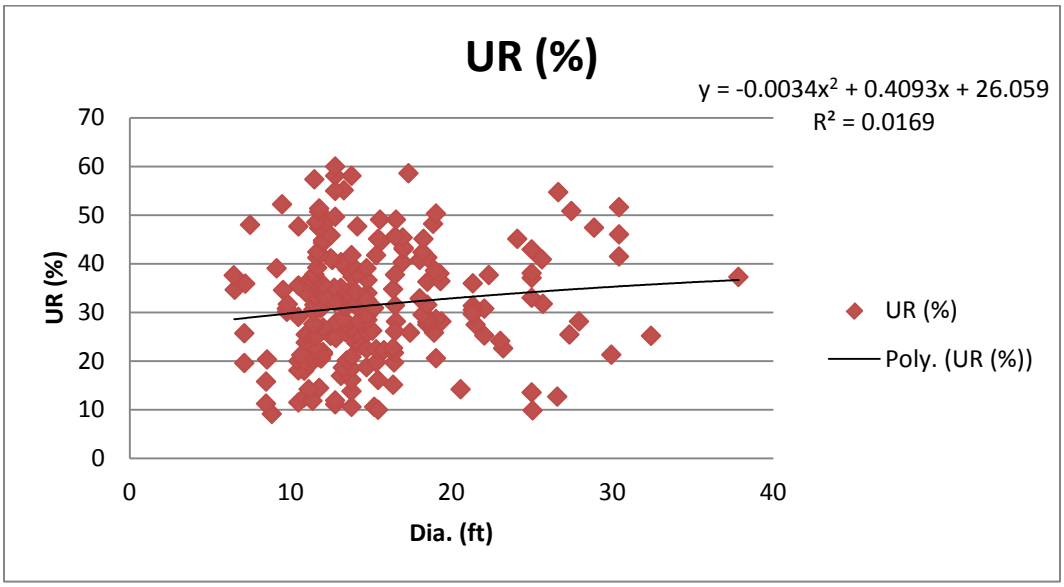

SUMMARY OUTPUT

Regression Statistics	
Multiple R	0.129825211
R Square	0.016854585
Adjusted R Square	0.008115515
Standard Error	11.25859405
Observations	228

ANOVA

	df	*SS*	*MS*	*F*	*Significance F*
Regression	2	488.9350308	244.4675154	1.928647412	0.147739891
Residual	225	28520.08648	126.7559399		
Total	227	29009.02151			

	Coefficients	*Standard Error*	*t Stat*	*P-value*
Intercept	26.05943177	6.340163412	4.110214528	5.53997E-05
Dia.	0.4092828	0.722486509	0.566491961	0.571624022
Dia. Square	-0.003422111	0.01874069	-0.182603251	0.855273756

Figure A-14 Polynomial Order-2 Regression Analysis of UR vs. Dia.

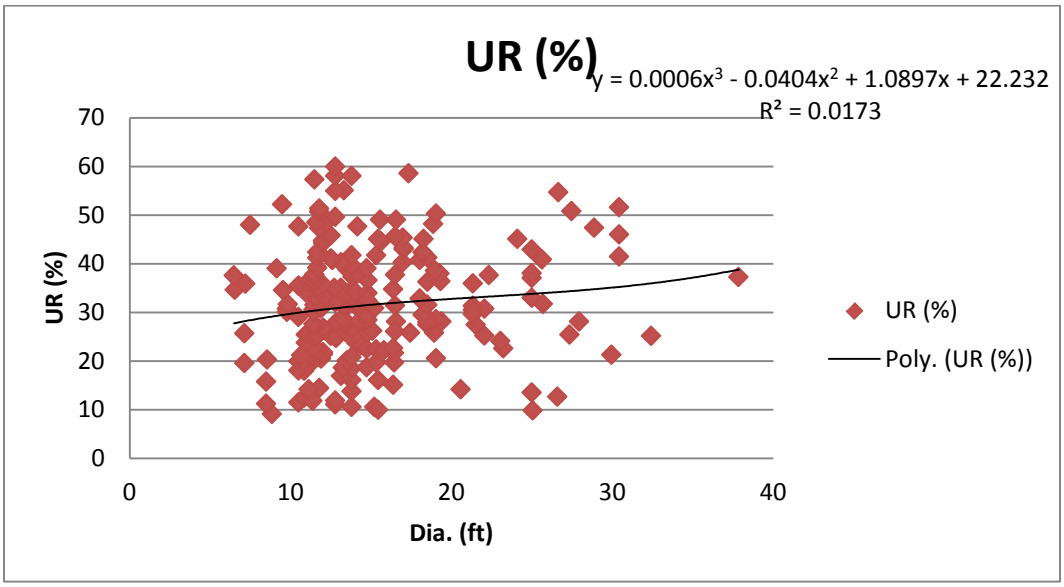

SUMMARY OUTPUT

Regression Statistics	
Multiple R	0.131398272
R Square	0.017265506
Adjusted R Square	0.004103883
Standard Error	11.28133851
Observations	228

ANOVA

	df	*SS*	*MS*	*F*	*Significance F*
Regression	3	500.8554304	166.9518101	1.311806777	0.271355873
Residual	224	28508.16608	127.2685986		
Total	227	29009.02151			

	Coefficients	*Standard Error*	*t Stat*	*P-value*
Intercept	22.23243309	14.0259744	1.585090095	0.114356571
Dia.	1.089746686	2.3383043	0.466041432	0.641638701
Dia. Square	-0.040401412	0.122280273	-0.330400077	0.741406498
Dia. Cube	0.00061234	0.002000821	0.306044639	0.759854908

Figure A-15 Polynomial Order-3 Regression Analysis of UR vs. Dia.

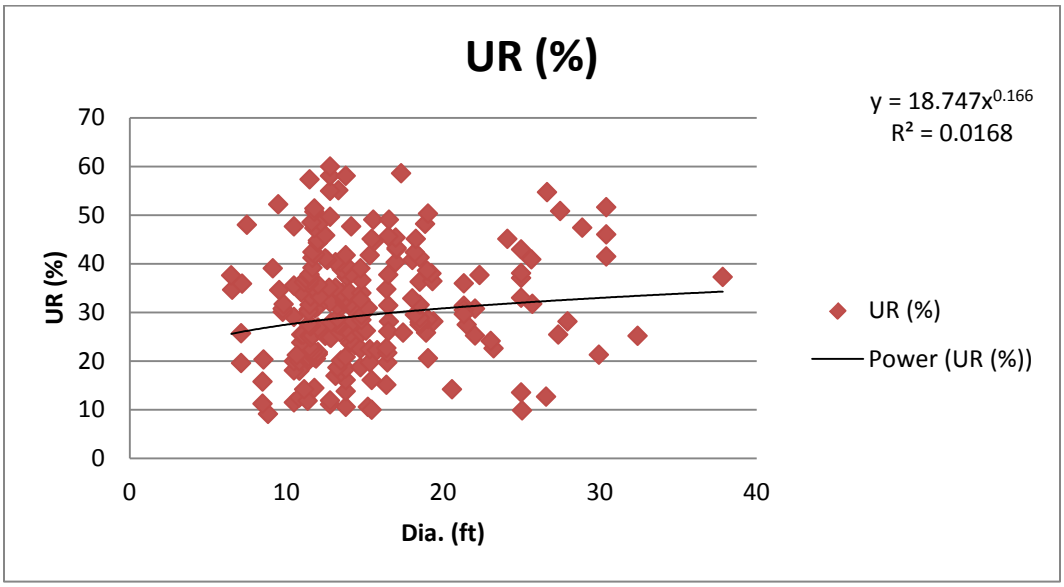

SUMMARY OUTPUT

Regression Statistics	
Multiple R	0.129508923
R Square	0.016772561
Adjusted R Square	0.012421997
Standard Error	0.396525285
Observations	228

ANOVA

	df	*SS*	*MS*	*F*	*Significance F*
Regression	1	0.606171626	0.606171626	3.855261421	0.050816479
Residual	226	35.53450014	0.157232302		
Total	227	36.14067177			

	Coefficients	*Standard Error*	*t Stat*	*P-value*
Intercept	2.931023625	0.226743687	12.92659416	5.53906E-29
Dia.	0.165976834	0.084531887	1.963481964	0.050816479

Figure A-16 Power Law Regression Analysis of UR vs. Dia.

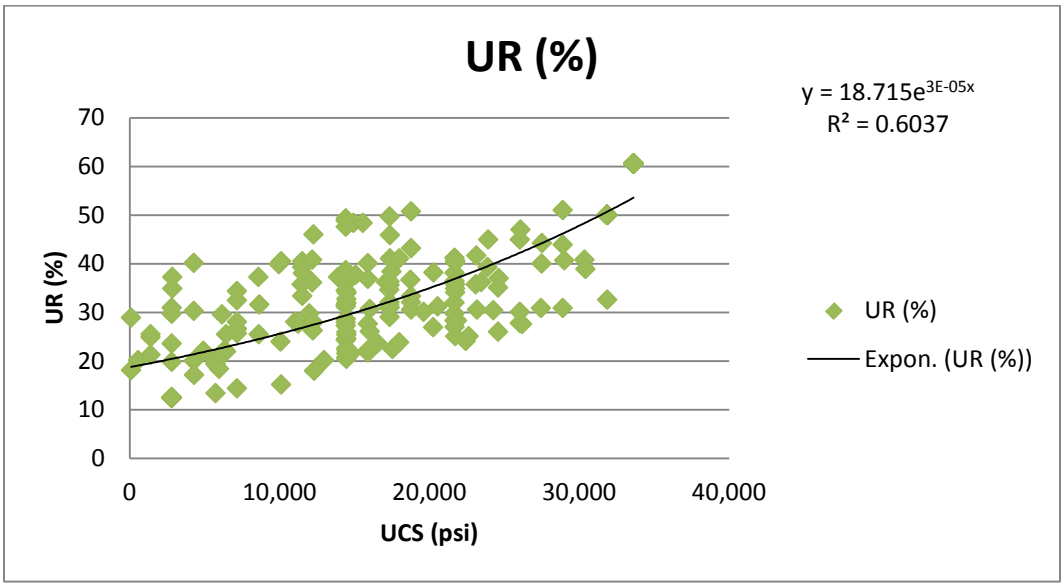

SUMMARY OUTPUT

Regression Statistics	
Multiple R	0.776950351
R Square	0.603651848
Adjusted R Square	0.601816903
Standard Error	0.259415195
Observations	218

ANOVA

	df	*SS*	*MS*	*F*	*Significance F*
Regression	1	22.1388098	22.1388098	328.975418	2.72156E-45
Residual	216	14.53598857	0.067296243		
Total	217	36.67479837			

	Coefficients	*Standard Error*	*t Stat*	*P-value*
Intercept	2.92930026	0.036132056	81.07206127	1.0699E-163
UCS	3.1271E-05	1.72409E-06	18.13767951	2.72156E-45

Figure A-17 Exponential Regression Analysis of UR vs. UCS

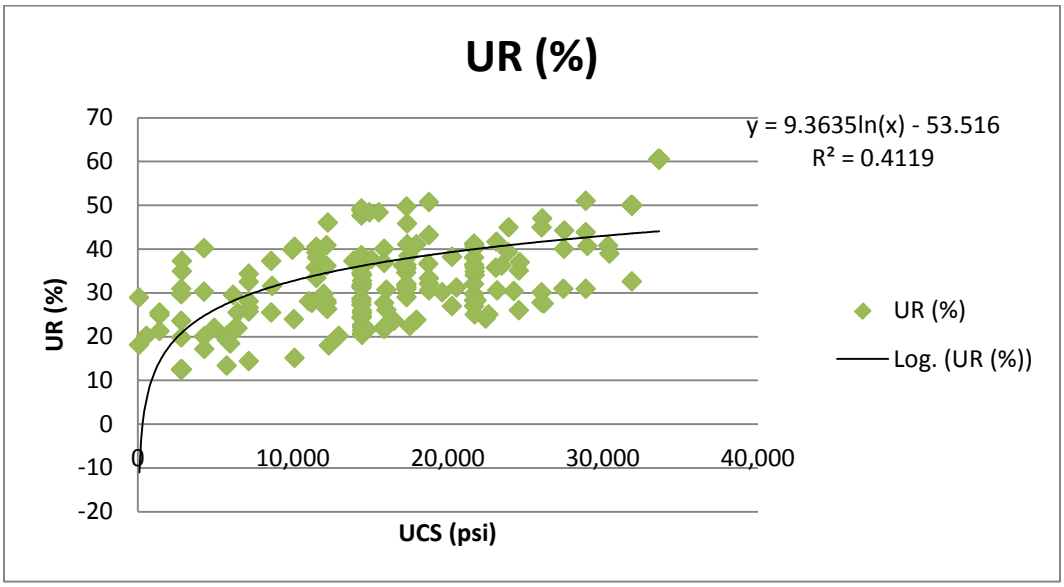

SUMMARY OUTPUT

Regression Statistics	
Multiple R	0.641825441
R Square	0.411939896
Adjusted R Square	0.409217396
Standard Error	10.41086647
Observations	218

ANOVA

	df	*SS*	*MS*	*F*	*Significance F*
Regression	1	16399.84121	16399.84121	151.3093935	1.05085E-26
Residual	216	23411.40638	108.3861407		
Total	217	39811.24759			

	Coefficients	*Standard Error*	*t Stat*	*P-value*
Intercept	-53.51568008	7.301147282	-7.32976312	4.55354E-12
LnUCS	9.36347493	0.761209337	12.30078833	1.05085E-26

Figure A-18 Logarithmic Regression Analysis of UR vs. UCS

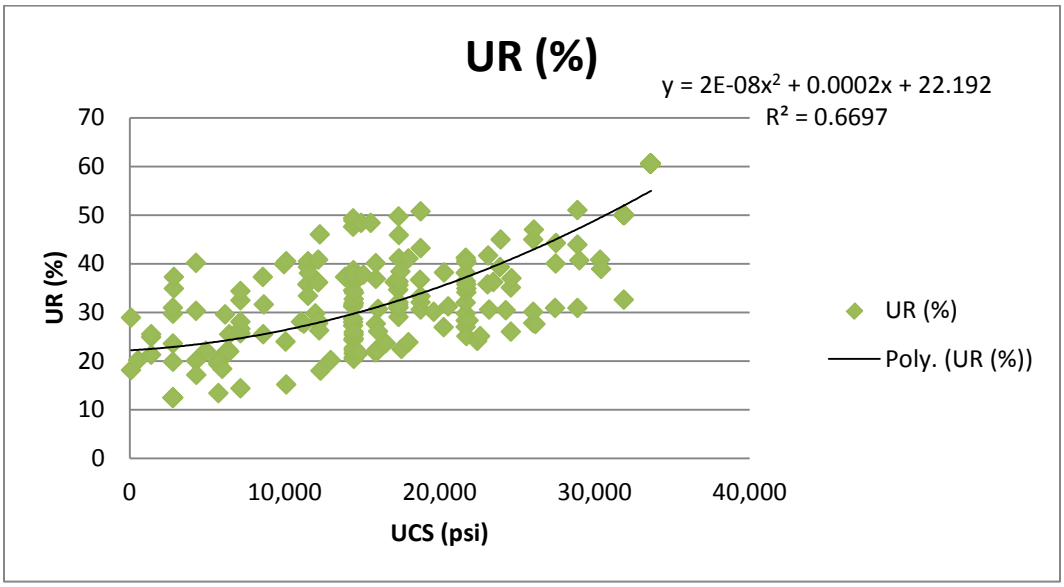

SUMMARY OUTPUT

Regression Statistics	
Multiple R	0.81834084
R Square	0.66968173
Adjusted R Square	0.666609002
Standard Error	7.820778057
Observations	218

ANOVA

	df	*SS*	*MS*	*F*	*Significance F*
Regression	2	26660.86517	13330.43258	217.9437003	1.92865E-52
Residual	215	13150.38242	61.16456942		
Total	217	39811.24759			

	Coefficients	*Standard Error*	*t Stat*	*P-value*
Intercept	22.19161031	1.715112326	12.93886702	1.06358E-28
UCS	0.000179744	0.000209518	0.857892124	0.391907362
UCS Square	2.36593E-08	5.44648E-09	4.343956191	2.15674E-05

Figure A-19 Polynomial Order-2 Regression Analysis of UR vs. UCS

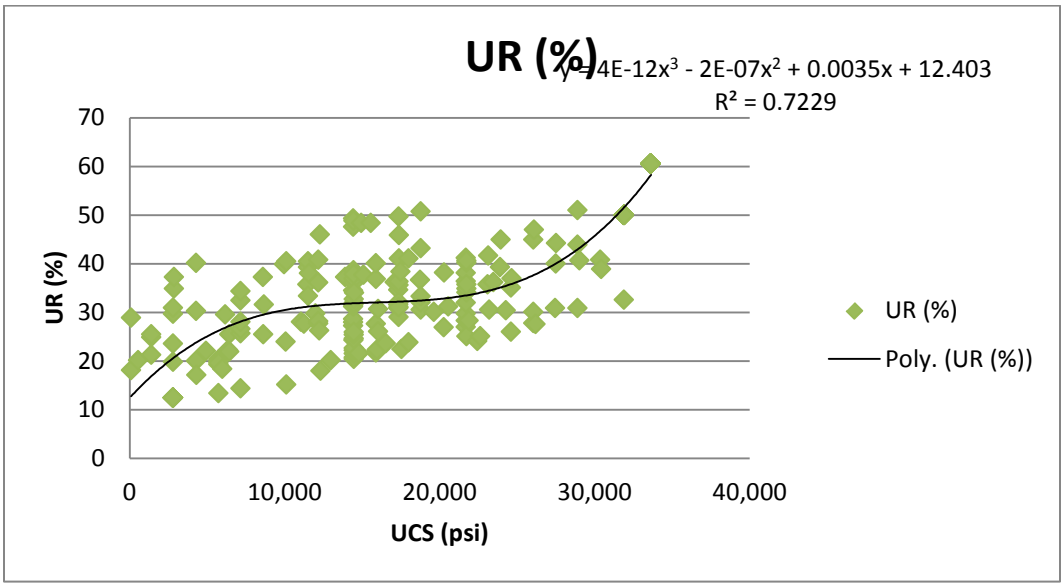

SUMMARY OUTPUT

Regression Statistics	
Multiple R	0.850246457
R Square	0.722919037
Adjusted R Square	0.719034725
Standard Error	7.179585158
Observations	218

ANOVA

	df	*SS*	*MS*	*F*	*Significance F*
Regression	3	28780.30878	9593.43626	186.1124783	2.27978E-59
Residual	214	11030.93881	51.54644304		
Total	217	39811.24759			

	Coefficients	*Standard Error*	*t Stat*	*P-value*
Intercept	12.40267267	2.193065438	5.65540474	4.94287E-08
UCS	0.003480043	0.000549451	6.333678486	1.3896E-09
UCS Square	-2.11453E-07	3.70054E-08	-5.71412004	3.6676E-08
UCS Cube	4.41648E-12	6.88755E-13	6.412266776	9.03251E-10

Figure A-20 Polynomial Order-3 Regression Analysis of UR vs. UCS

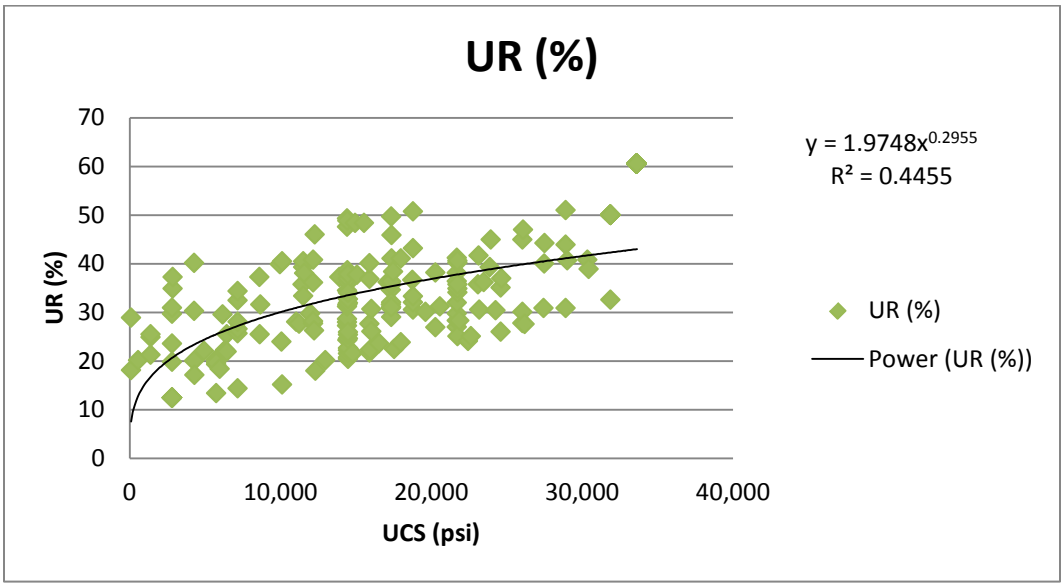

SUMMARY OUTPUT

Regression Statistics	
Multiple R	0.667462536
R Square	0.445506237
Adjusted R Square	0.442939136
Standard Error	0.306835302
Observations	218

ANOVA

	df	*SS*	*MS*	*F*	*Significance F*
Regression	1	16.33885142	16.33885142	173.544508	1.77083E-29
Residual	216	20.33594695	0.094147903		
Total	217	36.67479837			

	Coefficients	*Standard Error*	*t Stat*	*P-value*
Intercept	0.680452512	0.215183793	3.162192206	0.001790896
UCS	0.295547978	0.022434818	13.17362926	1.77083E-29

Figure A-21 Power Law Regression Analysis of UR vs. UCS

Appendix B

Performance Chart Data

Table B-1 Performance Chart Data

Dia. (ft)	3.62 psi	145 psi	725 psi	3,625 psi	7,250 psi	14,500 psi	36,250 psi
6	6.505	6.511	6.530	6.503	6.253	5.370	2.532
7	6.193	6.199	6.217	6.191	5.953	5.112	2.410
8	5.889	5.894	5.911	5.887	5.661	4.861	2.292
9	5.593	5.598	5.615	5.591	5.377	4.617	2.177
10	5.306	5.311	5.326	5.304	5.101	4.380	2.065
11	5.027	5.032	5.047	5.026	4.833	4.150	1.957
12	4.757	4.761	4.775	4.755	4.573	3.927	1.851
13	4.495	4.499	4.512	4.493	4.321	3.710	1.750
14	4.241	4.245	4.258	4.240	4.077	3.501	1.651
15	3.996	4.000	4.012	3.995	3.842	3.299	1.555
16	3.760	3.763	3.774	3.758	3.614	3.103	1.463
17	3.531	3.535	3.545	3.530	3.395	2.915	1.374
18	3.311	3.315	3.324	3.310	3.183	2.734	1.289
19	3.100	3.103	3.112	3.099	2.980	2.559	1.207
20	2.897	2.900	2.908	2.896	2.785	2.391	1.128
21	2.702	2.705	2.713	2.702	2.598	2.231	1.052
22	2.516	2.519	2.526	2.515	2.419	2.077	0.979
23	2.339	2.341	2.348	2.338	2.248	1.930	0.910
24	2.169	2.171	2.178	2.168	2.085	1.791	0.844
25	2.008	2.010	2.016	2.008	1.931	1.658	0.782
26	1.856	1.858	1.863	1.855	1.784	1.532	0.722
27	1.712	1.713	1.718	1.711	1.645	1.413	0.666
28	1.576	1.578	1.582	1.576	1.515	1.301	0.613
29	1.449	1.450	1.454	1.448	1.393	1.196	0.564
30	1.330	1.331	1.335	1.330	1.279	1.098	0.518
31	1.220	1.221	1.224	1.219	1.172	1.007	0.475
32	1.118	1.119	1.122	1.117	1.074	0.923	0.435
33	1.024	1.025	1.028	1.024	0.985	0.845	0.399
34	0.939	0.940	0.943	0.939	0.903	0.775	0.366
35	0.862	0.863	0.866	0.862	0.829	0.712	0.336
36	0.794	0.795	0.797	0.794	0.763	0.655	0.309
37	0.734	0.735	0.737	0.734	0.706	0.606	0.286
38	0.683	0.683	0.685	0.683	0.656	0.564	0.266
39	0.640	0.640	0.642	0.640	0.615	0.528	0.249
40	0.605	0.606	0.607	0.605	0.582	0.500	0.236
41	0.579	0.579	0.581	0.579	0.557	0.478	0.225
42	0.561	0.562	0.563	0.561	0.539	0.463	0.218

Table B-2 UCS vs. PRev Data

UCS (psi)	PRev (in./rev)	UCS (psi)	PRev (in./rev)	UCS (psi)	PRev (in./rev)	UCS (psi)	PRev (in./rev)
2,791	0.82	8,633	0.35	16,293	0.49	28,302	0.07
3,310	0.69	8,568	0.42	15,774	0.28	28,822	0.06
5,258	0.95	8,114	0.48	15,774	0.23	28,951	0.06
5,712	0.82	7,724	0.54	15,968	0.20	31,483	0.06
5,128	0.54	7,140	0.66	15,839	0.14	34,469	0.07
4,933	0.58	8,374	0.59	16,423	0.27	37,066	0.10
5,972	0.40	8,828	0.69	17,007	0.30	35,703	0.05
6,686	0.38	8,893	1.00	17,851	0.37	36,611	0.04
5,258	0.34	9,607	0.48	17,461	0.27	46,024	0.04
4,479	0.33	9,931	0.41	17,851	0.26		
4,673	0.38	9,412	0.37	18,565	0.25		
4,154	0.46	10,710	0.54	18,890	0.32		
3,959	0.38	11,360	0.89	20,513	0.29		
3,310	0.42	9,867	0.29	21,162	0.27		
3,375	0.52	10,451	0.27	20,253	0.21		
2,661	0.48	9,607	0.21	19,214	0.19		
2,466	0.38	9,023	0.18	18,435	0.18		
2,466	0.32	10,256	0.17	19,798	0.15		
2,336	0.27	11,360	0.20	19,798	0.12		
2,531	0.22	11,554	0.26	17,137	0.10		
3,375	0.26	11,100	0.30	21,421	0.11		
3,765	0.28	11,165	0.34	24,083	0.13		
3,959	0.31	12,528	0.25	24,602	0.13		
5,907	0.27	12,268	0.29	24,278	0.20		
6,556	0.26	12,139	0.37	25,446	0.19		
6,686	0.20	12,463	0.45	25,446	0.21		
5,907	0.18	13,047	0.48	23,888	0.10		
7,919	0.19	13,177	0.34	24,537	0.08		
7,075	0.22	13,761	0.31	25,446	0.08		
7,595	0.23	13,242	0.29	26,615	0.11		
8,179	0.22	13,307	0.25	27,458	0.12		
7,335	0.26	13,956	0.23	27,718	0.13		
7,854	0.29	14,216	0.23	27,978	0.12		
8,438	0.27	14,670	0.32	27,978	0.11		
8,893	0.25	14,930	0.53	27,329	0.10		
9,412	0.28	15,189	0.29	28,562	0.09		
8,828	0.30	15,774	0.39	31,288	0.12		

Table B-3 Diameter vs. RPM Data

Dia. (ft)	RPM	Dia. (ft)	RPM	Dia. (ft)	RPM	Dia. (ft)	RPM	Dia. (ft)	RPM	Dia. (ft)	RPM
6	12.99	11	12.14	14	11.49	18	5.87	27	5.22	4	13.20
6	12.38	11	12.51	14	7.52	18	5.13	27	6.03	4	20.20
6	9.49	11	13.40	14	10.58	18	7.50	27	3.33		
7	11.97	11	11.51	14	11.90	18	8.74	27	5.83		
7	12.42	11	6.30	14	11.97	18	4.50	28	2.01		
7	13.99	11	6.52	14	4.00	18	6.00	28	2.92		
7	8.99	11	11.30	14	6.02	18	5.00	28	3.01		
7	11.97	11	11.19	14	7.32	18	8.91	29	4.81		
8	11.99	11	9.99	14	7.37	18	5.15	30	4.03		
8	7.02	11	10.54	14	8.91	18	5.22	30	0.62		
8	8.02	11	10.97	14	9.99	19	8.04	30	1.73		
8	9.08	11	11.99	15	11.60	19	4.63	32	5.40		
8	13.01	11	11.58	15	11.99	19	6.02	32	5.40		
8	8.30	11	12.58	15	9.99	19	5.00	32	3.86		
8	15.49	12	9.30	15	8.00	19	7.15	37	2.06		
9	11.99	12	12.99	15	8.52	20	5.02	38	4.01		
9	15.96	12	10.30	15	11.49	20	6.91	19	9.70		
9	8.78	12	12.99	15	7.00	21	5.68	21	3.00		
9	14.14	12	10.51	16	7.30	21	5.79	25	2.50		
9	12.01	12	6.41	16	7.50	21	6.22	22	2.70		
10	12.62	12	11.99	16	10.02	21	3.83	17	3.00		
10	12.69	12	8.89	16	11.93	21	5.22	23	5.00		
10	16.72	12	10.58	16	6.00	22	5.03	22	6.50		
10	12.34	12	10.99	16	10.06	22	6.05	42	2.50		
10	10.21	12	10.49	16	7.00	22	6.22	22	4.20		
10	14.99	12	11.49	16	10.08	22	6.35	26	3.10		
10	6.91	13	9.99	16	7.30	22	3.77	26	2.80		
11	6.71	13	9.97	17	7.22	24	5.87	4	17.90		
11	12.45	13	11.49	17	10.50	24	4.01	4	17.00		
11	13.18	13	10.99	17	4.52	24	4.03	4	20.20		
11	12.49	13	7.02	17	6.30	24	6.61	5	17.30		
11	12.01	13	9.97	18	10.50	25	5.27	6	11.90		
11	10.62	13	10.99	18	9.30	25	5.09	6	10.60		
11	11.64	13	10.49	18	6.02	25	6.20	7	7.90		
11	9.52	14	5.02	18	10.78	26	6.03	7	7.20		
11	9.67	14	6.11	18	1.83	26	6.40	4	14.30		
11	10.80	14	9.99	18	3.72	26	3.23	4	13.50		

Table B-4 UCS vs. UR Data

UCS (psi)	UR (%)	UCS (psi)	UR (%)	UCS (psi)	UR (%)	UCS (psi)	UR (%)	UCS (psi)	UR (%)
94	18.12	9,971	39.85	14,476	24.61	18,739	36.62	26,047	27.75
94	28.89	10,073	23.93	14,476	25.38	18,786	30.51	26,047	30.09
563	20.12	10,112	15.13	14,476	25.94	18,786	32.06	26,094	47.00
1,406	21.23	10,112	40.48	14,476	31.94	18,786	33.29	26,196	27.54
1,406	24.90	11,056	28.04	14,476	32.72	18,786	43.17	27,453	30.87
1,406	25.45	11,240	27.65	14,476	36.05	18,786	50.73	27,500	40.00
2,811	12.46	11,478	35.71	14,476	36.94	19,629	30.07	27,513	44.23
2,811	19.79	11,525	33.37	14,476	37.83	20,270	26.92	28,905	51.00
2,811	23.57	11,525	39.26	14,485	34.01	20,285	38.18	28,905	30.87
2,811	29.68	11,525	40.49	14,804	21.61	20,566	31.18	28,905	43.87
2,811	30.90	11,572	38.04	14,945	48.38	21,691	26.96	29,018	40.69
2,858	34.90	11,993	29.73	15,085	37.72	21,691	28.29	30,357	40.77
2,858	37.24	12,181	27.71	15,554	48.39	21,691	29.74	30,428	38.91
4,280	40.16	12,181	28.15	15,896	27.65	21,691	31.96	31,886	32.55
4,280	30.25	12,181	36.15	15,896	36.83	21,691	36.41	33,626	60.51
4,280	20.03	12,181	40.82	15,896	40.06	21,691	38.07	31,886	50.00
4,310	17.13	12,228	26.27	15,896	21.70	21,691	41.18		
4,939	22.01	12,275	46.01	15,943	22.32	21,737	25.07		
5,738	20.24	12,321	17.93	16,037	26.08	21,737	34.07		
5,738	19.30	12,977	20.16	16,037	30.67	21,737	34.85		
5,738	19.93	13,914	37.27	16,537	23.61	21,737	35.74		
5,738	19.61	14,429	27.27	17,119	36.20	21,737	40.18		
5,738	13.35	14,429	27.94	17,334	30.84	21,737	40.63		
5,973	18.36	14,429	28.61	17,334	31.61	21,869	28.27		
6,161	29.52	14,429	31.16	17,334	34.61	22,433	24.10		
6,349	22.22	14,429	34.49	17,354	35.57	22,628	25.07		
6,443	25.45	14,429	47.61	17,354	32.03	23,096	35.74		
6,443	21.91	14,429	49.27	17,354	29.00	23,143	41.63		
7,168	14.36	14,438	31.61	17,354	31.09	23,190	30.52		
7,168	25.69	14,438	24.31	17,354	49.66	23,471	36.19		
7,168	26.58	14,438	48.82	17,354	36.30	23,892	39.30		
7,168	28.03	14,438	38.60	17,381	41.06	23,939	44.97		
7,168	32.47	14,476	20.38	17,381	45.84	24,267	30.41		
7,168	34.36	14,476	20.72	17,474	38.39	24,595	25.97		
8,607	37.24	14,476	21.49	17,542	22.43	24,597	35.05		
8,620	25.48	14,476	22.16	17,990	23.84	24,642	36.97		
8,667	31.59	14,476	22.61	17,990	41.06	26,047	44.97		

Appendix C

Case Studies

Chengdu Metro Line 2—Chengdu, China

General Information

- 31.45 miles of tunnel, split into 18 sections specified for EPB TBMs
- Ground consists of clayey and sandy soils with layered strata of pebbles, cobbles, and boulders. The pebbles, cobbles, and boulders have a high compressive strength (7,250 psi to 14,500 psi) and can result in abrasive ground conditions. The area's high groundwater levels interact with this matrix to form permeable ground conditions.
- This type of ground is unusual in China, and the Chengdu Metro represents the first instance of TBM tunneling in conditions with high cobble/pebble content and high groundwater in China.

Machine Specifications

- Machine Thrust: 36,000 kN (8.1 million lb)
- Maximum Torque: 6,876 kNm
- Maximum Stroke: 1,950 mm (77 in)
- Cutterhead Drive: Electric, Variable Speed
- Cutterhead Power: 900 kW (1,200 hp)
- Cutterhead Speed: 3.0 RPM
- Screw Conveyor: shaft type
- Screw Conveyor Diameter: 800 mm (31 in)
- Maximum Pressure: 4 bar
- Cutterhead Opening Ratio: 33%
- Cutterhead: Spoke Type, mixed ground
- Cutting Tools: Tungsten carbide knife-edge bits, 17-in. disc cutters

- Articulation: Active
- Back-filling: One-liquid type
- Segment Lining: Reinforced concrete, 12 in. thick, 5+1 arrangement
- Man Lock: Two-chamber type
- Tunnel Length: 2 x 0.8 mile. Left and Right Line tunnels with an intermediate station site.
- Contractor: China Railway Construction Corporation (CRCC), Bureau 23.

Advance Rates

The Robbins machine achieved advance rates of up to 423 ft per week, with average advance rates of approximately 223 ft per week (for the entire project, both sections of tunnel). These rates were affected as the EPB approached the intermediate station. The machine was slowed down at this point, because it was boring very fast and the station was not yet ready.

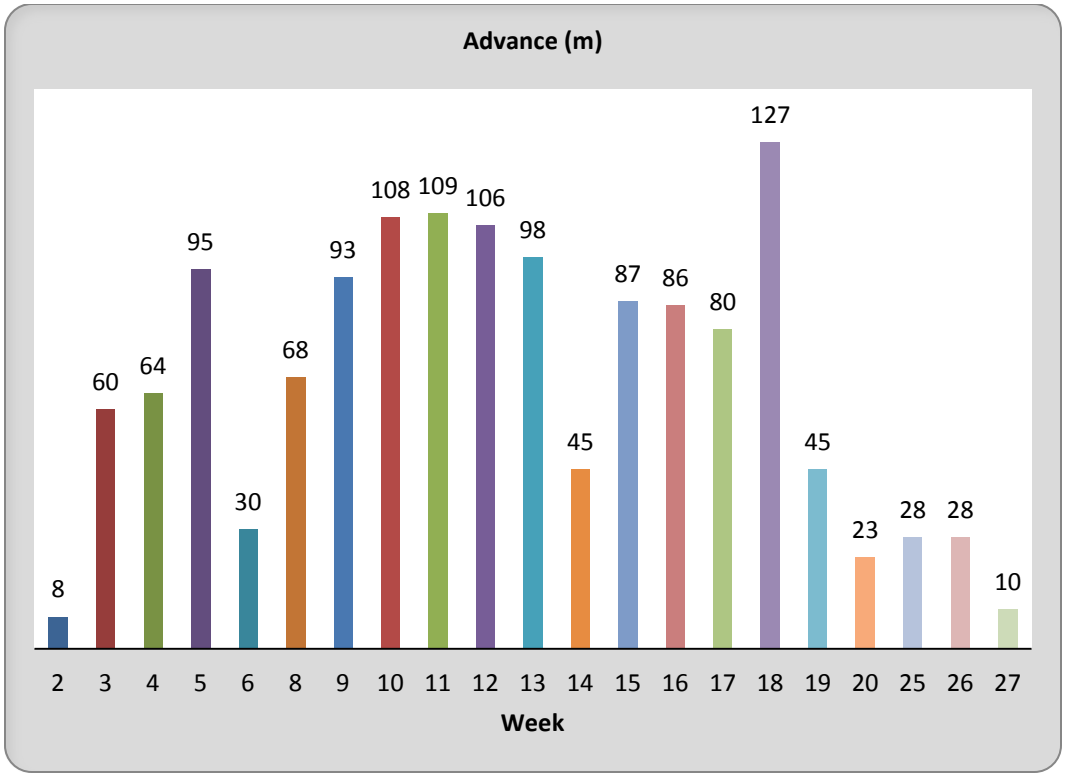

Max. daily rate	19rings ，28.5 m
Max. weekly rate	85rings ，127.5m
Max. monthly rate	305rings ，457.5m

Figure C-1 Advance Rates for the Robbins Chengdu Metro EPB, Left Line Tunnel.

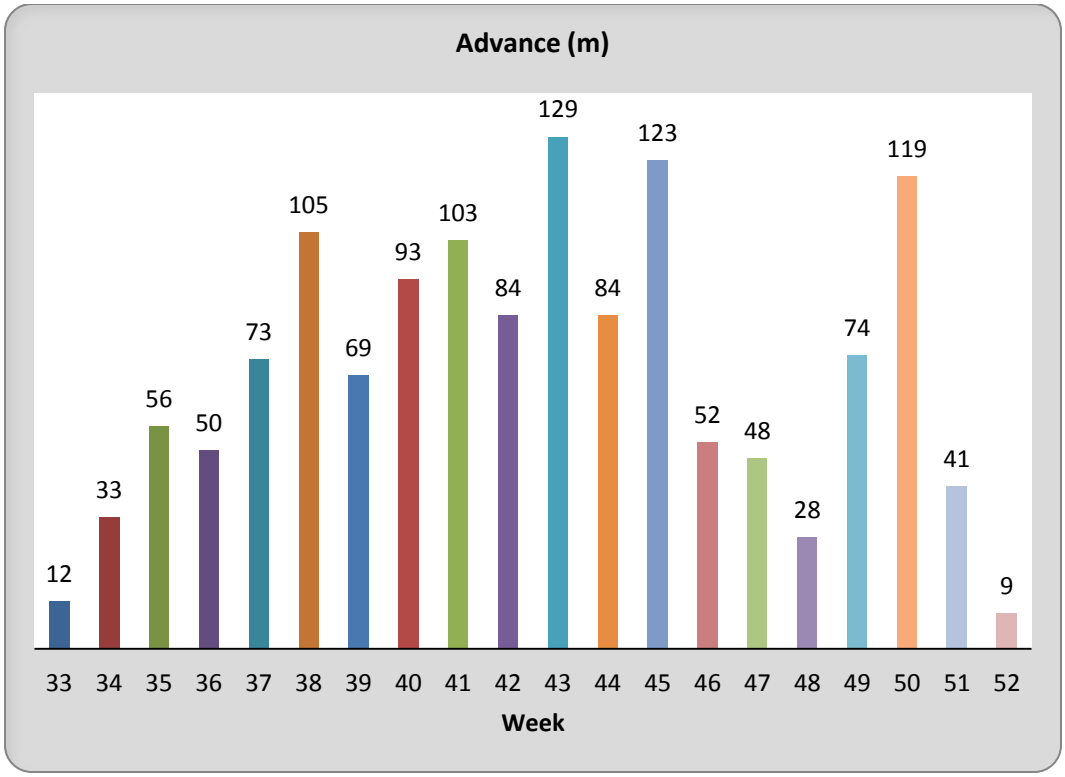

Max. daily rate	18rings ，27 m
Max. weekly rate	86rings ，129m
Max. monthly rate	298rings ，447m

Figure C-2 Advance Rates for the Robbins Chengdu Metro EPB, Right Line Tunnel.

Guangzhou Metro, Guang-Fo Line—Guangzhou, China

General Information

- The 20 mile long Guang-Fo line is China's first ever inter-city rail line, and will cut travel times between the cities of Guangzhou and Foshan to about 50 minutes by 2012.
- Ground consisted of a complex layered profile, ranging from highly weathered to slightly weathered granite, coarse sand, and silt at pressures up to 4 bar. About 70% of the tunneling was through a mixed face, with the alignment above the spring line in soft soils and the bottom half of the tunnel in rock of at least 7,250 psi UCS. The remaining 30% consisted of flowing sand with high water content.
- Robbins supplied two 20.53 ft diameter EPBs with mixed ground cutterheads.

Machine Specifications:

- Machine Thrust: 36,000kN (8.1 million lb)
- Maximum Torque: 5,628 kNm (4.2 million lb-ft)
- Maximum Stroke: 1, 950 mm (77 in)
- Cutterhead Drive: Electric, Variable Speed
- Cutterhead Power: 900 kW (1,200 hp)
- Cutterhead Speed: 3.0 rpm
- Screw Conveyor: shaft type
- Screw Conveyor Diameter: 800 mm (31 in)
- Maximum Pressure: 4 bar
- Cutterhead: Spoke Type, mixed ground
- Cutting Tools: Tungsten carbide knife-edge bits, 17 in. disc cutters

- Articulation: Active
- Back-filling: Two-liquid type
- Segment Lining: Reinforced concrete, 12 in. thick, 5+1 arrangement
- Man Lock: Two-chamber type
- Tunnel Length: 2 x 1.6 miles
- Contractor: China Communication Construction Corp., 2nd Navigation Engineering Bureau Ltd. (CCCC)

Advance Rates

The Robbins machines achieved advance rates of up to 1181 ft per month. The two EPBs operated at average 95% availability for the project duration, in expected ground conditions requiring few cutter changes.

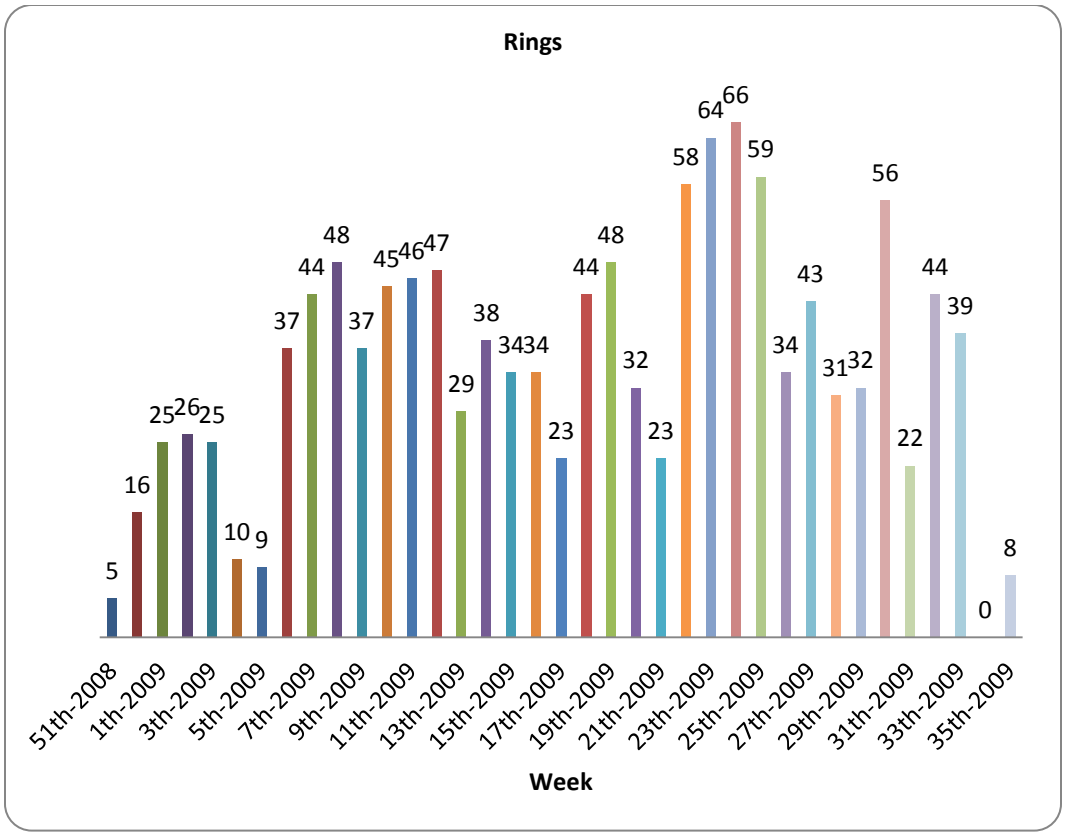

EPB 326 RECORD	
Max. daily rate	13 rings, 19.5m
Max. weekly rate	66 rings, 99.0 m
Max. monthly rate	240 rings, 360m

Figure C-3 Advance Rates for the Robbins Guangzhou Metro EPB 326.

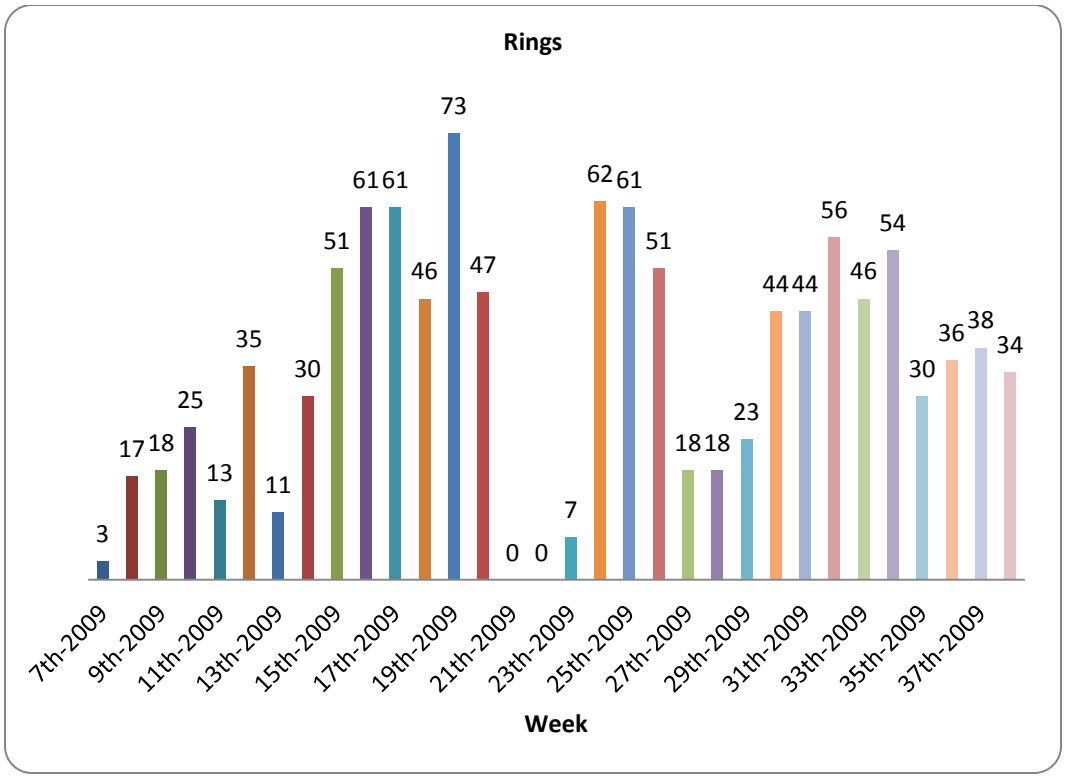

EPB 327 RECORD	
Max. daily rate	15 rings, 22.5m
Max. weekly rate	73 rings, 109.5 m
Max. monthly rate	224 rings, 336m

Figure C-4 Advance Rates for the Robbins Guangzhou Metro EPB 327.

Mexico City Metro Line 12—Mexico City, MX

General Information

- The Robbins EPB excavated 4.8 miles of the Mexican Federal District's first new rail route in ten years, traveling between the southern neighborhoods of Tláhuac and Mixcoac. During tunneling, the machine will pass through seven cut and cover station sites.
- The 33.5 ft diameter EPB is the largest TBM ever to bore in Mexico.
- Geotechnical investigations of the metro tunnel area showed an abundance of lake clays, interspersed with sections of sand, gravel, and boulders up to 800 mm in diameter. Long dormant and eroded volcanoes are buried throughout the area, where they have deposited volcanic rock and fields of boulders in the drained lake bed where modern Mexico City was founded. This type of soil composition is highly unusual, and has only one other analog in the world—in Sapporo, Japan.
- The Robbins EPB was assembled using Onsite First Time Assembly (OFTA) in just ten weeks. Components were lowered into the 56 ft deep launch shaft, located on Ermita Iztapalapa Avenue in downtown Mexico City.

Figure C-5 Robbins 33.5 ft Diameter EPB Excavating Line 12 of Mexico City Metro.

Machine Specifications

- Machine Thrust: 84,000kN (18.9 million lb)
- Normal Working Torque: 20,300 kNm (15 million lb-ft)
- Maximum Stroke: 2,300 mm (7.5 ft)
- Cutterhead Drive: Electric, Variable Speed
- Cutterhead Power: 2,280 kW (3,100 hp)
- Cutterhead Speed: 0-2.0 rpm
- Screw Conveyor: two-stage setup—initial ribbon-type screw followed by shaft-type screw

- Screw Conveyor Diameter: 1,200 mm (3.9 ft)
- Maximum Pressure: 4 bar
- Cutterhead: Spoke Type, soft ground
- Cutting Tools: Tungsten carbide knife-edge bits
- Articulation: Active
- Back-filling: Two-liquid type
- Segment Lining: Reinforced concrete, 16 in. thick, 7+1 arrangement
- Man Lock: Two-chamber type
- Tunnel Length: 4.8 miles
- Contractor: ICA Consortium (ICA, CARSO, and Alstom)

Advance Rates

- The machine completed excavation of the project on March 1, 2012, after achieving maximum advance rates of 443 ft per week.
- Despite multiple planned stoppages as the machine was walked through each of seven cut and cover station sites, the overall advance rates averaged 738 ft per month.

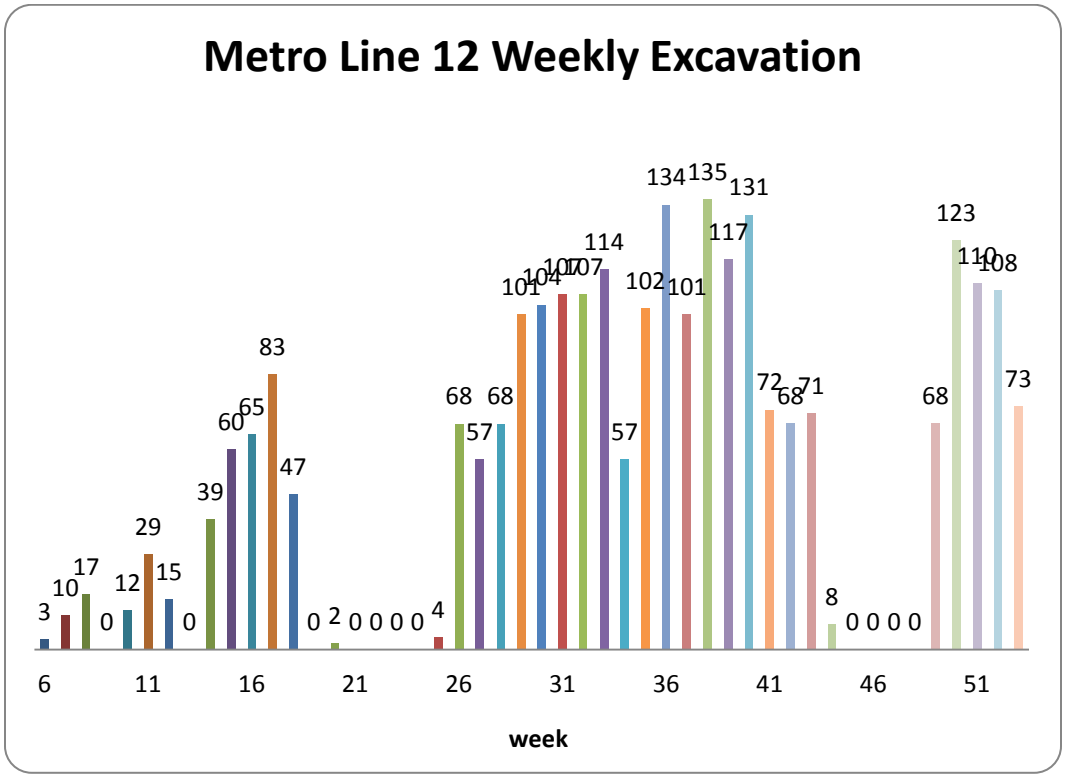

Figure C-6 Advance Rates at Mexico City Metro in March 2011.

New Delhi Metro Extension Project Phase II—New Delhi, India

General Information

- Two 21.4 ft diameter Robbins EPBs were commissioned to bore the BC-16 contract of the New Delhi Metro Extension Project, Phase II, running between Udyog Bhawan and Jor Bagh areas in Delhi. Each TBM bored parallel tunnels of 1.2 miles in length, with an intermediate station in between.
- Approximately 10 mi of TBM drives were involved in Phase II of the project, with about 19 mi of underground works in total including cut and cover stations. The 14 other TBMs were manufactured by competitors. The project was on a tight schedule, which called for all tunneling to be complete by December 2009, in advance of the 2010 Commonwealth Games.
- Ground conditions consisted of watery to sticky clay, silty sand, and gravels with pressures up to 3 bar.

Machine Specifications

- Machine Thrust: 32,000kN (7.2 million lb)
- Normal Working Torque: 6,178 kNm (4.5 million lb-ft)
- Maximum Stroke: 1,750 mm (69 inches)
- Cutterhead Drive: Electric
- Cutterhead Power: 810 kW (1,085 HP)
- Cutterhead Speed: 0-1.5 RPM
- Screw Conveyor: shaft-type
- Screw Conveyor Diameter: 850 mm (33 inches)
- Maximum Pressure: 5 bar
- Cutterhead: Spoke Type

- Cutting Tools: Tungsten carbide drag bits and knife-edge bits; two hydraulic copy cutters
- Articulation: Non-articulated
- Back-filling: Two-liquid type
- Segment Lining: Reinforced concrete, 11 in. thick, 5+1 arrangement
- Man Lock: Two-chamber type
- Tunnel Length: 2 x 1.2 miles
- Contractor: Continental Engineering Corporation / Soma JV
- Project Owner: Delhi Metro Rail Corporation (DMRC)
- Muck Removal: Rail muck cars

Advance Rates

- The machines excavated from May 2008 to July 2009, with one machine (EPB - 324) achieving 600 ft in one week
- At the end of contractual tunneling in March 2009, one machine was selected to bore an additional 1800 ft long drive because the competitor machine slated to tunnel it was still excavating its previous tunnel. The Robbins machine completed this bore in July 2009.

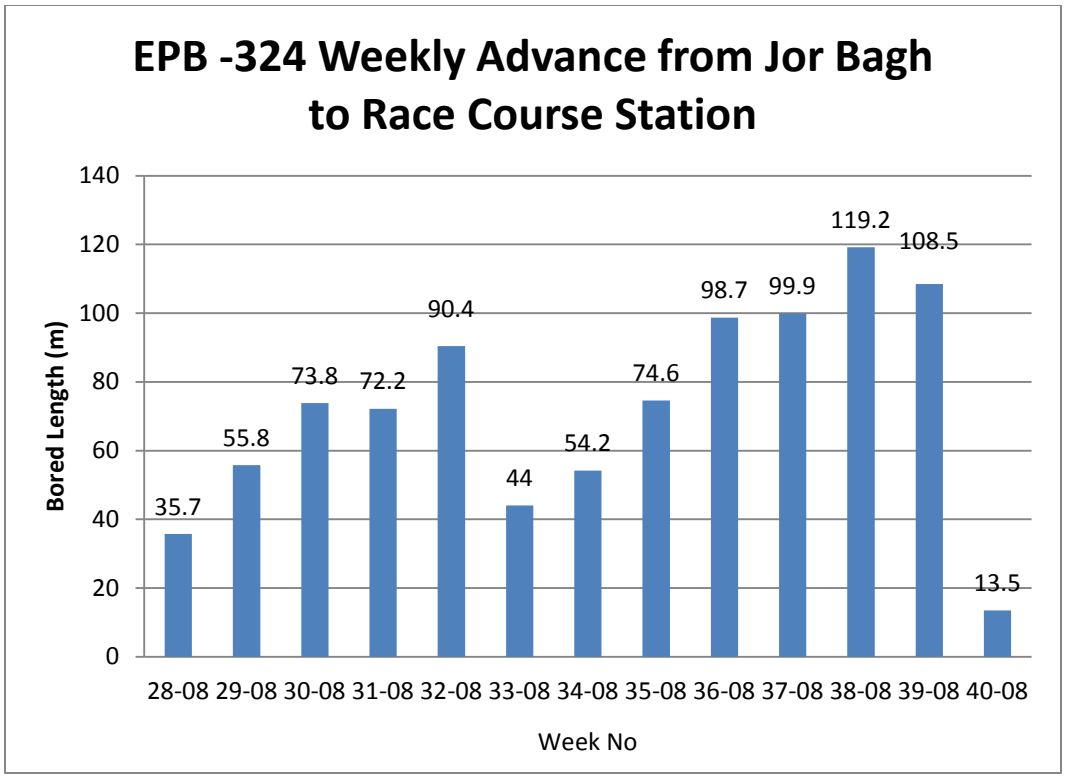

Figure C-7 First Section of Tunneling for EPB-324.

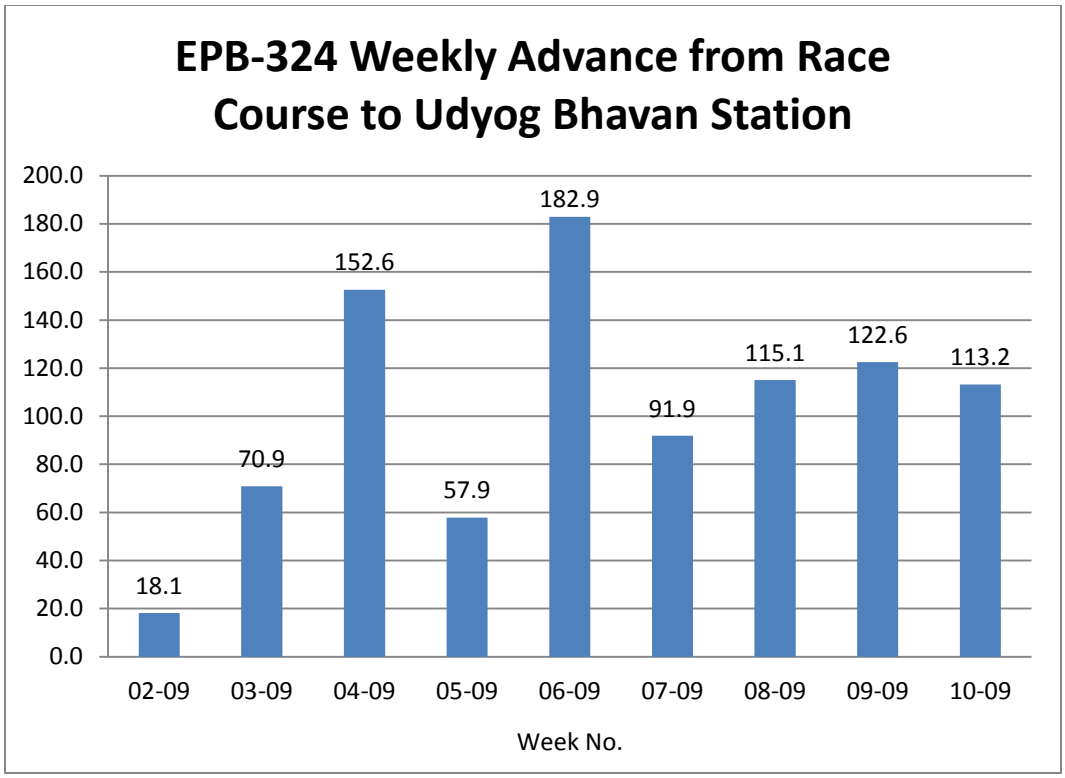

Figure C-8 Second Section of Tunneling for EPB-324, With a Record Rate of 600 ft in One Week.

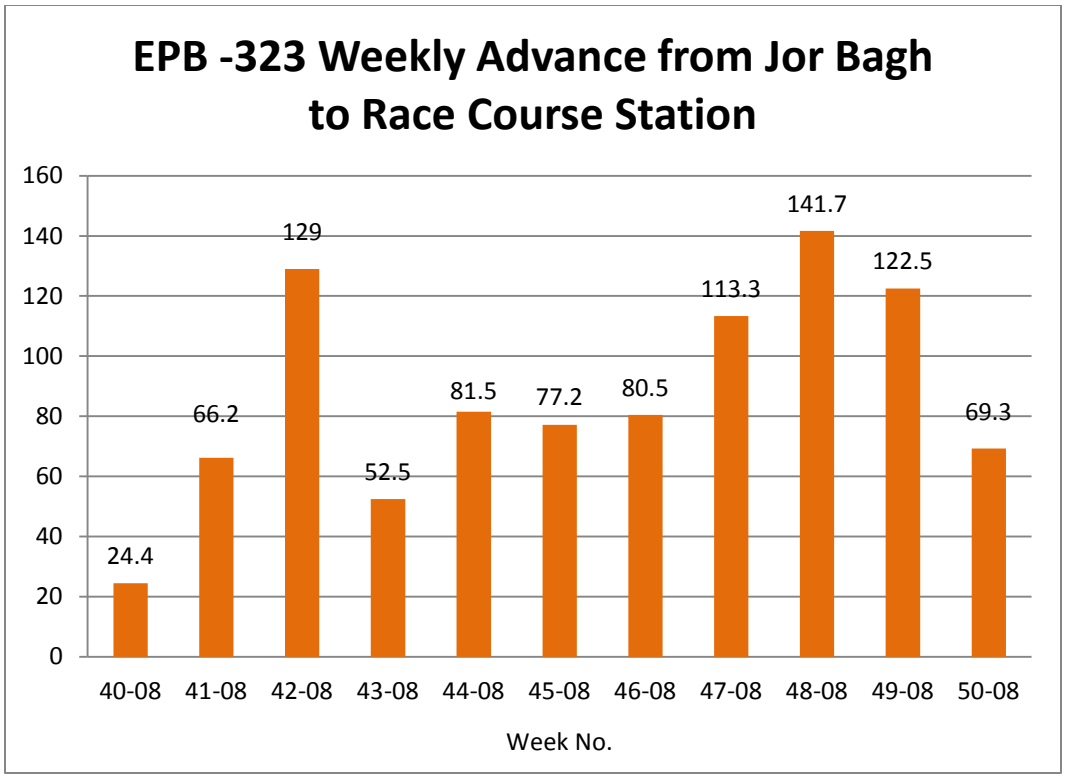

Figure C-9 First Section of Tunneling for EPB-323.

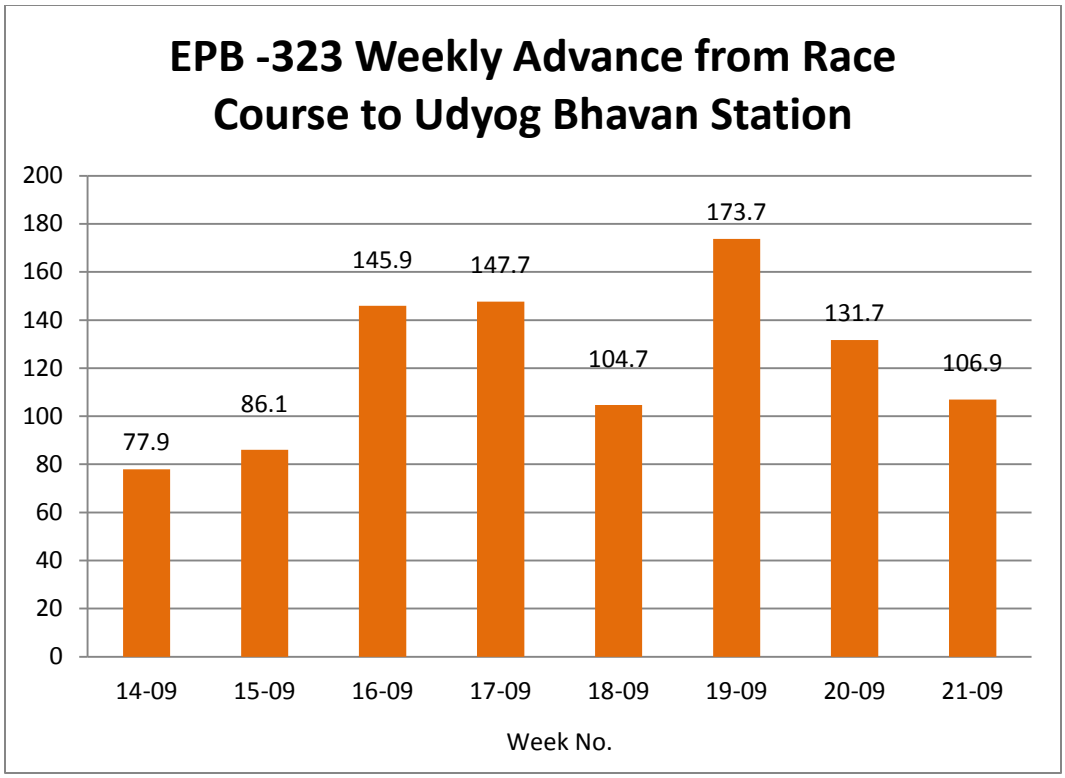

Figure C-10 Second Section of Tunneling for EPB -323.

Table C-1 Overall Rates for Both Robbins EPBs

	EPB -323	EPB -324
Average Advance Rate (all tunnels, in meters)	104.4	87.6
Maximum Advance Rate (all tunnels, in meters)	173.7	182.9

Figure C-11 EPB -324 at its Intermediate Breakthrough in October 2008.

Upper Northwest Interceptor Sewer 1 & 2—Sacramento, California, USA

General Information

- The Robbins 13.9 ft diameter EPB excavated a 3.7 mile long tunnel for Sacramento's Upper Northwest Interceptor (UNWI) sewer project. The sewer line will convey up to 560 million liters (148 million gallons) of wastewater per day. The tunnels, for project owner Sacramento Regional County Sanitation District (SRCSD), will add capacity to existing interceptor systems in the area that are close to overflowing during heavy rains.
- The EPB was designed for use with a novel tunnel liner, never before used in the U.S. Precast concrete segments 9 in. thick were molded with embedded PVC sheets 0.07 in. thick. Designed as a single pass system, the PVC inner liner protects the sewer from corrosive gases that can degrade concrete.
- Bore holes along the tunnel alignment indicated layers of clay and sand, with no boulders expected. Below the spring line, the tunnel profile consisted mostly of sand, while the upper portion of the tunnel face was in clay.

Machine Specifications

- Machine Thrust: 18,000kN (4 million lb)
- Normal Working Torque: 1,866 kNm (1.3 million lb-ft)
- Maximum Stroke: 2,590 mm (102 inches)
- Cutterhead Drive: Hydraulic
- Cutterhead Speed: 0-1.6 RPM
- Screw Conveyor: shaft-type

- Screw Conveyor Diameter: 650 mm (26 inches)
- Maximum Pressure: 5 bar
- Cutterhead: Spoke Type, with plates
- Cutting Tools: Tungsten carbide knife-edge bits, shell bits, interchangeable with disc cutters
- Articulation: Active
- Back-filling: Two-liquid type
- Segment Lining: Reinforced concrete, 9 in. thick, 5+1 arrangement, PVC inner liner
- Man Lock: Two-chamber type
- Tunnel Length: 3.7 miles
- Contractor: Traylor/Shea JV
- Project Owner: Sacramento Regional County Sanitation District (SRCSD)
- Muck Removal: Robbins Continuous Conveyor System

Advance Rates

- The machine excavated from December 2008 to November 2009. During that time it achieved a record for EPB machines in the 13 to 16 ft diameter range. Multiple advances of 690 ft per week were recorded (5 days excavation per week), as well as daily rates of 165 ft in two 8-hour shifts. The average advance rate recorded for the project was 351 ft per week.
- The Robbins-supplied conveyor system performed at over 90% availability for the duration of the project.

Figure C-12 Breakthrough on November 21, 2009.

Zhengzhou Metro, Line 1—Zhengzhou, China

General Information

- Once complete in 2013, Line 1 of Zhengzhou Metro will include 16 mi of tunnel and 22 stations. The Zhengzhou Metro company has invested Yuan 10.2 billion (USD 1.5 billion / EUR 1.1 billion) in the new metro lines, which will total 117 mi by their completion between 2015 and 2030.
- The parallel 2.2 mi long tunnels pass through four intermediate stations between Kaixuan and Tongbo areas of the city
- Ground consists of soft soils including clay, fine sand, loess, and pebbles.
- Robbins supplied two 20.6 ft diameter EPBs with soft ground cutterheads.

Machine Specifications:

- Machine Thrust: 36,000kN (8.1 million lb)
- Maximum Torque: 4,785 kNm (3.5 million lb-ft)
- Maximum Stroke: 1, 950 mm (77 in)
- Cutterhead Drive: Electric, Variable Speed
- Cutterhead Power: 750 kW (1,005 HP)
- Cutterhead Speed: 0.3 to 2.0 RPM
- Screw Conveyor: shaft type
- Screw Conveyor Diameter: 800 mm (31 in.)
- Cutterhead: Spoke Type, soft ground
- Cutting Tools: Tungsten carbide knife-edge bits
- Articulation: Active
- Back-filling: One-liquid type

- Segment Lining: Reinforced concrete, 12 in. thick, 5+1 arrangement
- Man Lock: Two-chamber type
- Tunnel Length: 2 x 2.2 miles
- Contractor: China Railway Construction Corp. (CRCC), 11th Bureau
- Owner: Zhengzhou Metro Company

Advance Rates

The machines were launched in November and December 2010, and by March 2011 had both achieved breakthroughs into an intermediate cut and cover station site at the 4,250 ft mark of tunneling.

The metro's first TBM, one of two 20.7 ft diameter Robbins EPBs for Zhengzhou's Line 1, achieved a project record of 2,362 ft in one month. Daily rates have been as high as 22 rings (108 ft) in two 10-hour shifts. The rates are not only a project record amongst nine other machines, but also rank as some of the highest rates ever recorded for Chinese EPB TBMs in the 20 to 23 ft diameter range.

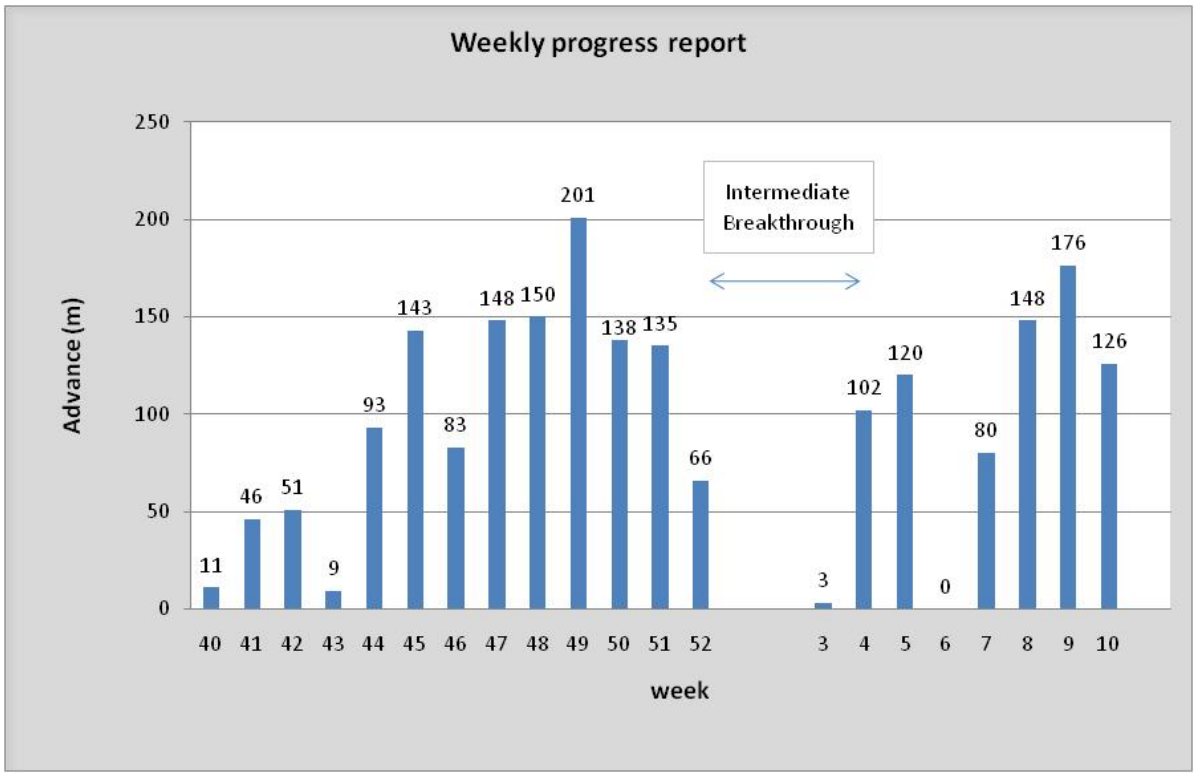

Max. daily rate	21rings ，31.5 m
Max. weekly rate	134rings ，201m
Max. monthly rate	401ings，601.5m

Figure C-13 Advance Rates for the Robbins Zhengzhou Metro EPB 345.

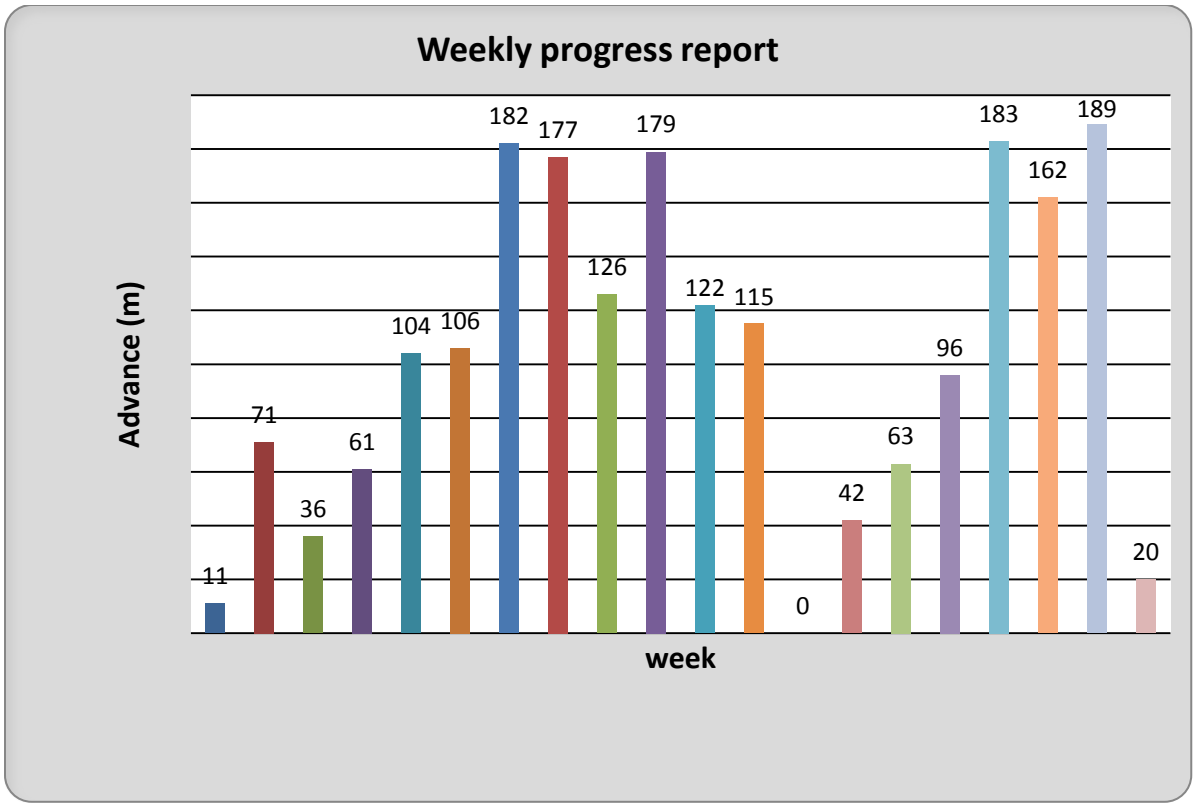

Max. daily rate	23rings ，34.5 m
Max. weekly rate	126rings ，189m
Max. monthly rate	480ings ，720m

Figure C-14 Advance Rates for the Robbins Zhengzhou Metro EPB 346.

LIST OF ACRONYMS AND ABBREVIATIONS

AR	Advance Rate
CAI	Cerchar Abrasivity Index
CSM	Colorado School of Mines
CUIRE	Center for Underground Infrastructure Research and Education
EMI	Earth Mechanics Institute
EPB	Earth Pressure Balanced
Fn	Normal Cutterdisc Force
FPI	Field Penetration Index
ISRM	International Society for Rock Mechanics
ITA	International Tunneling Association
LCM	Linear Cutting Machine
NTH	Norwegian Institute of Technology
NTNU	Norwegian University of Science and Technology
PR	Penetration Rate
PRev	Penetration per Revolution
RMCI	Rock Mass Cuttability Index
RME	Rock Mass Excavability
RMR	Rock Mass Rating
RPM	Revolutions per Minute
RQD	Rock Quality Designation
RSR	Rock Structure Rating
SP	Specific Penetration
TBM	Tunnel Boring Machine
UCS	Uniaxial Compressive Strength
UR	Utilization Rate

LIST OF DEFINITIONS

Advance Rate: Amount of average progress of the complete tunnel (with segmental linings erected) (Laughton, 1998).

Cerchar Abrasivity Index: An index for classifying the abrasivity of a rock material. It measures the wear on the tip of a steel stylus (Sundin and Wanstedt, 1994).

Field Penetration Index: The normal cutterdisc force divided by the penetration rate of TBM. Higher the values indicate greater difficulty off boring (Hassanpour et al., 2009).

Normal Cutterdisc Force: Amount of perpendicular to cutterdisc axis force from the ground to a single cutterdisc as a result of TBM moving forward (Laughton et al., 1995).

Penetration per Revolution: The amount of average progress a TBM can make for one revolution of its cutterhead.

Penetration Rate: The amount of average progress of tunnel considering 100% utilization of cutterhead (Laughton, 1998).

Revolution per Minute: The number of revolutions the TBM cutterhead can do in one minute.

Rock Mass Cutability Index: An index used to classify different rocks based on their resistance to cutting forces (Hassanpour et al., 2009).

Rock Mass Excavability: Boreability predictor of a rock mass that a TBM is encountering (Bieniawski et al., 2006).

Rock Mass Rating: Geomechanical classification system for rocks (Ribachi and Lembo Fazio, 2005).

Rock Quality Designation: A rough measure of the degree of jointing or fractures in a rock mass, measured as a percentage of the drill core in length (Khademi et al., 2010).

Rock Structure Rating: A quantitative method for describing quality of a rock mass for appropriate ground support (Cassinelli, 1982).

Specific Penetration: The amount of penetration per revolution divided by the normal cutterdisc force. Specific penetration is the reverse form of field penetration index (Ribachi and Lembo Fazio, 2005).

Utilization Rate: The time of cutterhead rotation in one cycle of TBM boring divided by the total time of the cycle (Laughton, 1998).

References

Abd Al-Jalil, Y., 1998. Analysis of performance of tunnel boring machine-based systems, The University of Texas at Austin, 427 p.

Abdul-Kadir, M. R., & Price, A. D. F. 1995. Conceptual phase of construction projects. International Journal of Project Management, 13(6), 387-393.

Alber, M., 2000. Advance rates of hard rock TBMs and their effects on projects economics, Tunnelling and Underground Space Technology 15 (1) (2000), pp. 55–84.

Alvarez Grima, M., 2000b. Neuro-fuzzy modeling in Engineering Geology: applications to mechanical rock excavation, rock strength estimation and geological mapping, Ph.D.Thesis, Delft University of Technology, 252 pp, Balkema, Rotterdam.

Alvarez Grima, M., P.A., 2000a. Bruines and P.N.W. Verhoef, Modeling tunnel boring machine performance by neuro-fuzzy methods, Tunnell. Undergr. Space Technol. 15 (3), pp. 259–269.

Bamford, W.F., 1984. Rock test indices are being successfully correlated with tunnel boring machine performance. In: Proceedings of the 5th Australian Tunneling Conference, Melbourne, vol. 2, pp. 9–22.

Barla, G., Pelizza, S., 2000. TBM tunneling in difficult ground conditions, Proceedings of GeoEng 2000, Proceedings of the International Conference on Geotechnical & Geological Engineering, Melbourne, November 19–24, 2000, Technomic Publishing Company, Lancaster, pp. 329–354.

Barton, N., 1999. TBM performance in rock using QTBM, Tunnels Tunnell. Int. 31, pp. 41–48.

Barton, N., 2000. TBM tunneling in jointed and faulted rock. A.A. Balkema Publishers, Rotterdam.

Barton, N., 2011. TBM prognosis for open-gripper and double-shield machines tunneling through hard jointed rock with weakness zones, Proceedings of World Tunneling Congress (WTC), May 20-26, Helsinki, Finland.

Bencorinc, 2017. http://www.bencorinc.com/uploads/case-studies/portland-cso-west-east/Portland-CSO_PumpStation.jpg, Visited: 11/1/2017

Bieniawski, Z.T., Celada B, Galera, JM., 2007a. TBM excavability: prediction and machine–rock interaction. In: Proceedings of the Rapid Excavation and Tunneling Conference (RETC), Toronto, Canada, pp 1118–1130. 256

Bieniawski, Z.T., Celada, B., Galera Fernandez, J.M., 2007b. Predicting TBM Excavability-Part I. Tunnels & Tunneling International, p. 25.

Bieniawski, Z.T., Celada, B., Galera, J.M., Álvares, M., 2006. Rock Mass Excavability (RME) index: a New Way to Selecting the Optimum Tunnel Construction Method, Proc. ITA World Tunneling Congress, Seoul.

Bieniawski, Z.T., Celada, B., Galera, J.M., Tardáguila, I., 2008. New applications of the excavability index for selection of TBM types and predicting their performance, ITA World Tunneling Congress, Agra, India.

Boyd, R.J., 1986. Hard rock continuous mining machine: Mobile Miner MM-120. In: D.F. Howarth et al., Editors, Rock excavation engineering seminar, Dept. Mining and Met. Eng, University of Queensland.

Bruland, A., 1998a. Hard rock tunnel boring. Ph.D. Thesis, The Norwegian University of Science and Technology, Trondheim.

Bruland, A., 1998b. Prediction Model for Performance and Costs, The Norwegian University of Science and Technology, Trondheim, Norwegian Tunneling society, NFF, Publication No. 11, pp. 29-34.

Cassinelli, F., Cina, S., Innaurato, N., Mancini, R., Sampaolo, A., 1982. Power consumption and metal wear in tunnel-boring machines: analysis of tunnel-boring operation in hard rock. Tunneling ‘82, London, Inst. Min. Metall., pp. 73–81.

Deere D. and Miller R.D., 1966. Engineering classification and index properties for intact rock. Univ. of Illinois, Tech. Rept. No. AFWL-TR-65-116, 1966.

Farmer, I.W., Glossop, N.H., 1980. Mechanics of disc cutter penetration, Tunnels Tunnell. Int. 12 (6), pp. 22–25.

Farrokh, E., 2013. Study of utilization and advance rate of hard rock TBMs, Ph.D. thesis, The Pennsylvania State University.

Frenzel, Ch., Käsling, H., Thuro, K., 2008. Factors Influencing Disc Cutter Wear. Geomechanik und Tunnelbau 1, pp. 55-60.

Goel, R. K., 2008. Evaluation of TBM performance in a Himalayan tunnel, World Tunnel Congress 2008 - Underground Facilities for Better Environment and Safety – India, 1522-1532.

Gong, Q.M., 2005. Development of a rock mass characteristics model for TBM penetration rate prediction, Ph.D. thesis, Nanyang Technology University.

Graham, P.C., 1976. Rock exploration for machine manufacturers. In: Z.T. Bieniawski, Editor, Exploration for Rock Engineering, Balkema, Johannesburg, pp. 173–180.

Halpin, D. W., 2010. Construction management. John Wiley & Sons.

Hamilton, W.H., and, Dollinger, G.L., 1979. Optimizing tunnel boring machine and cutter design for greater boreability, RETC Proceedings, Atlanta 1, pp. 280–296.

Hansen T.H., 1988. Rock properties. Norwegian Rock and Soil Assoc., Publ. no 5, 3 pp.

Hassanpour, J., 2009. Investigation of the effect of engineering geological parameters on TBM performance and modifications to existing prediction models. Ph.D. Thesis, Tarbiat Modares University, Tehran, Iran.

Hassanpour, J., 2009a. Investigation of the effect of engineering geological parameters on TBM performance and modifications to existing prediction models. Ph.D. Thesis, Tarbiat Modares University, Tehran, Iran.

Hassanpour, J., Rostami, J., Khamehchiyan, M., Bruland, A., 2009b. Development new equations for performance prediction. Geo Mechanics and Geoengineering: An International Journal 4 (4), 287-297.

Hassanpour, J., Rostami, J., Khamehchiyan, M., Bruland, A., and Tavakoli, H.R., 2009a. TBM performance analysis in pyroclastic rocks: a case history of Karaj water conveyance tunnel, Rock Mech. Rock Eng.

Hassanpour, J., Rostami, J., Khamehchiyan, M., Bruland, A., Tavakoli, H.R., 2009b. TBM performance analysis in pyroclastic rocks: a case history of Karaj water conveyance tunnel, Rock Mech. Rock Eng.

Herenknecht, 2017a. https://www.herrenknecht.com/typo3temp/pics/Intake-shaft_Jan2012_1920x620_02_0072795517.1442322678.jpg, Visited: 11/1/2017

Herenknecht, 2017b. www.herrenknecht.com/uploads/pics/130308_TPG_Schnittgrafik_Einfachschild__TBM_960x614_01.1365179020.jpg, Visited: 11/1/2017

Herget G., 1982. Probabilistic slope design for open pit mines. Rock Mechanics, Suppl. 12, 163-178, 1982.

Hoek, E., and Brown, E.T., 1980. Underground Excavations in Rock. London: Instn Min. Metall., 527 pages.

Howarth, D.F., 1986. Review of rock drillability and boreability assessment methods, Trans IMM Sect A Min Ind 9, The Institution of Mining and Metallurgy, London, pp. A191–A202.

Hughes, H.M., 1986. The relative cuttability of coal-measures stone, Min. Sci. Technol. 3 (2), pp. 95–109.

Innaurato, N., Mancini, R., Rondena, E., Zaninetti, A., 1991. Forecasting and effective TBM performances in a rapid excavation of a tunnel in Italy. In: Proceedings of the Seventh International Congress ISRM, Aachen, pp. 1009–1014.

Iseley, T., Najafi, M., & Tanwani, R., 1999. Trenchless construction methods and soil compatibility manual. National Utility Contractors Association, Arlington, VA.

International Society for Rock Mechanics (ISRM), Commission on classification of rocks and rock masses, 1980. Basic geotechnical description of rock masses. Int. J. Rock Mech. Min. Sci. & Geomech. Abstr., Vol. 18, pp. 85 110.

International Society for Rock Mechanics (ISRM), Commission on standardization of laboratory and field tests, 1978. Suggested methods for the quantitative description of discontinuities in rock masses. Int. J. Rock Mech. Min. Sci. & Geomech. Abstr., Vol. 15, No. 6, pp. 319-368.

ITA/AITES WG. 14, 2000. Recommendations and Guidelines for Tunnel Boring Machine, Lausanne.

Jencopale, N., 2013. Improving Productivity of Tunnel Boring Machines. Master Thesis, University of Texas at Arlington.

Jjboring, 2017. http://jjboring.com/wp-content/uploads/2016/06/hand-tunnels024x768.jpg, Visited: 11/1/2017

Johannessen, O., 1988. NTH Hard Rock Tunnel Boring. Project Report 1–88, NTH/NTNU Trondheim, Norway, 1988.

Khademi Hamidi, J., Shahriar, K., Rezai, B., Bejari, H., 2009. Application of Fuzzy Set Theory to Rock Engineering Classification Systems: An Illustration of the Rock

Mass Excavability Index, Rock Mechanics and Rock Engineering, Volume 43, Number 3, pp. 335-350.

Khademi Hamidi, J., Shahriar, K., Rezai, B., Rostami J., 2010. Performance prediction of hard rock TBM using Rock Mass Rating (RMR) system, Tunnell. Undergr. Space Technol. 25 (4), pp. 333-345.

Kim, T., 2004. Development of a Fuzzy Logic Based Utilization Predictor Model for Hard Rock Tunnel Boring Machines. Ph.D. Thesis Dissertation, Colorado School of Mines.

Klein, S., Schmoll, M., Avery, T., 1995. TBM performance at four hard rock tunnels in California. In: Proceedings of the Rapid Excavation & Tunnelling Conference, pp. 61–75 (Chapter 4).

Laughton, C., 1998. Evaluation and prediction of tunnel boring machine performance in variable rock masses. Ph.D. Thesis, The University of Texas, Austin, USA.

Laughton, C., Nelson, P.P., Abd Al-Jalil Y., 1995. The probabilistic prediction of tunnel boring machine performance in practice. NSF Workshop on Transferring Research into Practice, ASCE Press.

Lislerud A., 1983. Hard rock tunnel boring, Project report 183, Norwegian Institute of Technology, Trondheim.

Maidl, B., Schmid, L., Ritz, W., Herrenknecht, M., 2008. Hard Rock Tunnel Boring Machines. 347 pages.

Maidl, B., Herrenknecht, M., Anheuser, L., 1994. Maschineller Tunnelbau im Schildvortrieb. Verlag Ernst & Sohn, Berlin.

Maidl, B., Schmid, L., Ritz, W., Herrenknecht, M., 2001. Tunnel bohrmaschinen im Hartgestein. Verlag Ernst & Sohn, Berlin.

Mole, 2017. http://mole.my/wp-content/uploads/2017/09/tbm.jpg, Visited: 11/1/2017

Najafi, M. 2013. Trenchless technology: Planning, equipment, and methods. McGraw Hill Professional.

Nelson, P., O'Rourke, T.D., Kulhawy, F.H., 1983. Factors affecting TBM penetration rates in sedimentary rocks. In: Proceedings, 24th US Symposium on Rock Mechanics, Texas A&M, College Station, TX, pp. 227–237.

Nelson, P. P., Abd Al-Jalil, Y., Laughton, C., 1994a. Tunnel boring machine project data bases and construction simulation, Geotechnical Engineering Center Report GR 94-4. The University of Texas at Austin.

Nelson, P. P., Abd Al-Jalil, Y., Laughton, C., 1994b. Probabilistic Estimates of Time to Complete Tunnel for Six Inland Feeder Project Tunnel Drives using Level 1 Data Base Searching and Simulation Methodologies. Report to the Metropolitan Water District. Geotechnical Engineering Center, University of Texas at Austin, TX.

Nelson, P.P., Abad-Aljali, Y., Laughton, C., 1999. Improved strategies for TBM performance prediction and project management. RETC, pp. 963–979.

Ozdemir, L., Miller, R., Wang, F.D., 1978. Mechanical Tunnel Boring Prediction and Machine Design. Final Project Report to NSF APR73-07776-A03, Colorado School of Mines, Golden, Co.

Patching T.H. and Coates D.F., 1968. A recommended rock classification for rock mechanics purposes. CIM Bull., Oct. 1968, pp 1195-1197.

Piteau D.R., 1970. Geological factors significant to the stability of slopes cut in rock. Proc. Symp. on Planning Open Pit Mines, Johannesburg, South Africa, 1970, pp. 33-53.

Ramezanzadeh, A., 2005. Performance analysis and development of new models for performance prediction of hard rock TBMs in rock mass, Ph.D. thesis, INSA, Lyon, France, p. 333.

Ribacchi, R, Lembo-Fazio, A., 2005. Influence of rock mass parameters on the performance of a TBM in a Gneissic formation (Varzo tunnel). Rock Mech Rock Eng., 38 (2):105–127

Robbins, R.J., 1992. Large diameter hard rock boring machines: State-of-the-art and development in view of alpine base tunnels, Felsbau, Vol. 10, No. 2, 56-62.

Robbins, 2017a. http://www.therobbinscompany.com/wp-content/uploads/2017/05/Latest-News_Slide1.jpg, Visited 11/1/2017

Robbins, 2017b. http://www.therobbinscompany.com/wp-content/uploads/2017/05/GrosvenorLaunch_CrossoverXRE_large-1.jpg, Visited: 11/1/2017

Rostami, J., 1993. Design optimization, performance prediction and economic analysis of tunnel boring machine for the construction of the proposed Yucca Mountain nuclear waste repository. Ms. Thesis, Colorado School of Mines, Golden, Colorado, USA.

Rostami, J., 1997. Development of a force estimation model for rock fragmentation with disc cutters through theoretical modeling and physical measurement of crushed zone pressure. Ph.D. Thesis, Colorado School of Mines, Golden, Colorado, USA, p. 249.

Rostami, J., 2008. Hard Rock TBM cutterhead modeling for design and performance prediction, Geomechanik und Tunnelbau, Ernst & Sohn, (Austrian Journal of Geotechnical Eng.), pp. 18-28.

Rostami, J., Ozdemir, L., 1993. A new model for performance prediction of hard rock TBM. In: Bowerman, L.D., et al. (Eds.), Proceedings, Rapid Excavation and Tunnelling Conference, pp. 793–809.

Roxborough, F.F., Phillips H.R., 1975. Rock excavation by disc cutter, Int. J. Rock Mech. Min. Sci. Geomech. Abstr. 12, pp. 361–366.

Sanio, H.P., 1985. Prediction of the performance of disc cutters in anisotropic rock, Int. J. Rock Mech. Min. Sci. Geomech. Abstr. 22, pp. 153–161.

Sato, K., Gong, F., Itakura, K., 1991. Prediction of disc cutter performance using a circular rock cutting ring. In: Proceedings, The first International Mine Mechanization and Automation Symposium, Colorado School of Mines, Golden, Colorado, USA.

Sharp, W., Ozdemir, L., 1991. Computer Modelling for TBM Performance Prediction and Optimization. Proceedings of the International Symposium on Mine Mechanization and Automation, CSM/USBM, vol. 1(4), pp. 57–66.

Snowdon, R.A., Ryley, M.D., Temporal, J., 1982. A study of disc cutting in selected British rocks, Int. J. Rock Mech. Min. Sci. 19, pp. 107–121.

Stevenson Garry, W., 1999. Empirical estimates of TBM performance in hard rock; Proc. RETC,. AIME, pp. 993–1006.

Sundin, N.O., Wanstedt, S., 1994. A boreability model for TBM's. In: Nelson, P., Laubach, S.E. (Eds.), Rock Mechanics Models and Measurements Challenges from Industry. Proceedings of the 1st North American Rock Mechanics Symposium, The University of Texas at Austin, Balkema, Rotterdam, pp. 311–318.

Tarkoy, P.J., 1973. Predicting TBM penetration rates in selected rock types. In: Proceedings, 9th Canadian Rock Mechanics Symposium, Montreal.

Thuro, K., Plinninger, R.J., 2003. Hard rock tunnel boring, cutting, drilling and blasting: rock parameters for excavability. In: Proceedings of the 10th ISRM International Congress on Rock Mechanics, Johannesburg, South Africa, 1227-1234.

Tunnelingonline, 2017. http://www.tunnelingonline.com/wp-content/uploads/2013/06/feat-move-robins1.jpg, Visited: 11/1/2017

Tunneltalk, 2017a. https://www.tunneltalk.com/images/Hong-Kong-drainage/Hong-Kong-double-deck-blast-analysis.jpg, Visited: 11/1/2017

Tunneltalk, 2017b. https://www.tunneltalk.com/images/Dublin/DublinPortTunnel-Pic4.jpg, Visited: 11/1/2017

US Army Corps of Engineers. 1997. Engineering and Design Tunnels and Shafts in Rock, Appendix C: Tunnel Boring Machine Performance-Concepts and Performance Prediction, Washington, D.C.

VTC, 2017. http://tycnw01.vtc.edu.hk/cbe2024/3-Tunnel.pdf, Visited: 11/1/2017

WBI-PRINT 6. 2007. Stability Analysis and Design for Mechanized Tunneling, Prof. Dr.-Ing. W. Wittke Consulting Engineers for Foundation Engineering and Construction in Rock Ltd.

Wpengine, 2017. 35r8vq1qfmha1cecht1675qy.wpengine.netdna-cdn.com/wp-content/uploads/2017/04/Double-Shield_bodycopy_3Dsideview-2-1024x352.jpg, Visited: 11/1/2017

Yagiz, S., 2002. Development of rock fracture and brittleness indices to quantifying the effects of rock mass features and toughness in the CSM Model basic penetration for hard rock tunneling machines. Ph.D. Thesis. T-5605, p. 289, Colorado School of Mines, Co., USA.

Biographical Information

Saeed Janbaz graduated in 2011 with a Bachelor of Science (B.S.) in Civil Engineering from Tabriz University, Tabriz, Iran. During his studies, he worked for Parket Constructional Company as a project engineer and welding inspector and at the same time taught English conversation at Kish Language Institute, in Iran. After graduation, he moved to Malaysia to pursue his Master's in Construction Management at the University Technology Malaysia (UTM). Saeed graduated from UTM with honors within three semesters while working to cover his expenses. After completing his Master of Science degree in 2013, he returned to Iran and started a family business as a private residential contractor until August of 2014, when he came to the University of Texas at Arlington (UTA) to pursue a Doctor of Philosophy degree in civil engineering with focus in Construction Engineering. During his time at UTA, Saeed was a teaching assistant for various graduate courses such as construction field operations, trenchless technology, construction contracts, construction best practices, and construction sustainability. Also during his time as a Ph.D. student, he was appointed as the lead estimator for a research project granted to Center for Underground Infrastructure Research and Education (CUIRE) by the Texas Department of Transportation (TxDOT). The work on this project gave him the idea for his Ph.D. dissertation to work on advance rate of tunnel boring machines (TBMs). Saeed foresees a bright and successful future in the tunneling industry and is looking forward to having a long tunneling career around the globe.